CALIFORNIA
ENERGY COMMISSION

Energy Research and Development Division

FINAL PROJECT REPORT

Performance-Based Earthquake Engineering Assessment Tool for Natural Gas Storage and Pipeline Systems

Task 3 – *OpenSRA* Final Report

Gavin Newsom, Governor
January 2023 | CEC-500-XXXX-XXX

PREPARED BY:

Primary Author:
Barry Zheng, Micaela Largent, Jennie Watson-Lamprey, Tom Clifford

Slate Geotechnical Consultants
2927 Newbury St., Suite A
510-277-3325
https://slategeotech.com/

Contract Number: PIR-18-003

PREPARED FOR:
California Energy Commission

Yahui Yang
Project Manager

Laurie ten Hope
Deputy Director
ENERGY RESEARCH AND DEVELOPMENT DIVISION

Drew Bohan
Executive Director

DISCLAIMER

This report was prepared as the result of work sponsored by the California Energy Commission. It does not necessarily represent the views of the Energy Commission, its employees or the State of California. The Energy Commission, the State of California, its employees, contractors and subcontractors make no warranty, express or implied, and assume no legal liability for the information in this report; nor does any party represent that the uses of this information will not infringe upon privately owned rights. This report has not been approved or disapproved by the California Energy Commission nor has the California Energy Commission passed upon the accuracy or adequacy of the information in this report.

ACKNOWLEDGEMENTS

The authors thank California Energy Commission for funding this project, the project partners Pacific Earthquake Engineering Research Center (PEER), UC Berkeley, UC San Diego, University of Nevada Reno, the NHERI SimCenter at UC Berkeley, and subcontractors Lettis Consultants International (LCI) and Thomas O'Rourke, as well as the Technical Advisory Committee for providing project guidance.

This research study was funded by the California Energy Commission, under Contract No. PIR 18-003. The opinions, findings, conclusions, and recommendations expressed in this publication are those of the authors and do not necessarily reflect the view of California Energy Commission and its employees, the State of California, the Pacific Earthquake Engineering Research (PEER) Center, and the Regents of the University of California.

PREFACE

The California Energy Commission's (CEC) Energy Research and Development Division manages the Natural Gas Research and Development Program, which supports energy-related research, development, and demonstration not adequately provided by competitive and regulated markets. These natural gas research investments spur innovation in energy efficiency, renewable energy and advanced clean generation, energy-related environmental protection, energy transmission and distribution and transportation.

The Energy Research and Development Division conducts this public interest natural gas-related energy research by partnering with RD&D entities, including individuals, businesses, utilities and public and private research institutions. This program promotes greater natural gas reliability, lower costs and increases safety for Californians and is focused in these areas:

- Buildings End-Use Energy Efficiency.
- Industrial, Agriculture and Water Efficiency
- Renewable Energy and Advanced Generation
- Natural Gas Infrastructure Safety and Integrity.
- Energy-Related Environmental Research
- Natural Gas-Related Transportation.

The *Task 3 - OpenSRA Final Report* is the final report for the Performance-Based Earthquake Engineering Assessment Tool for Natural Gas Storage and Pipeline Systems project (PIR-18-003) conducted by the University of California, Berkeley. The information from this project contributes to the Energy Research and Development Division's Natural Gas Research and Development Program.

For more information about the Energy Research and Development Division, please visit the CEC's research website (www.energy.ca.gov/research/) or contact the CEC at 916-327-1551.

ABSTRACT

This report is one of a series of reports documenting the methods and findings of a multi-year, multi-disciplinary project conducted by the Pacific Earthquake Engineering Research Center (PEER) with the Lawrence Berkeley National Laboratory (LBNL) and funded by the California Energy Commission (CEC). The overall project is titled "*Performance-based Earthquake Engineering Assessment Tool for Natural Gas Storage and Pipeline Systems*" hereafter referred to as the "*OpenSRA* Project."

The overall goal of the *OpenSRA* project is to create an open-source research-based seismic risk assessment tool for natural gas infrastructure that can be used by utility stakeholders to better understand state-wide risks, prioritize mitigation, plan new gas infrastructure, and help focus post-earthquake repair work.

The project team includes researchers from LBNL, UC Berkeley, UC San Diego, University of Nevada Reno, the NHERI SimCenter at UC Berkeley, and Slate Geotechnical Consultants and its subcontractors Lettis Consultants International (LCI) and Thomas O'Rourke. Focused research to advance the seismic risk assessment tool was conducted by Task Groups, each addressing a particular area of study and expertise, and collaborating with the other Task Groups.

This report focuses on the implementation of models into *OpenSRA* and the overall development of the software. *OpenSRA* calculates the seismic risk of natural gas infrastructure by calculating the seismic demands (fault displacement, ground shaking, and ground displacement) and the component fragility (buried pipelines, wells and caprocks, and well-trees and pressure vessels).

Keywords: *OpenSRA*, open-source, software, risk framework, fragility

Zheng, Barry; Micaela Largent; Tom Clifford; Jennie Watson-Lamprey. 2023. *Performance-Based Earthquake Engineering Assessment Tool for Natural Gas Storage and Pipeline Systems, Task 3 - OpenSRA Final Report*. California Energy Commission. Publication Number: CEC-500-202X-XXX.

TABLE OF CONTENTS

LIST OF FIGURES

Page

LIST OF TABLES

Page

EXECUTIVE SUMMARY

Introduction

This report is one of a series of reports documenting the methods and findings of a multi-year, multi-disciplinary project conducted by the Pacific Earthquake Engineering Research Center (PEER) with the Lawrence Berkeley National Laboratory (LBNL) and funded by the California Energy Commission (CEC). The overall project is titled "*Performance-based Earthquake Engineering Assessment Tool for Natural Gas Storage and Pipeline Systems*" henceforth referred to as the "*OpenSRA* Project."

The overall goal of the *OpenSRA* project is to create an open-source research-based seismic risk assessment tool for natural gas infrastructure that can be used by utility stakeholders to better understand state-wide risks, prioritize mitigation, plan new gas infrastructure, and help focus post-earthquake repair work.

The project team includes researchers from LBNL, UC Berkeley, UC San Diego, University of Nevada Reno, the NHERI SimCenter at UC Berkeley, and Slate Geotechnical Consultants and its subcontractors Lettis Consultants International (LCI) and Thomas O'Rourke of Cornell University. Focused research to advance the seismic risk assessment tool was conducted by Task Groups, each addressing a particular area of study and expertise, and collaborating with the other Task Groups.

This report specifically discusses the capabilities within the *OpenSRA* software. The following will touch on the inputs needed, the user interface, assumptions made throughout the calculations, and outputs.

Project Purpose

The goal of this project is to create an open-source research-based seismic risk assessment tool for natural gas infrastructure. The following report describes the software (*OpenSRA*) in great detail. This report is not meant to be used as a manual, it is simply to describe the capabilities and components that have been implemented into the software to date. The research and models implemented are further outlined in previously submitted CEC reports.

CHAPTER 1: Introduction

This report is one of a series of reports documenting the methods and findings of a multi-year, multi-disciplinary project conducted by the Pacific Earthquake Engineering Research Center (PEER) with the Lawrence Berkeley National Laboratory (LBNL) and funded by the California Energy Commission (CEC). The overall project is titled "*Performance-based Earthquake Engineering Assessment Tool for Natural Gas Storage and Pipeline Systems*" henceforth referred to as the "*OpenSRA* Project."

The overall goal of the *OpenSRA* project is to create an open-source research-based seismic risk assessment tool for natural gas infrastructure that can be used by utility stakeholders to better understand state-wide risks, prioritize mitigation, plan new gas infrastructure, and help focus post-earthquake repair work.

The probabilistic seismic risk tool developed in this project follows the widely accepted risk methodology pioneered by Cornell (1968). A seismic source characterization is used to develop a suite of earthquake scenarios with associated rates of occurrence to represent the seismic hazard. Fault ruptures and the resulting ground deformation are generated for each earthquake scenario to represent the seismic loading, which includes a map of ground motion parameters. This scenario-based seismic parameter map is overlaid on the infrastructure system, and the seismic loading is related to the capacities of the infrastructure to calculate the seismic performance of the natural gas system for the scenario. By repeating the process for all the scenarios in the suite, the tool can evaluate the seismic risk to the system.

A user-driven research approach was used to develop *OpenSRA* to be used easily by regulators and utilities, and to include updated models and methods for the seismic demands and capacities that control the seismic risk for natural gas systems. The project includes several innovative approaches that improve the basic methodology and distinguish this project's approach from standard approaches currently used. Current risk studies developed by the utilities use risk scoring approaches that are highly subjective and qualitative. They do not incorporate properly the uncertainties in the seismic demand and in the fragility of the system and its components. Targeted research was conducted in this project to improve the characterization of uncertainty of key inputs to the seismic risk assessment tool. The seismic risk methodology employed in this project provides quantitative estimates of the probabilistic seismic risk. For risk-informed decision-making processes, the reliability of the risk estimates needs to be considered because this can be significant, particularly for large, rare earthquakes.

The project team includes researchers from LBNL, UC Berkeley, UC San Diego, the University of Nevada, Reno, the NHERI SimCenter at UC Berkeley, and Slate Geotechnical Consultants and its subcontractors Lettis Consultants International (LCI) and Thomas O'Rourke. Focused research to advance the seismic risk assessment tool was conducted by Task Groups, each addressing a particular area of study and expertise, and collaborating with the other Task Groups. The Task Groups are:

- Task A: Fault Displacement

- Task B: Liquefaction-induced deformation and seismically induced slope displacement
- Task C: Performance of natural gas storage well casings and caprock
- Task D: Performance of gas storage and pipeline system surface infrastructure
- Task E: Smart gas infrastructure sensing of wells and pipeline connections performance
- Task F: Synthesis of component fragilities into a system performance model

This report focuses on the development of the *OpenSRA* program, and the calculation framework within the software. The following outlines the calculation models and implementation workflow, assumptions made throughout, and the overall user experience.

CHAPTER 2:
Project Approach

2.1 Introduction

OpenSRA follows the Performance-Based Earthquake Engineering (PBEE) risk methodology developed by PEER (Moehle and Deierlein, 2004) to assess the seismic risk of natural gas infrastructure. To perform the calculations within *OpenSRA* in a timeframe that will be useful to the user, we have implemented Polynomial Chaos (PC). This methodology places requires clearly defined means, aleatory variabilities and epistemic uncertainties for each step of the PBEE risk methodology. This chapter describes this process as it is implemented in *OpenSRA*.

2.2 *OpenSRA*

Each stage in the PEER risk framework typically involves the evaluation of one analytical or regression model. The resulting metrics and their distributions from this evaluation are then propagated into the next stage until the probability of failure is assessed. Prior to this project, models existed in literature that fall into the earlier stages of the PEER risk framework (e.g., models that predicts system response given seismic intensity), but the knowledge for the latter stages of the framework was lacking (e.g., damage models for damage given system response and fragility models for probability of failure given damage). One of the primary goals of this research study is to perform analyses to develop new models that can be used to fill in this knowledge gap. The new models are then incorporated into *OpenSRA* and combined with the existing models described in the previously submitted CEC reports (Thompson 2021, Bain et al. 2022) to perform a more complete seismic risk assessment.

2.2.1 PEER Risk Framework

In the PEER risk framework the annual rate of exceedance of a decision variable is calculated by:

$$\lambda_{dv} = \int_{DM} \int_{EDP} \int_{IM} P\{DV > dv|dm\}\, p\{dm|edp\}\, p\{edp|im\}\, \lambda_{im} d(im) d(edp) d(dm) \qquad (2.1)$$

In the above equation, IM is the intensity measure (e.g., peak ground acceleration), EDP is the engineering demand parameter (e.g., ground deformation), DM is the damage measure (e.g., pipe strain), DV is the decision variable (e.g., rate of rupture), λ is the annual rate, the operations of $p\{y|x\}$ and $P\{Y > y|x\}$ are the conditional probability density function (PDF) and cumulative distribution function (CDF), respectively, of y given x. Given these definitions, λ_{IM} is the annual rate of occurrence of the seismic event, $p\{edp|im\}$ is the probability of a system response computed using geohazard models given the seismic demand, $p\{dm|edp\}$ is the fragility assessment given the system response, and $p\{dv|dm\}$ is the loss estimate given the damage level. The mathematical formulations for $p\{y|x\}$ and $p\{Y > y|x\}$ are given by the following equations, assuming that the random variables X and Y are both lognormally distributed:

$$p\{y|x\} = \frac{1}{\sqrt{2\pi}\sigma_Y y} e^{-\frac{\left(ln(y)-\left(\mu_Y(x)+\sigma_{\mu_Y}\xi\right)\right)^2}{2\sigma_Y^2}} \quad (2.2)$$

$$P\{Y > y|x\} = 1 - \Phi\left(\frac{ln(y) - \left(\mu_Y(x) + \sigma_{\mu_Y}\xi\right)}{\sigma_Y}\right) \quad (2.3)$$

where $\mu_Y(x)$ is the mean of Y given X=x, σ_Y is the aleatory variability, σ_{μ_Y} is the epistemic uncertainty on $\mu_Y(x)$, ξ is a standard normal random variable, and the operator Φ is the error function. Note that $\mu_Y(x)$ represents the engineering models, such as those presented in this report.

In current practice, damage to natural gas pipelines is parameterized as a function of intensity measures (Watson-Lamprey et al. 2020). These simplified fragility curves are easy to develop as they only require estimates of damage and ground shaking intensity, but they are associated with large epistemic uncertainties. By following the PBEE risk methodology, *OpenSRA* is able to incorporate recent scientific advances in our understanding of geohazards, ground response, and the influence of infrastructure characteristics into the evaluation. As additional research is performed, and our understanding continues to improve, this can be incorporated into *OpenSRA* and will lead to reductions in epistemic uncertainty and improved accuracy.

2.2.2 Efficient Evaluation of the PBEE Risk Framework

Risk calculations are typically performed using Monte-Carlo sampling, which may take hours to days to perform a large risk calculation of the type implemented in *OpenSRA*. To develop a user-friendly version of *OpenSRA* that runs in significantly less time, a numerical approximation called polynomial chaos (PC) is implemented. As discussed in Lacour and Abrahamson (2021), the triple integral for the PBEE risk framework presented in Equation (2.1) can be approximated numerically using various traditional quadrature rules (e.g., the rectangle rule or the trapezoidal rule). These numerical methods for integration can be computationally very efficient for evaluating one-dimensional integrals; however, they become exponentially more expensive in computation for evaluating multidimensional integrals.

To reduce the complexity of Equation (2.1), *OpenSRA* implements the three efficient computation methods presented in Lacour and Abrahamson (2021):

1. Simplify Equation (2.1) from a triple integral to three one-dimensional integrals.
2. Approximate the engineering models for $\mu_Y(x)$ using linear functions to compute the integration analytically and avoid numerical integration.
3. Analytically propagate the epistemic uncertainty through the integrals using PC approximation, over the traditional Monte-Carlo sampling approach.

2.2.3 Simplification of the Triple Integral to One-Dimensional Integrals

According the Lacour and Abrahamson (2021), one practical property of the PBEE risk equation is that the conditional models of IM, EDP, DM and DV are typically one-dimensional functions of these parameters (e.g., IM is used for the conditioning of the median EDP only, and not additionally for the conditioning of DM and DV). If we enforce these one-dimensional

relationships between parameters IM, EDP, DM and DV, we can rewrite the triple integral in Equation (2.1) with one-dimensional integrals:

$$\lambda_{dv} = \int_{DM} P\{DV > dv|dm\}\, d(dm) * \int_{EDP} p\{dm|edp\}\, d(edp) * \int_{IM} p\{edp|im\}\, \lambda_{im} d(im) \qquad (2.4)$$

where the first integral is performed over the domain of IM only, then a second integral is performed over the domain of EDP only, and finally a third integral is performed over the domain of DM only. This reduces the computational complexity in the integration from exponential to linear.

2.2.3.1 Analytical Integration using Linear Approximation of Models

As mentioned previously, the conditional probabilities $p\{y|x\}$ and $P\{Y > y|x\}$ in Equations (2.2) and (2.3) are functions of $\mu_Y(x)$ calculated using the damage and fragility models. When the equations for $p\{y|x\}$ and $P\{Y > y|x\}$ are substituted into the simplified PEER risk equation in Equation (2.4), this equation can be solved analytically if the models for $\mu_Y(x)$ are linear. By taking advantage of the analytical solution to calculate risk, the computation time is significantly faster compared to approximation using numerical integration. To do this, we approximate the models for $\mu_Y(x)$ that are used in the risk equation using linear functions given by the following form:

$$\mu_Y(x) \approx a_Y * \ln(x) + b_Y \qquad (2.5)$$

where a_Y and b_Y are the slope and intercept for the linear model. For the full derivation and verification of the linear approximation approach, see Lacour and Abrahamson (2021).

2.2.3.2 Polynomial Chaos Approximation for Propagation of Epistemic Uncertainty

Epistemic uncertainty is used to capture the uncertainty in the mean prediction of a parameter. According the Lacour and Abrahamson (2021), epistemic uncertainty in civil engineer problems is traditionally propagated using a brute-force Monte-Carlo sampling approach. For the simplified risk equation in Equation (2.4), this brute force method can be applied to propagate uncertainty by considering separate logic trees for the parameters IM, EDP, DM, and DV (i.e., ξ_{IM}, ξ_{EDP}, ξ_{DM}, and ξ_{DV}) and then sampling each ξ independently. However, this approach requires a large number of samples (i.e., simulations) before the results converge, which is computationally inefficient.

Lacour and Abrahamson (2021) presents PC approximation as an efficient approach to propagate epistemic uncertainty. The method approximates PDFs and CDFs as linear combinations of a set basis functions (analogous to Taylor expansion of analytical functions), which are then incorporated into the analytical solution mentioned in the previous section. The basic forms of the PC expansion for PDFs and CDFs are presented below.

$$p\{x\} \approx \sum_{i=0}^{P} c_i(x)\Psi_i[\{\xi\}] \qquad (2.6)$$

$$P\{X > x\} \approx \sum_{i=0}^{P} C_i(x)\Psi_i[\{\xi\}] \tag{2.7}$$

where c_i and C_i are the coefficients for the PC expansion, Ψ_i are the known polynomial functions (specifically the Hermite family of polynomial for approximating normal distributions), and P is the number of PC terms to use to approximate the distribution. By substituting these functions into Equation (2.4) for risk, λ_{dv} is now a direct a function of the PC coefficients, the polynomial functions, and just one set of samples for the overall epistemic uncertainty of the entire problem. The primary computation required for PC is the intermediate calculation of the PC terms, which are functions of the various σ_Y and σ_{μ_Y} for IM, EDP, DM, DV, and the linear approximation coefficients for EDP, DM, DV. This set of intermediate calculations is very fast and efficient to perform, as the PC terms are evaluated analytically. Furthermore, the polynomial functions are known mathematical functions, and the sampling of the uncertainty is performed only once during post-processing after the PC terms have been fully computed for all events. Overall, as discussed in Lacour and Abrahamson (2021), the use of PC over traditional Monte-Carlo sampling can easily improve the computation time by two to three orders of magnitude. For additional details to the application of PC to the risk framework and validation examples, please refer to the Lacour and Abrahamson PEER report.

2.2.4 *OpenSRA* Overview

Figure 2.1 to Figure 2.3 show the workflow of *OpenSRA* and how the PEER risk methodology shown in Equation (2.4) is conceptually incorporated into the seismic risk assessment of each of the three infrastructure types: below ground pipelines, wells and caprocks, and above ground subsystem components. The PEER risk methodology serves as the backbone to the *OpenSRA* risk assessment workflow. The user defines the infrastructure type that will be analyzed by *OpenSRA* and inputs their component characteristics. *OpenSRA* then steps through the PEER risk methodology as shown in the flow charts in these figures to perform the risk assessment.

Figure 2.4 shows a flow chart of the overall user process for *OpenSRA* and how the PEER risk framework is wrapped into the user experience.

As shown in Figure 2.1, the workflow for below ground pipelines utilize the full form of the triple integral given in Equation (2.4) in order to capture the influence of seismic intensity on ground deformation, the influence of ground deformation on pipe strain, and finally the influence of pipe strain on the probability of failure in the form of failure and leakage. The models to relate seismic intensity to ground deformation are based on state-of-the-art models that have been published in literature (see Bain et al. 2022). The models to relate deformation to pipe strain and pipe strain to failure are developed as part of the focus of Task B and Task F. These models are described in detail in Section 3.2 and Appendix A in Watson-Lamprey et al. (2022).

Figure 2.2 shows the workflow for wells and caprocks. For this category, Task Groups C and F developed damage models for well casings and tubings that are dependent on fault rupture deformation and ground shaking. These models are considered as two independent modes of failure for wells. Because both branches of the workflow for wells consist of only two integrals, Equation (2.4) is adjusted accordingly to reflect the workflow. For caprocks, results of the numerical study suggest that probability of leakage is not significantly dependent on the tested model parameters, hence its distribution is independent on seismic and geohazard demands, and the overall risk is a constant distribution. Please refer to Section 3.3 and Appendix B in Watson-Lamprey et al. (2022) for details to the development of these models.

Figure 2.3 shows the workflow for above ground subsystem components, specifically failure associated with wellheads and pressure vessels. Research by Task D and F resulted in models for joint rotations and strains for wellheads and moment ratios for pressure vessels, both of which are dependent on the seismic intensity (i.e., peak ground acceleration). The intensity of the strains and moment ratios are then used to inform the levels of failure associated with wellheads and pressure vessels respectively. Please refer to Section 3.4 and Appendix C in Watson-Lamprey et al. (2022) for details to the development of these models.

Figure 2.1: PEER Risk Methodology Applied to Below Ground Pipelines

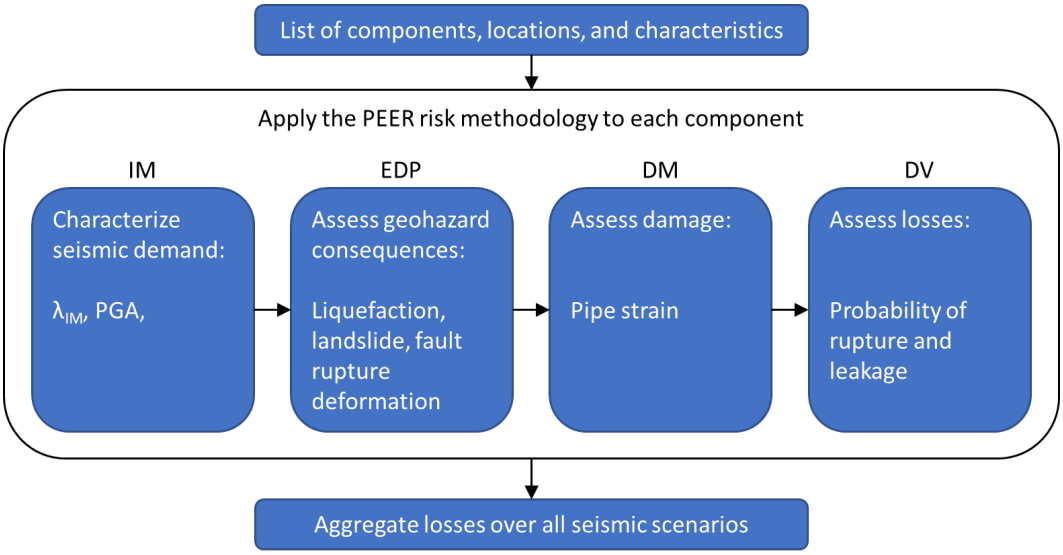
List of components, locations, and characteristics
Apply the PEER risk methodology to each component
IM
EDP
DM
DV
Characterize seismic demand:
λ_{IM}, PGA,
Assess geohazard consequences:
Liquefaction, landslide, fault rupture deformation
Assess damage:
Pipe strain
Assess losses:
Probability of rupture and leakage
Aggregate losses over all seismic scenarios

Figure 2.2: PEER Risk Methodology Applied to Wells and Caprocks

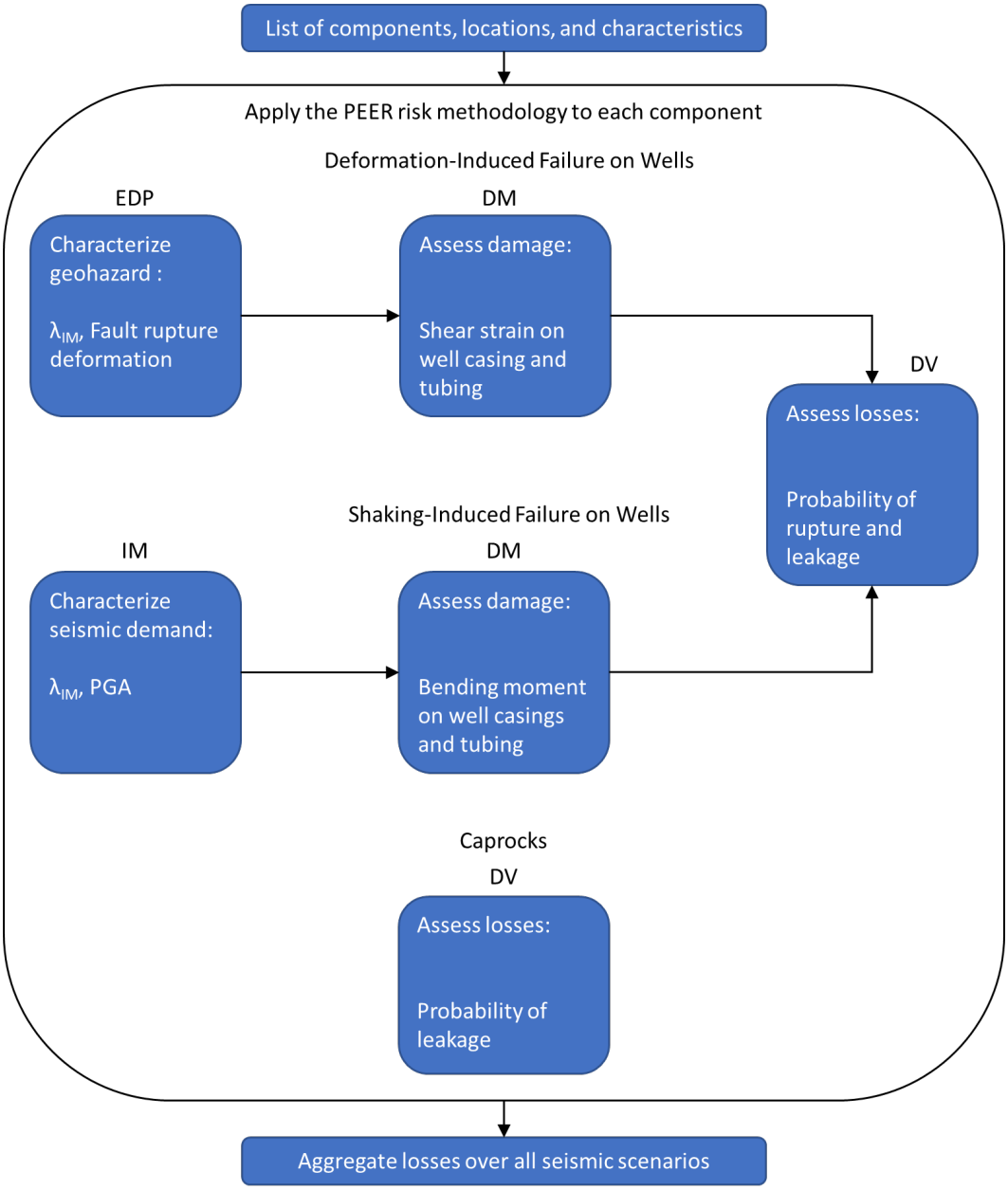

Figure 2.3: PEER Risk Methodology Applied to Above Ground Components

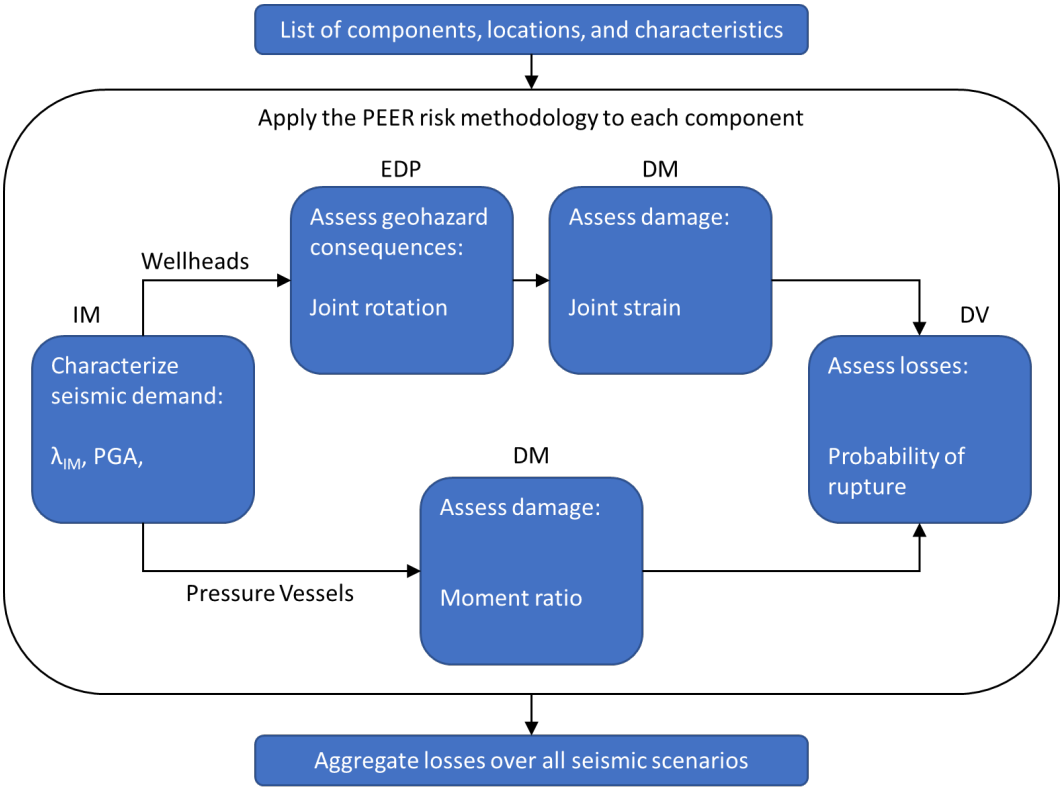

Figure 2.4: *OpenSRA* User Experience Flow Chart

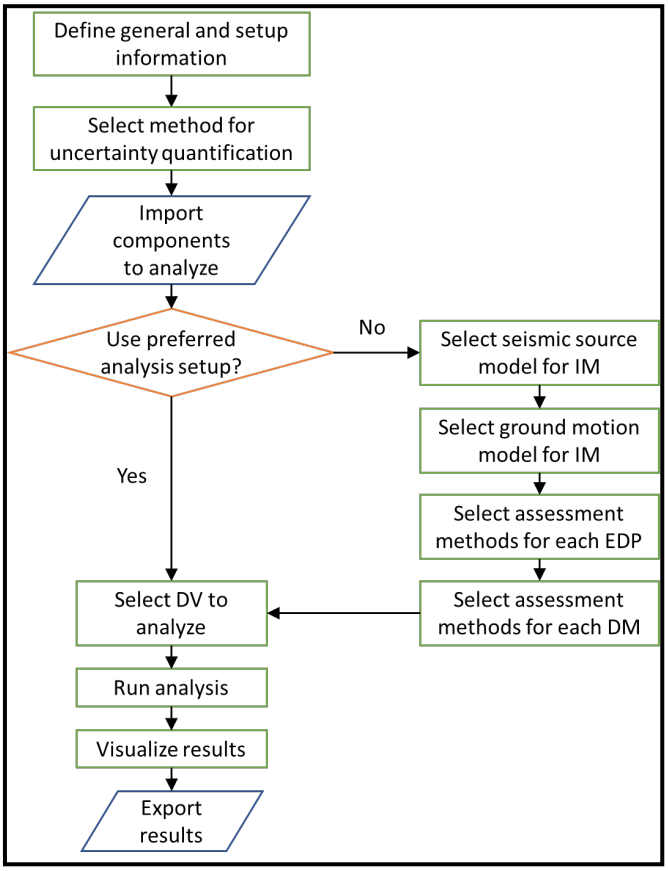

2.3 Calculating Risk in *OpenSRA*

The following subsections describe how *OpenSRA* uses Polynomial Chaos to perform efficient risk calculations.

2.3.1 Required Inputs to Run Polynomial Chaos

Required inputs to PC are determined by the number of integrals being performed. The inputs are outlined in Table 1. In Table 1 "step" refers to the current integral, μ, σ_{epi}, and σ are the mean, epistemic uncertainty, and aleatory variability of the conditioned random variable for that category (e.g., PGA for IM), and a and b are the slope and intercept used in the linear approximation of the mean of the random variable for that category (e.g., permanent ground deformation for EDP, see Equation (2.5).

Table 1: Inputs Needed for Polynomial Chaos

Number of Integrals	Integral Number	Inputs
One Integral (e.g., IM to DV, EDP to DV, DM to DV) ➢ Total of 6 inputs	Step 0	μ_0, $\sigma_{epi,0}$, σ_0
	Step 1 (first integral)	μ_1, $\sigma_{epi,1}$, σ_1
Two Integrals (e.g., IM to DM to DV) ➢ Total of 10 inputs	Step 0	μ_0, $\sigma_{epi,0}$, σ_0
	Step 1 (first integral)	a_1, b_1, $\sigma_{epi,1}$, σ_1
	Step 2 (second integral)	μ_2, $\sigma_{epi,2}$, σ_2
Three Integrals (e.g., IM to EDP to DM to DV) ➢ Total of 14 inputs	Step 0	μ_0, $\sigma_{epi,0}$, σ_0
	Step 1 (first integral)	a_1, b_1, $\sigma_{epi,1}$, σ_1
	Step 2 (second integral)	a_2, b_2, $\sigma_{epi,2}$, σ_2
	Step 3 (third integral)	μ_3, $\sigma_{epi,3}$, σ_3

2.3.2 Steps to calculate risk in *OpenSRA*

Below is the step-by-step procedure that *OpenSRA* follows to perform a risk calculation, using Polynomial Chaos, namely a DV at a given time (e.g., probability of rupture, probability of leakage). Note that each version of the risk integral shown in Table 1 is referred to as one workflow (i.e., from Step 0 to the final step).

1. Determine all possible workflows from the combinations of IM, EDP, DM, DV (e.g., one workflow could be from IM to DM to DV like the case for pressure vessels, and another workflow may be from IM to EDP to DM to DV for most of the analyses for buried pipelines).
2. Once all the workflows have been determined, retrieve all common random and fixed variables from the models/methods to be used.
3. Users decide whether to use the "preferred" distributions/values to model the random/fixed variables or use information from their own knowledge. "Preferred" refers to recommendations from the researchers.
4. For each random variable, determine which part of its distribution is provided (mean, sigma/CoV, low, high, distribution type):
    a. If any part of the distribution is not provided, infer the missing part(s) from the "preferred" distributions;
    b. If the user has specified to use their own knowledge, then depending on the source of type of input:
        i. Shapefile – find corresponding attribute at the point of intersection;
        ii. Raster – search for nearest neighbor;
        iii. Input table/shapefile – assign values in specific column;
        iv. Single value – assigned to all components;

5. Once the distributions of the random variables are fully defined, perform Latin hypercube sampling of the input random variables to generate $N_{RV\ sample}$ samples.
6. To estimate each of the inputs to polynomial chaos:
    a. Step 0:
        i. μ_0, $\sigma_{epi,0}$, and σ_0 known inputs and do not require any additional processing
    b. Step 1 to Step N-1, where N=number of integrals:
        i. Use the μ from the previous step and samples of the required input random variables for the method to generate $N_{RV\ sample}$ of the prediction of the mean for the current step
        ii. From the $N_{RV\ sample}$ of the mean prediction:
            - Calculate mean of the $N_{RV\ sample}$ predictions of mean, $\mu_{current\ step}$:

$$\mu_{current\ step} = \frac{1}{N_{RV\ sample}} \sum_{i=1}^{N_{RV\ sample}} prediction_i \tag{2.8}$$

            - Calculate $\sigma_{epi,input\ RV}$ using:

$$\sigma_{epi,input\ RV} = \sqrt{\frac{\sum_{i=1}^{N_{RV\ sample}} \left(prediction_i - \mu_{current\ step}\right)^2}{N_{RV\ sample}}} \tag{2.9}$$

            - Calculate the total σ_{epi} for current step, with $\sigma_{epibase}$ being the base uncertainty in the model/method to account for uncertainty in the model coefficients:

$$\sigma_{epi,current\ step} = \sqrt{\sigma_{epi,base}^2 + \sigma_{epi,input\ RV}^2} \tag{2.10}$$

            - Estimate the linear approximation coefficients a and b as follows, with Δ_{step} as the step size to use in forward Euler approximation of the derivative (currently, Δ_{step}=1%):

$$a_{current\ step} = \frac{f\left(\left(1 + \Delta_{step}\right) * \mu_{previous\ step}\right) - \mu_{current\ step}}{\Delta_{step}} \tag{2.11}$$

$$b_{current\ step} = \mu_{current\ step} - a_{current\ step} * \mu_{previous\ step} \tag{2.12}$$

7. Once the inputs to PC are determined for each workflow, the PC coefficients are calculated from the analytical solutions (see Lacour and Abrahamson, 2021).
    a. The default PC order is 4, which means:
        i. For one integral, there are 15 unique PC coefficients to be computed;

ii. For two integrals, there are 30 unique PC coefficients to be computed;
iii. For three integrals, there are 70 unique PC coefficients to be computed;

b. The number of unique PC coefficients is computed from a "N choose K" logic, where N is the sum of the number of integrals + 1 and the PC order, and K is the number of integrals + 1.

8. Generate $N_\xi = 1000$ realizations of the Hermite polynomials ($\Psi_i[\{\xi\}]$ in Equations (2.6) and (2.7)) to use given the number of integrals and the expansion order to use for PC approximation.
9. Sum the product of the unique PC coefficients from Step 7 with the Hermite polynomial functions from Step 8 according to Equations (2.6) and (2.7) to get N_ξ samples of DV.
10. From the N_ξ samples of DV in Step 9, sort the samples in ascending order and locate the 5th, 16th, 50th, 84th, and 95th percentile values:
    a. For $N_\xi = 1000$, this means the samples at position 51, 161, 501, 841, and 951 after sorting are chosen as the fractiles.
11. Compute the mean of the N_ξ samples of DV to get the mean of the DV.
12. If multiple seismic events are expected to be run, then the PC coefficient results from Step 7 are weighted by the annual rate of occurrence of that event and stored. Then *OpenSRA* reruns Steps 6 and 7 for the next event and add the weighted PC coefficients to those from the previous event. This process is repeated for all seismic events, after which *OpenSRA* proceeds into Step 8 through Step 11 with the weighted sum of the PC coefficients from all the events.

CHAPTER 3:
Project Results

The following chapter outlines how the fragility curves presented in the previously submitted CEC reports (Thompson 2021, Bain et al. 2022, Pantoli et al. 2022, Rutqvist et al. 2022, Watson-Lamprey et al. 2022) are implemented in *OpenSRA*. We present this implementation according to the seismic demands that are handled in *OpenSRA* (fault displacement, ground shaking, and ground movement) and the infrastructure types (buried pipelines, wells and caprocks, and well-trees and pressure vessels). To utilize the most detailed data available we subdivide the seismic demands by coverage area of the available data into four distinct levels.

3.1 Levels of Analysis

Given the vast network of pipelines and other natural gas infrastructure in California four levels were assigned to the analyses to help classify the level of detail needed.

Level 1: includes data that is geospatially continuous at a uniform resolution over the entire state of California. With its lower level of resolution and without site-specific or subsurface data, the state-wide data lead to very high uncertainty.

Level 2: includes data that is at regional scales collected at higher resolution than Level 1 data. Level 2 data are not necessarily geospatially continuous over the entire state of California. There is minimal, generic subsurface data or estimated engineering properties. Use of Level 2 data leads to high uncertainty, but less uncertainty than with Level 1 data.

Level 3: includes data that is site-specific including geologic and topographic mapping and includes subsurface data through CPTs, borings with SPT, and soil/rock index tests. Subsurface data can be used in performance-based liquefaction, lateral spreading, slope displacement, and settlement procedures. Level 3 data enable assessment with medium uncertainty.

Level 4: includes data that is high-quality laboratory test data with the Level 3 site-specific geologic, topographic, and geotechnical data. Use of Level 4 data enable the performance of advanced numerical analyses. Level 4 analyses will have the least uncertainty in estimating the effects of earthquake-induced ground deformation on buried pipes. Due to the high level of data required they will not be employed commonly. Level 4 analysis is outside the scope of *OpenSRA*.

Within *OpenSRA* these levels are handled by choice of model and data availability, and the epistemic uncertainty decreases with increasing level. The user does not specifically assign a level. The user either selects the data (i.e. specific geologic maps or site specific data) and models they would like to use or based on the data given *OpenSRA* will assign a distribution of models. For more information on the development of models and literature review on current standard of practice please see Bain et al. (2022), for the fragility curves described below see Watson-Lamprey et al. (2022).

3.2 Seismic Demands

The following section walks through the different seismic demands addressed within *OpenSRA*. These include fault displacement hazard, ground shaking, and ground displacement.

3.2.1 Fault Displacement Hazard

A report titled "Fault Displacement Hazard Characterization for *OpenSRA*" by Thompson (2021) was submitted to CEC. This section summarizes the implementation of the methods described in this CEC report. Please refer to the previously submitted report for additional details on the model.

3.2.1.1 Fault Displacement Hazard Matrix

Guidance for implementing the fault displacement hazard element to *OpenSRA* for the various levels is captured in hazard matrix table in Thompson (2021). The recommended models, inputs, and outputs are presented in Table 2.

Table 2: Fault displacement models implemented into *OpenSRA*

Level	Model	Inputs	Outputs
Level 1	Wells and Coppersmith (1994)	UCERF3-linked Q-fault scenarios including: magnitude, dip, strike, rake	Fault displacement magnitude and direction
Level 2	Petersen et al. (2011)	UCERF3-linked Q-fault scenarios including: magnitude, dip, strike, rake	Fault displacement magnitude and direction
Level 3	PFDHA models (currently under development)	Not yet available	Fault displacement magnitude and direction

3.2.1.2 Implementation of Hazard Matrix

Level 1 and 2 utilize the Quaternary faults (Q-faults) and folds database (USGS and CGS, 2006) for the fault location and the Uniform California Earthquake Rupture Forecast, Version 3 (UCERF3, Field et al., 2013) for the rupture scenario (magnitude and geometry). UCERF3 is a recent and comprehensive model of seismic sources that includes buried faults and multiple models to accommodate those faults that are widely recognized to exist but lack the geologic and seismic expression to define a single, specific fault plane. For the purposes of this project the 3.1 model was used (herein referred to as UCERF3.1).

Fault Shear through Buried Pipeline

The fault mapping and predicting pipeline crossing algorithm for Levels 1 and 2 uses Q-faults to map fault location while continuing to utilize UCERF3.1 for the rupture geometry (strike, dip, rake) and magnitude. A 100-meter buffer around the Q-fault traces defines the fault polygon and the nearest UCERF3 fault defines the rupture attributes. Figure 3.1 depicts the Q-fault locations along with pipeline crossings (shown with stars). Figure 3.2 shows both the primary and secondary fault zones developed by Thompson (2021). The pipeline shapefile is divided into straight, 100-meter segments in order to track the specific segments that cross fault zones.

Rupture displacement is estimated using the methodology of Petersen et al. (2011), which calculates displacement as a function of earthquake magnitude and the pipe crossing's location relative to the total rupture length scenario (this is based on the observation that faults rupture more in the center of the trace that at the ends). The net displacement vector direction is calculated based on its orientation from the mean strike, dip, and rake values from UCERF3.1. *OpenSRA* then splits the net displacement vector into components for horizontal along-strike slip, horizontal dip direction slip (following the right-hand rule), and vertical slip. Each component has a displacement magnitude and the horizontal components have a slip direction (clockwise from north, 0-360°). The rupture parameters indicate the motion of the hanging wall block by convention, so the pipeline segment is also vectorized to be pointing towards the hanging wall. The algorithm then calculates the pipe crossing angle, β, as the angle between the horizontal slip vectors and the pipeline vector. β is then the primary input value for the strain fragility models of Bain et al. (2022) and Hutabarat et al. (2022) discussed later in Section 3.3.1.

Figure 3.1: Intersections of Natural Gas Pipelines in California with Fault Traces from the U.S. Quaternary Fault and Fold Database (2019 edition)

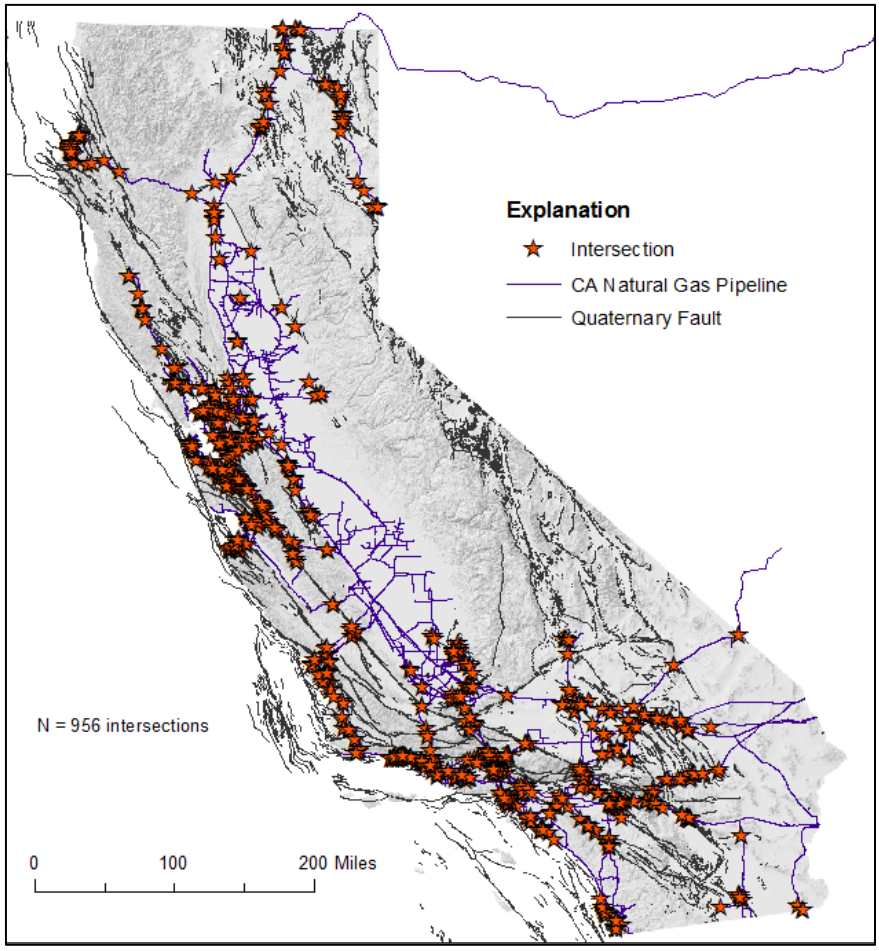

Map of California showing natural gas pipelines (in blue) and fault traces from the U.S. Quaternary Fault and Fold Database (in gray). The 956 intersections of these two linear datasets are indicated by red stars.

Sources: Pipeline database from CEC. Fault source traces from USGS and CGS (2006).

Figure 3.2: Level 2 Primary and Secondary Fault Hazard Zones and California Pipelines in the San Francisco Bay Area

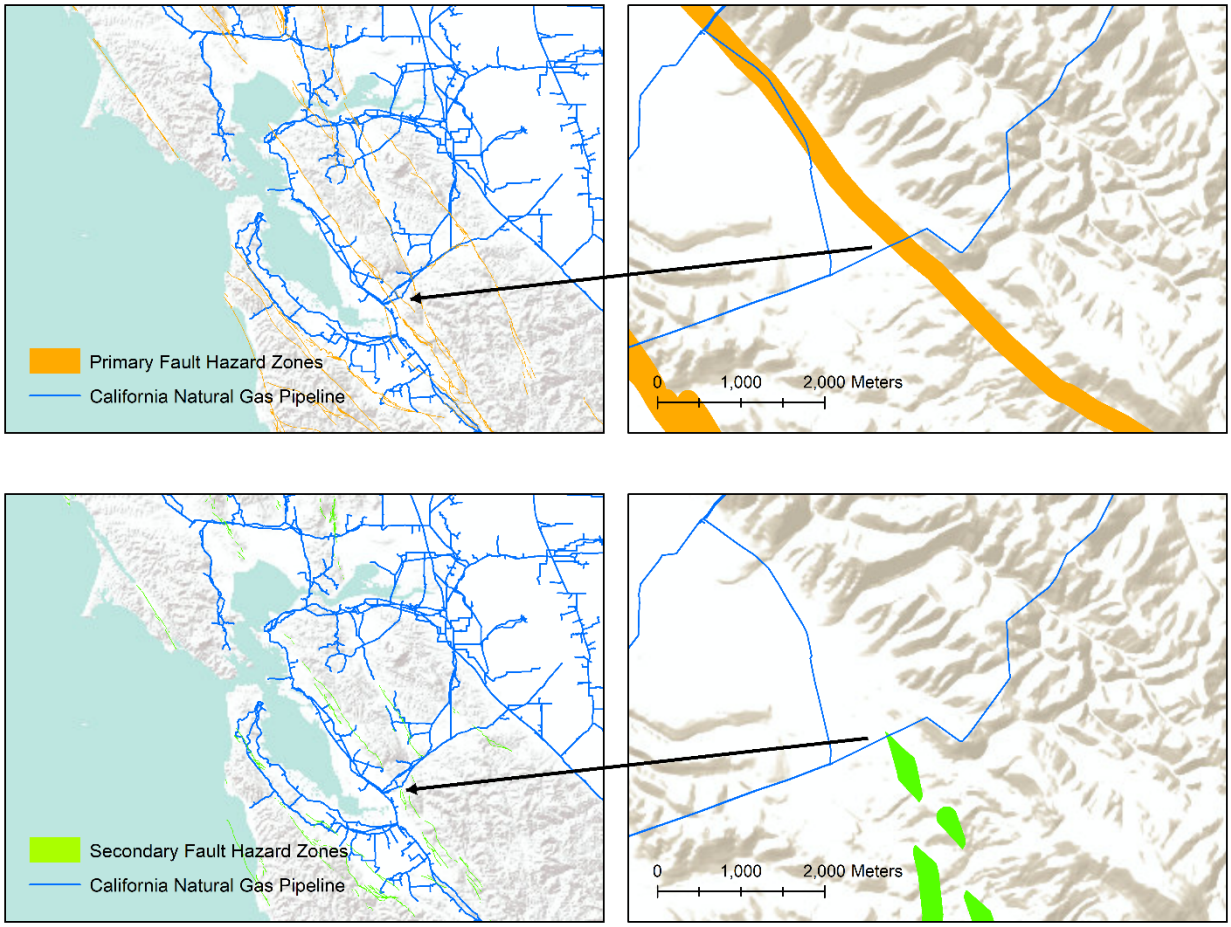

Primary (orange) and Secondary (green) fault hazard zones. Right side figures show examples of pipeline-fault zone intersections.

Sources: Pipeline database from CEC. Fault source zones developed by Thompson (2021).

Fault shear Through a Well

Similar to the pipe crossing implementation workflow for buried pipelines, fault shear is only a problem on wells if the fault plane crosses the wells. Below is the implementation workflow to determine well crossing, assuming that (1) wells and fault planes both three-dimensional objects, and (2) the trace to define 3D orientation of the well is provided (at the minimum the top and bottom node of a well).

1. Represent the finite fault plane with the equation for an infinite plane ($Ax + By + Cz + D = 0$).
2. Loop through the list of well trace.
    a. For each pair of consecutive well traces, create a 3D vector using the pair of trace.
    b. Determine the intersection between the trace vector and the infinite plane.

c. Check if the intersection:
    i. Lies within the two traces that defines the well segment vector.
    ii. Lies on the finite fault plane.
d. If both conditions are true in Step C, then the current well crosses the fault plane and the program exits the loop for Step 2; otherwise continue the loop with the next well segment

3. Repeat Steps 1 and 2 for all fault planes in the Q-fault database.

3.2.2 Ground Shaking

The ground shaking at a site is estimated by performing a probabilistic seismic hazard analysis (PSHA) using a combination of UCERF3 scenarios and ground motion prediction equations (GMPEs) presented in the Next Generation Attenuation Relationships for Western US (NGA-West2) Project.

The PSHA is performed in a preprocessing step that follows the approach first developed by Cornell (1968) with the inclusion of parameters for randomization and the consideration of epistemic uncertainty.

A Poisson process is used to compute the frequency that a specified level of ground motion will be exceeded at a site. The PSHA computes the annual number of events that produce a ground motion parameter, Z, that exceeds a specified level, z. This number of events per year, ν, is also called the "annual frequency of exceedance," the inverse of which is called the "return period."

The calculation of the annual frequency of exceedance, ν, considers the rate of earthquakes of magnitudes 5 or greater, the rupture dimension of the earthquakes, the distance of the site relative to the earthquake, and the attenuation of the ground motion from the earthquake rupture to the site. The annual rate of exceedance of a ground motion test value, z, from a source, *i*, for a given earthquake that occurred on the source, *i*, is given by the equation:

$$\nu_i(Z > z) = N_i(E_i)P(Z > z|E_i)$$

where:

E_i is the given earthquake from source *i*, with a known magnitude and distance; and

$N_i(E_i)$ is the annual rate of the given earthquake per year from source *i*

The seismic hazard (and therefore predicted ground motion) is calculated within *OpenSRA*. Similar to the fault displacement hazard, the rupture scenarios are determined using UCERF3.1. Running the entire list of rupture scenarios within *OpenSRA* would require a long computing time as it is comprised of 253,394 rupture scenarios. For the purposes of this hazard, the UCERF3.1 scenarios were reduced to 1194 scenarios with a magnitude step size 0.5. Additional information about the reduced list of rupture scenarios can be found in Lacour and Abrahamson (2022).

The ground motion is characterized by using a suite of four ground motion prediction equations (GMPEs) from NGA-West2. The NGA-West2 models were developed as part of a multi-year effort to improve attenuation models for active tectonic regions such as California. This project addressed important issues such as: modeling of directionality, verification for

recent small, moderate and large magnitude events, and evaluation of soil amplification factors.

The GMPEs selected for this analysis were Abrahamson et al. (2014), Boore et al. (2014), Campbell and Bozorgnia (2014) and Chiou and Youngs (2014). The GMPEs were given equal weight. The NGA-West2 models use the average shear wave over the top thirty meters (V_{S30}) as an index of site response. Basin response is included in the model by the depth to a shear wave velocity of 1,000 m/s ($Z_{1.0}$) and 2,500 m/s ($Z_{2.5}$). These shear wave velocity parameters are predicted using various sources using the mapped values already implemented into OpenSHA (Field et al. 2003). *OpenSRA* then uses a latitude and longitude grid of California, finds the closest node to the analysis, and pulls the parameters from the estimated values with the priority listed below. In summary the preprocessing that is implemented into *OpenSRA* is as follows:

1. For all components, filter out scenarios that are >200 km from source
2. Using UCERF3.1 predict ruptures within 200 km
3. Estimate V_{s30}, $Z_{1.0}$ and $Z_{2.5}$, where the default values were retrieved from OpenSHA (Field et al. 2003) by:
    a. Discretized the California state boundary into grid nodes spaced at 0.01 degrees;
    b. Used OpenSHA to obtain the "best" estimate based on its internally assigned priority of the datasets.
    c. Priority for sources for V_{s30}:
        i. CGS/Wills V_{s30} Map (2015)
        ii. Thompson V_{s30} Map (2018)
        iii. CGS/Wills Site Classification Map (2006)
        iv. Global V_{s30} from Topographic Slope (Wald & Allen 2007)
    d. Priority for sources for $Z_{1.0}$ and $Z_{2.5}$ (for reference to these maps, refer to OpenSHA in Field et al. 2003):
        i. SCEC Community Velocity Model Version 4, Iteration 26, Basin Depth
        ii. SCEC CCA, Iteration 6, Basin Depth
        iii. SCEC Community Velocity Model Version 4 Basin Depth
        iv. SCEC/Harvard Community Velocity Model Version 11.9.x Basin Depth
        v. SCEC CCA, Iteration 6, Basin Depth
        vi. USGS Bay Area Velocity Model Release 8.3.0
4. Calculate ground motion at different periods by performing a PSHA using equally weighted NGA-West2 GMPEs

Ground motions can also be predicted directly by using ShakeMaps online (Wald et al. 2005). *OpenSRA* is able to calculate the closest point of ground shaking (from ShakeMaps) to wherever the analysis bounds are. Finally, users can also perform a deterministic scenario by defining a simple fault and using the same weighted NGA-West2 Models (see above).

3.2.3 Ground Displacement

The following section discusses the models implemented into *OpenSRA* regarding ground displacement hazard. The hazards include liquefaction, liquefaction induced settlement, lateral spreading, and seismic-induced landsliding. Each of the hazard models uses a ground motion metric (PGA or PGV), moment magnitude (from UCERF3.1), and mapped values of surficial geology and groundwater level. The default values for these models can be found in Appendix A.

The list of inputs used across the different ground displacement models are presented in Table 3. For Levels 1 and 2, the models include inputs from mapped values (such as geologic unit or V_{s30}), these maps can be found in Appendix A.

Table 3: Parameters used in the ground displacement models

Parameter	Description
PGA	peak ground acceleration (g)
PGV	peak ground velocity (cm/s, ft/sec)
M_w	moment magnitude
V_{s30}	time-weighted average shear wave velocity in the top 30 meters (m/s, ft/s)
Precipitation	mean annual precipitation (cm/in)
D_c	distance to nearest coast (km/miles)
D_r	distance to nearest river (km/miles)
D_w	distance to nearest waterbody (km/miles)
GWT	groundwater table depth (m/ft)
SPT	standard penetration test
CPT	Cone penetration test
Geologic Maps	Statewide for Level 1 (e.g., Wills et al. 2015) and surficial Quaternary maps for Level 2 (e.g., Witter et al. 2006, and Bedrossian et al. 2006)
γ	Soil unit weight (kPa/pcf)
ϕ	Soil friction angle (degree)
c	Soil cohesion
c_r	Root cohesion
t	Thickness of slope parallel to ground surface (m/ft)
Topographic slope	Slope in degrees
Free-face ratio	V:H ratio at a free-face

3.2.3.1 Liquefaction

Table 4 outlines the models for liquefaction implemented into *OpenSRA*, the parameters needed, and outputs

Table 4: Liquefaction models implemented into *OpenSRA*

Level	Model	Inputs	Model
Level 1	Zhu et al 2017	PGV, V_{s30}, precipitation, D_c, D_r, D_w, GWT	Probability of liquefaction
Level 2	Youd and Perkins (1978) with Hazus (FEMA, 2020)	Surficial Quaternary geologic maps, PGA, M_w, GWT	Liquefaction susceptibility converted to probability of liquefaction
	Model under development by Task Group B	Surficial Quaternary geologic maps, PGA, M_w, GWT	Probabilistic assessment of liquefaction triggering and lateral spread displacement
Level 3	Boulanger and Idriss (2016)	CPT, PGA, M_w, GWT	Probability of liquefaction
	Probabilistic Modification to Robertson and Wride (1998) updated as Robertson (2009) from Ku et al. (2012)	CPT, PGA, M_w, GWT	Probability of liquefaction
	Moss et al. (2006)	CPT, PGA, M_w, GWT	Probability of liquefaction

3.2.3.2 Liquefaction Induced Settlement

Table 5 outlines the models for liquefaction induced settlement models implemented into *OpenSRA*, the parameters needed, and outputs.

Table 5: Liquefaction induced settlement models implemented into *OpenSRA*

Level	Model	Inputs	Model
Level 1	Zhu et al (2017) combined with Hazus (FEMA, 2020)	PGV, V_{s30}, precipitation, D_c, D_r, D_w, GWT	Liquefaction Susceptibility Class Converted to Settlement Estimate
Level 2	Zhu et al (2017) with Hazus (FEMA, 2020)	PGV, V_{s30}, precipitation, D_c, D_r, D_w, GWT	Liquefaction Susceptibility Class Converted to Settlement Estimate
	Youd and Perkins (1978) with Hazus (FEMA, 2020)	Surficial Quaternary geologic maps, PGA, M_w, GWT	Liquefaction-induced settlement according to liquefaction susceptibility category
Level 3	Cetin et al. (2009)	SPT, GPA, Mw, GWT	Free-field, level-ground settlement
	Zhang et al. (2002)	CPT, PGA, Mw, GWT	Free-field, level-ground settlement

3.2.3.3 Lateral Spreading

Table 6 outlines the models for lateral spread models implemented into *OpenSRA*, the parameters needed, and outputs.

Table 6: Lateral spread models implemented into *OpenSRA*

Level	Model	Inputs	Outputs
Level 1	Zhu et al. (2017) with Hazus (2020) (FEMA, 2020)	PGV, V_{s30}, precipitation, D_c, D_r, D_w, GWT	Liquefaction susceptibility class converted to settlement estimate
Level 2	Youd and Perkins (1978) with Hazus (FEMA, 2020)	Surficial Quaternary geologic maps, PGA, M_w, GWT	Liquefaction susceptibility converted to lateral spread displacement
	Proposed model presented in Bain et al. (2022)	Surficial Quaternary geologic maps, PGA, M_w, GWT	Probabilistic assessment of liquefaction triggering and lateral spread displacement
Level 3	Zhang et al. (2004)	CPT, PGA, M_w, GWT, topographic slope or free-face ratio	Estimate of lateral spread displacement
	Idriss & Boulanger (2008) combined with Zhang et al. (2004)	CPT or SPT	Estimate of lateral spreading displacement

3.2.3.4 Landsliding

Table 7 outlines the models for landslide models implemented into *OpenSRA*, the parameters needed, and outputs.

Table 7: Seismic-induced Landslide models implemented into *OpenSRA*

Level	Model	Inputs	Outputs
Level 1	Infinite slope analysis using strength distributions presented in Table B.15 in Bain et al. (2022)	Statewide Geologic Map	Estimate of Seismic Slope Displacement
Level 2	Grant et al. (2016)	topographic slope, ϕ, γ, c, c_r, t, PGA	Model predicts the type of slope movement (rock-slope failures, disrupted soil slides, coherent rotational slides, and lateral spreads) and estimates seismic slope displacement distribution
	Bray & Macedo (2019)	topographic slope, ϕ, γ, c, t, PGA, M_w	Seismic Slope Displacement Distribution
Level 3	Zhang et al. (2004)	CPT, PGA, M_w, GWT, topographic slope or free-face ratio	Estimate of lateral spread displacement
	Idriss & Boulanger (2008) combined with Zhang et al. (2004)	CPT or SPT	Estimate of lateral spreading displacement

3.3 Fragility of Natural Gas Infrastructure

The following section outlines the implementation procedure for each natural gas component addressed within *OpenSRA*. These procedures are presented as a fragility implementation workflow with accompanying implementation tables. For information regarding the specific fragility models see the previously submitted CEC reports (Thompson 2021, Bain et al. 2022, Pantoli et al. 2022, Rutqvist et al. 2022, Watson-Lamprey et al. 2022).

3.3.1 Buried Pipelines

Using the information from Section 3.1 and Section 3.2, the probability of ground movement is used to predict the probability of rupture and leakage given tensile and compressive strains using the fragility models presented in Watson-Lamprey et al. (2022).

3.3.1.1 Tensile and Compressive Strain Damage Models

The numerical modeling in this study analyzed abrupt ground movements. Abrupt ("knife-edge") ground movements result in locally higher strain concentrations compared to distributed ground movements, which were not studied. The assumption of knife-edge ground movements is appropriate for many practical cases, and it introduces a moderately conservative bias to the pipe strain fragility models for the cases involving distributed ground movements.

Pure strike-slip tension, pure strike-slip compression, pure normal-slip, and pure reverse-slip modes of ground deformation were analyzed using Abaqus for the *OpenSRA* Project. Although each of these modes of ground deformation can have an oblique component of movement, such deformation was not evaluated. A fifth mode of ground deformation where a pipeline crosses a ground deformation zone that displaces parallel to the longitudinal pipeline axis and places the pipeline in pure tension at the landslide or lateral spread scarp and pure compression at the landslide or lateral spread toe without induced bending strains was analyzed using an analytical model presented by O'Rourke & Liu (2012).

Figure 3.3 summarizes the ground deformation modes assessed for the *OpenSRA* Project. The strike-slip tension (Figure 3.3a), strike-slip compression, (Figure 3.3b), normal-slip (Figure 3.3c), and reverse-slip (Figure 3.3d) modes of ground deformation were assessed using Abaqus with input parameters provided by Jung et al. (2016) and O'Rourke et al. (2014, 2016). An intermediate "bending" model for the strike-slip and normal-slip modes of ground deformation was employed to transition from ground deformation that induces tension to deformation that induces compression. Movement parallel to the pipeline axis without induced bending strains (similar to Figure 3.3e) was assessed using an analytical model presented in O'Rourke & Liu (2012). Two-dimensional views of abrupt soil deformation are shown in Figure 3.3a and Figure 3.3b, whereas three-dimensional views of same are shown in Figure 3.3c through Figure 3.3f.

Figure 3.3: Assessed Ground Deformation Modes

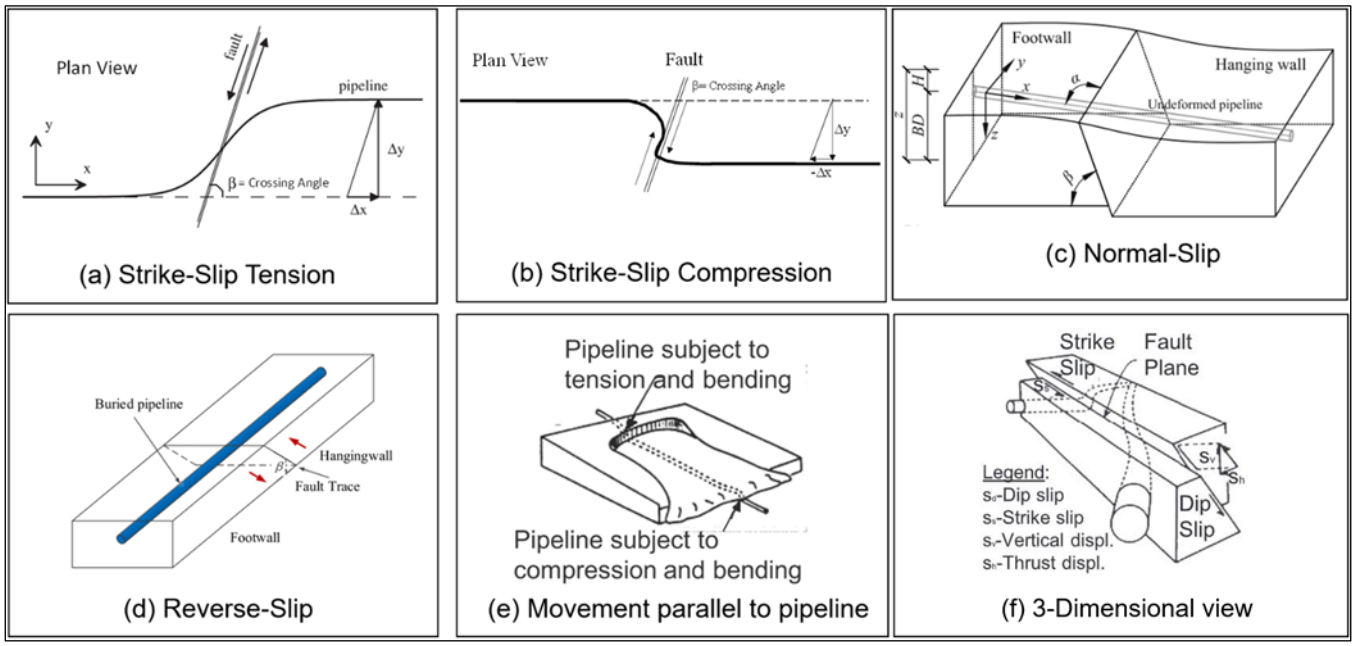

Ground deformation modes assessed to derive pipe strain fragility models

Pipelines that cross landslides or lateral spreads parallel to the direction of displacement can be reasonably modeled using the normal-slip mode at the scarp and reverse-slip mode at the toe or as the fifth case of ground deformation where no bending strains are induced. Pipelines that cross landslides or lateral spreads perpendicular or at an oblique angle can be modeled as the strike-slip tension or strike-slip compression ground deformation mode where the pipe transitions from moving, unstable soil to stationary, stable soil. Ground settlement can be modeled as vertical normal-slip deformation.

The logic tree for model selection with each of the geohazards (fault rupture, landslide, lateral spread, settlement) is presented in APPENDIX B:. Details of the models can be found in Appendix A of the System Wide Response and Fragility Report (Watson-Lamprey et al. 2022).For buried pipelines, the Task Group recommends to separately calculate the probabilities of failure for tension and compression, as the metrics μ_{mean}, σ_{epi}, and σ, may be quite different between the two modes of failures to be combined into one model for failure.

3.3.1.2 Tensile Strain Failure Model

Figure 3.4 presents the suggested lognormal cumulative distribution functions (CDFs) for these damage state fragility functions assuming a constant aleatory variability, σ=0.30, for both leakage and rupture, which was estimated using expert opinion (Abrahamson, 2022). The 10th and 90th percentiles are presented for the fragility functions assuming constant epistemic uncertainty, σ_{epi}=0.20, for both leakage and rupture, a common assumption for structural systems. σ represents the aleatory variability in the fragility models due to inherent randomness in the loading conditions (e.g., eccentricities in the pipe alignment, nonuniform backfill soil conditions) and pipe properties (e.g., post-yield stress-strain behavior, weld quality, corrosion). σ_{epi} represents the epistemic uncertainty in the mean or median value (i.e., uncertainty resulting from whether the suggested models are the correct models).

Figure 3.4: Tensile Damage State Fragility Model

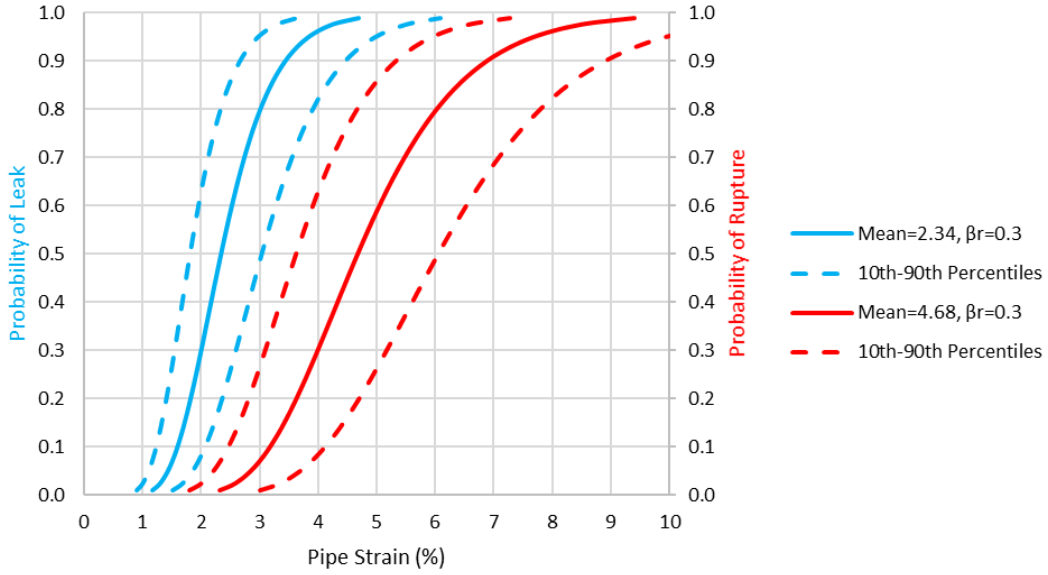

3.3.1.3 Compressive Strain Failure Model

To account for greater uncertainty associated with field conditions, the aleatory variability, σ, is increased from 0.407 to 0.50, as explained in Appendix D in Bain et al. (2022).

Pipelines can often sustain more axial strain after the initiation of buckling or pipe wall wrinkling before pipe wall tearing or rupturing occurs. The probability of compressive rupture (due to buckling or pipe wall wrinkling) fragility function accounts for this additional capacity by shifting the 50% probability of exceedance values in the original fragility function up to the 20% probability of exceedance level in the final function, as explained in Appendix D in Bain et al. (2022).

Additional details of the pipeline fragility models are provided in Appendix D in Bain et al. (2022). Below is the equation for probability of compressive rupture, along with the supplementary equations. Figure 3.5 plots the 10th, median (50th), and 90th percentiles of the probability of compressive rupture for a number of D/t ratios.

Figure 3.5: Probability of Compressive Rupture for Select D/t Ratios

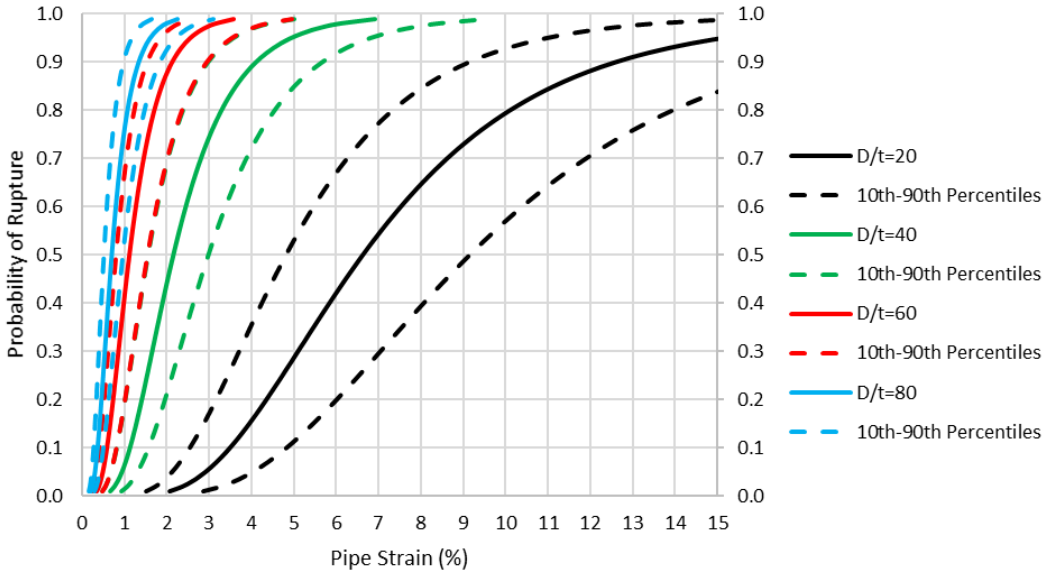

3.3.1.4 Preprocessing for Buried Pipelines for Pipe Strain Calculation

While the above sections describe the methodology for estimating the mean pipe strains, this section discusses the preprocessing steps regarding the locations where pipe strains occur (i.e., pipe crossings), as these are the only locations where the methods will be applied. This is done as a preprocessing phase in *OpenSRA*, where:

1. Pipelines are discretized into segments less than or equal to 100 meters.
2. Using polygons of known deformation pattern (e.g., California's landslide inventory, CGS, 2016), the horizontal slip direction (i.e., slip azimuth) is determined from comparing all elevations along the boundary of the polygon and finding the direction of maximum downhill slope.
3. The pipe crossing analysis begins with finding intersections of 100-meter pipeline segments and the deformation zone polygons, similar to the fault rupture analysis described in Section 3.2.1. However, only the segments that directly intersect the boundary of the deformation zone are considered. This is because pipe strain is a result of differential deformation, and only segments at the crossings experience differential deformation; segments fully within or outside the deformation zones are assumed to experience uniform deformation.
4. The pipe crossing angle is calculated from the angle between the pipe vector (a vector parallel to the pipe segment pointing into the deformation polygon) and the horizontal slip azimuth. The vertical angle of slip is currently not considered within *OpenSRA* and the default value of 75 degrees is used while more study is performed to develop the algorithm.
5. *OpenSRA* then checks the anchorage length of the intersection, where the anchorage length is defined as the distance to location where pipeline is fixed in location (such as a significant bend). The algorithm first sets the anchorage length for each intersection to a default value (30 meters). Then the algorithm looks at the first 30 meters of the segment (within the landslide zone) to identify any bends in the pipeline. If the bend angle is greater than 40 degrees, the algorithm then sets the anchorage length to be

the distance between the zone intersection and the vertex of the bend. Finally, if the subsection of the pipe that crosses the deformation zone is less than 30 meters, the anchorage length is reduced to that distance. If the pipeline crosses the deformation zone in less than 30 meters, the anchorage length is reduced to the total crossing distance.

6. The algorithm outputs the 100-meter pipe segment file with additional columns for pipe crossing angle, strike, dip, slip azimuth, and anchorage length, which are used in the pipe strain methodology.

3.3.2 Wells and Caprocks

Using the information in Section 3.1 and Section 3.2 the probability of failure for wells and caprocks is calculated within the *OpenSRA* framework.

The implementation workflow of determining the well mode to use given casing and tubing sizes for wells is shown in Figure 3.6. This is utilized in *OpenSRA* to determine the fragility curves to use (further described below).

Figure 3.6: Implementation Workflow for Determining Well Mode based on Tubing and Casing Sizes

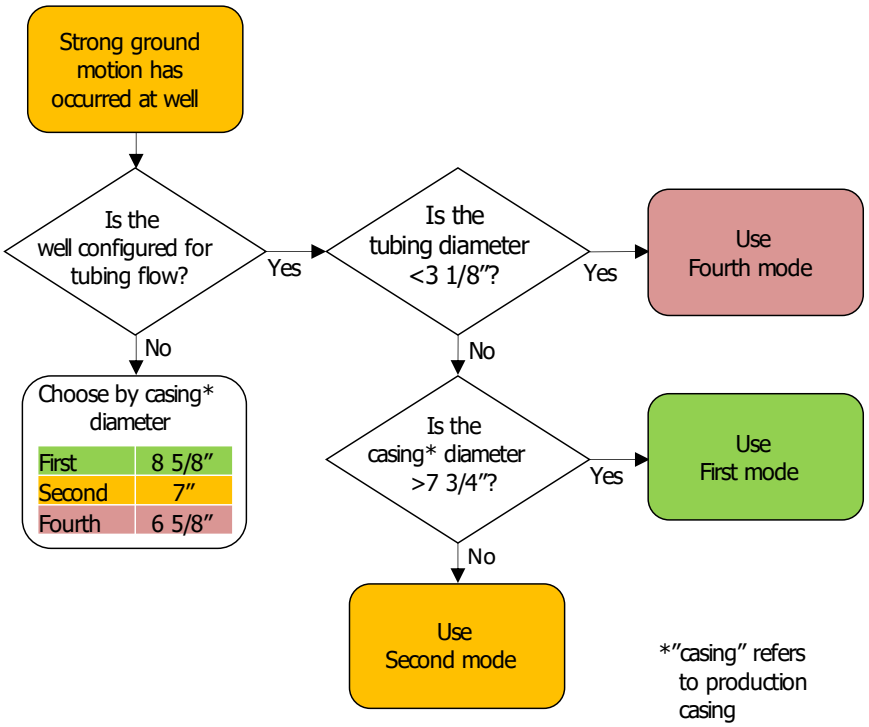

The damage model is used to estimate the range of the damage state that results from the geohazard, and then the fragility model is used to estimate the probabilities of failure. Sections 3.3.2.1 and 3.3.2.2 provide the methodology to determine the distribution of the probability of failure for wells given fault shear and ground shaking hazards. Once the probability of failure has been determined, the probability of leakage for wells can be determined following the implementation workflow in Figure 3.7. For fault shear, if the well is configured for casing flow, the leakage probability is equal to the casing failure probability. If

the well is configured for tubing-only flow, the leakage probability is equal to the tubing failure probability. The latter is because the casing failure probability is always greater than the tubing failure probability, given failure occurs progressively from the outermost well element inward as shearing progresses.

Figure 3.7: Implementation Workflow for Probability of Leakage for Wells Subject to Shaking Induced Failure

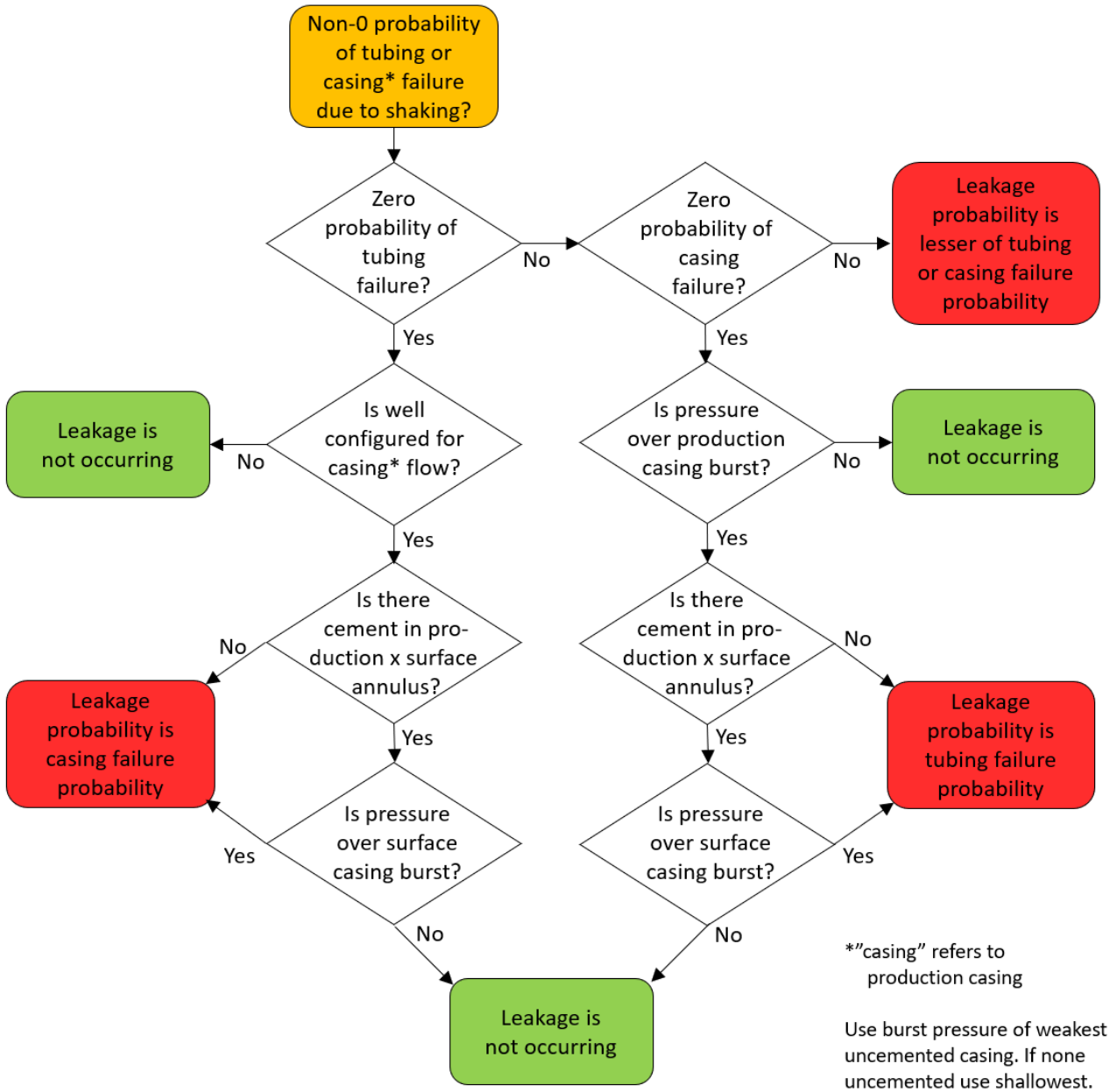

3.3.2.1 Fault Shear Induced Failure on Wells

Once the well crossings have been determined, then the wells that contain crossings will be subject to the analysis to determine the probability of failure using the damage and failure models described in Watson-Lamprey et al. (2022). The probability of failure given fault-displacement induced shear strain is presented in Figure 3.8 below.

Figure 3.8: Probability of Failure for Well Casing and Tubing due to Fault Offset

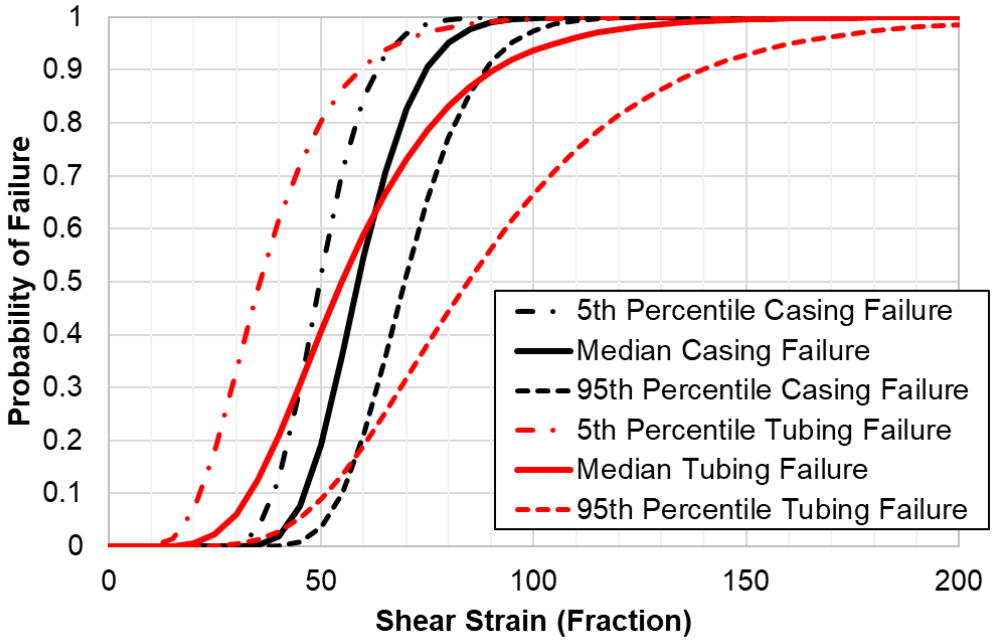

3.3.2.2 Shaking Induced Failure on Wells

Unlike fault displacement induced damage on wells presented in the previous section, there is no crossing implementation workflow associated with ground shaking induced damage on wells. All wells provided will be analyzed for shaking induced failure.

The probability of ground shaking induced failure is plotted in Figure 3.9 through Figure 3.12 for the conductor casing, production casing, surface casing, and well tubings. The median plastic moment at which 50% probability of failure occurs is compiled and estimated by the Task C researchers.

Figure 3.9: Probability of Failure for Conductor Casing due to Ground Shaking

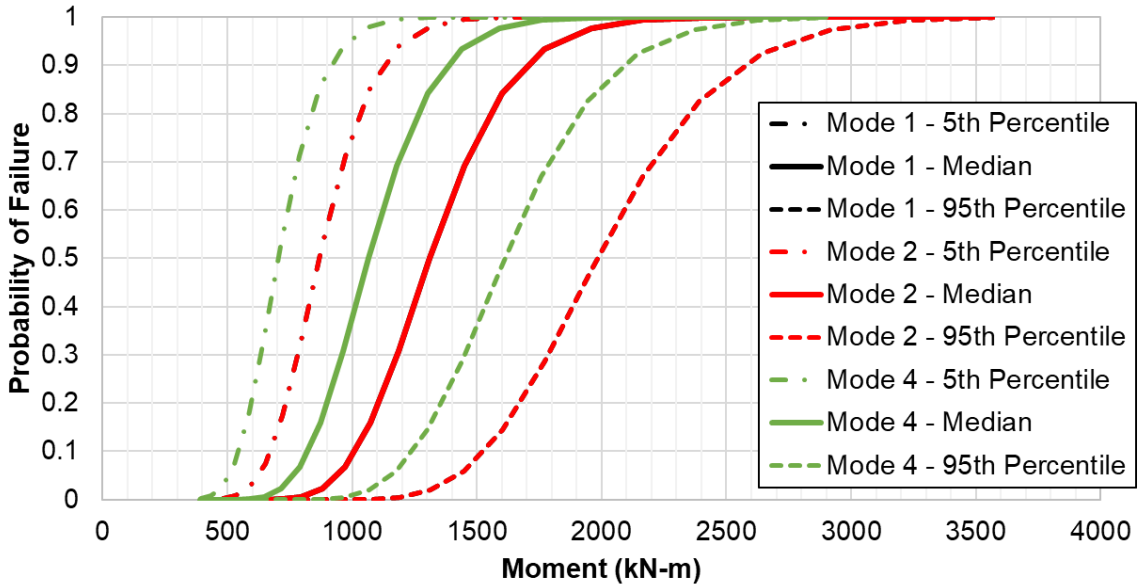

Figure 3.10: Probability of Failure for Surface Casing due to Ground Shaking

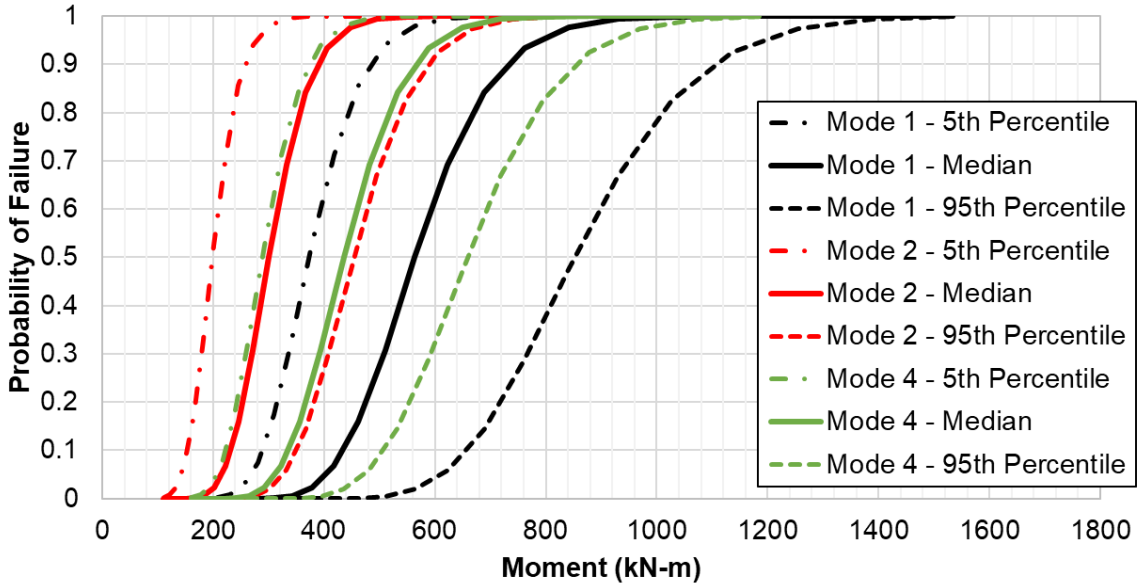

Figure 3.11: Probability of Failure for Production Casing due to Ground Shaking

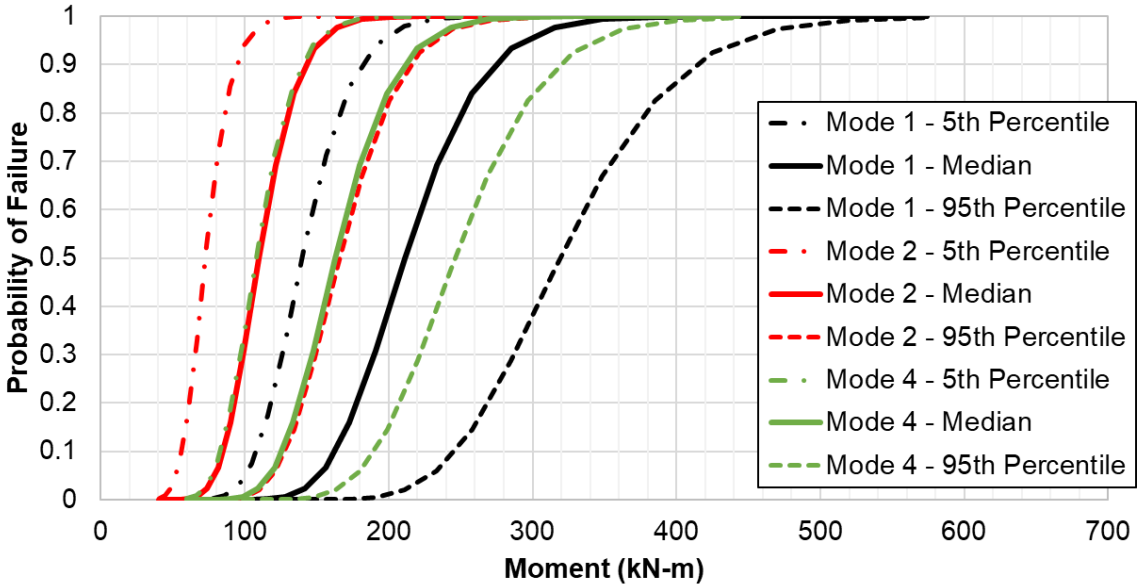

Figure 3.12: Probability of Failure for Tubing due to Ground Shaking

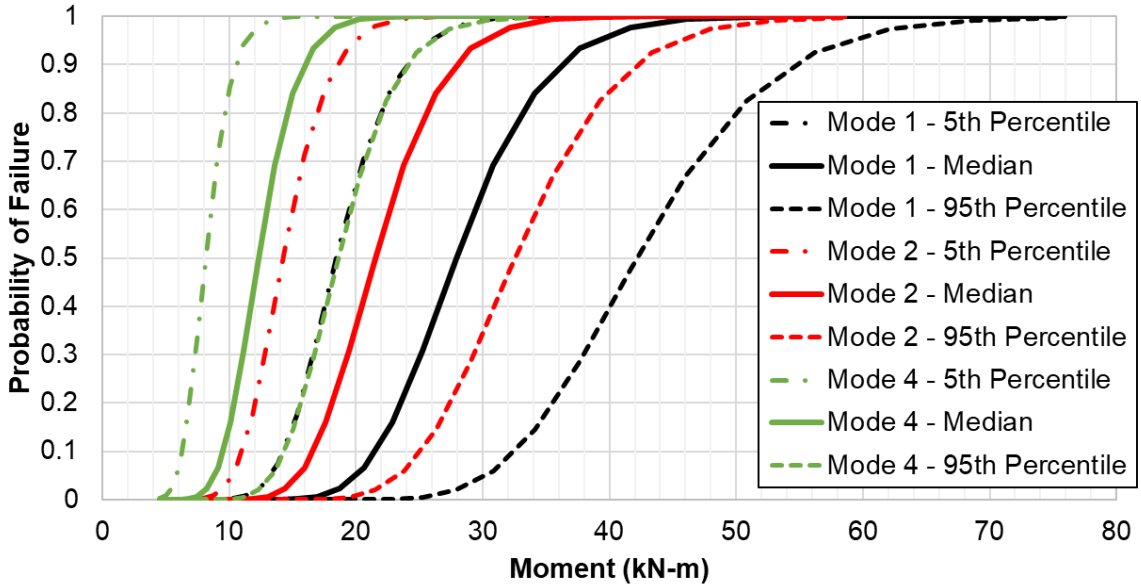

3.3.2.3 Fault Shear Induced Failure on Caprocks

Caprocks are currently assumed to be horizontal planes. The implementation workflow for caprocks crossing faults is simply:

1. Determine the trace of the fault at the elevation of caprock.
2. If the fault trace at this elevation intersects the caprock, then caprock crossings exist.

If caprock crossing exists, then the average probability of leakage for caprocks is 8.9%, with σ_{epi} of 0.86%

3.3.3 Above Ground Infrastructure

The following section outlines the implementation of above ground infrastructure fragility curves into *OpenSRA* for well-tree configurations and pressure vessels. The models for failure of above ground components are dependent on ground shaking. As seismic hazards are distributed over an area, all above ground components that are within 200 km of each fault trace will be evaluated for ground shaking induced failure.

3.3.3.1 Well tree

As described in Watson-Lamprey et al. (2022), methodologies for probability of failure provided for well trees that fall into one of the six cases presented in Table 8:

Table 8: Available Subsystem-Component Combinations

Conf.	Comp.	Schematic and name
P2	Elbow	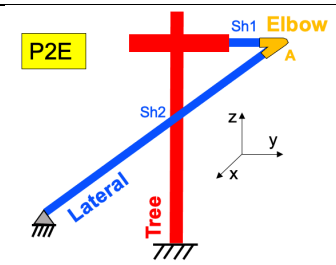
	Tee	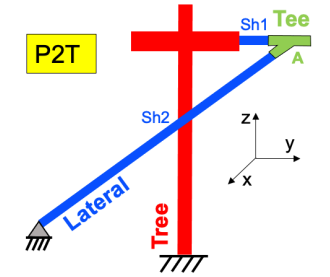
P3	Elbow	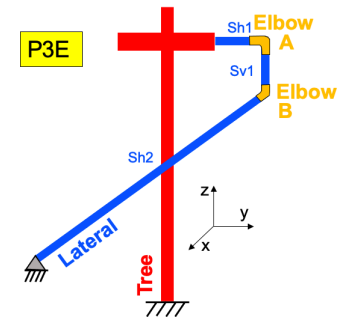
	Tee	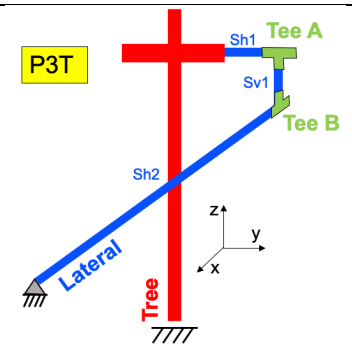
P4	Elbow	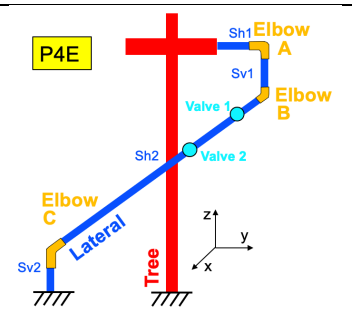

Conf.	Comp.	Schematic and name
P4	Tee	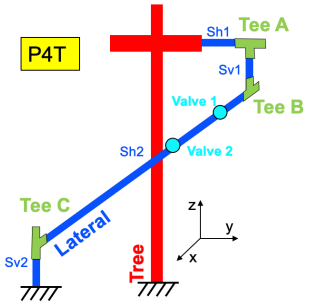

Within each subsystem-component combination, there are a number of models to calculate joint rotation for:

1. Direction of shaking (x-direction, y-direction)
2. Joint location (A, B, C)
3. Component orientation (open/close)

In total there are 22 unique models that may need to be computed to the distribution of joint rotation over the six subsystem-component combination. Each of the 22 unique rotation models are then propagated into models for longitudinal strain, and subsequently the probability of failure given longitudinal strain (see Figure 3.13 and Appendix C in Watson-Lamprey et al., 2022). Once the probability of failure for a specific subsystem-component combination, direction of shaking, joint location, and orientation is determined, then the distributions of probability of failure for all variations within each subsystem-component combination are averaged to obtain the overall average distribution for probability of failure. For example, for elbows in subsystem P2, there are 4 unique models:

1. x-direction, Joint A, closed orientation
2. x-direction, Joint A, open orientation
3. y-direction, Joint A, closed orientation
4. y-direction, Joint A, open orientation

OpenSRA computes the distribution of rotations for each of the four models above, then subsequently the distribution of longitudinal strain, and finally the probability of failure. Once the distributions of probability of failure are known for the four variations, then the distributions are averaged (i.e., sum and divided by 4) to obtain the average probability of failure for elbows in subsystem P2.

Figure 3.13: Probability of Failure for Wellheads due to Ground Shaking

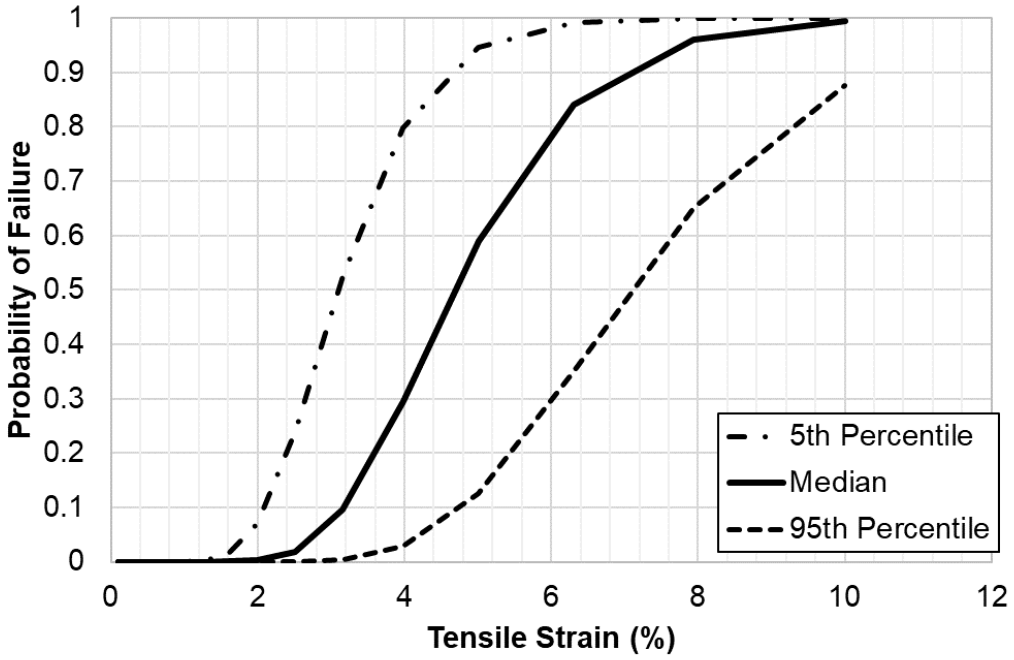

3.3.3.2 Pressure Vessels

For the pressure vessels, the critical component considered was the base of the pressure vessel. Two types of base connections were considered. The first represents the configuration of older pressure vessels, in which the base anchors are embedded in a concrete footing and thus designed as a fully fixed connection. In this case, no elongation of the anchor will occur, and minimal base rotation is anticipated, consequently the base of these pressure vessels is considered fixed. This case is labeled as "no stretch length". The second configuration is typical of newer pressure vessels. In this case, the anchors have a designed free stretch length of at least eight times the diameter of the anchor, as recommended by ACI 318-19 (2019). This allows the base to rotate, hence a nonlinear spring is incorporated in the model at the base of the vessel.

The workflow for pressure vessels is as follows:

1. Determine the distribution for moment ratio (see Appendix C in Watson-Lamprey et al. 2022).
2. Compute the probability of failure given the moment ratio (see Section 3.4.5 in Watson-Lamprey et al. 2022).

The distribution of the probability of failure for pressure vessels with ground shaking is shown in Figure 3.14.

Figure 3.14: Probability of Failure for Pressure Vessels due to Ground Shaking

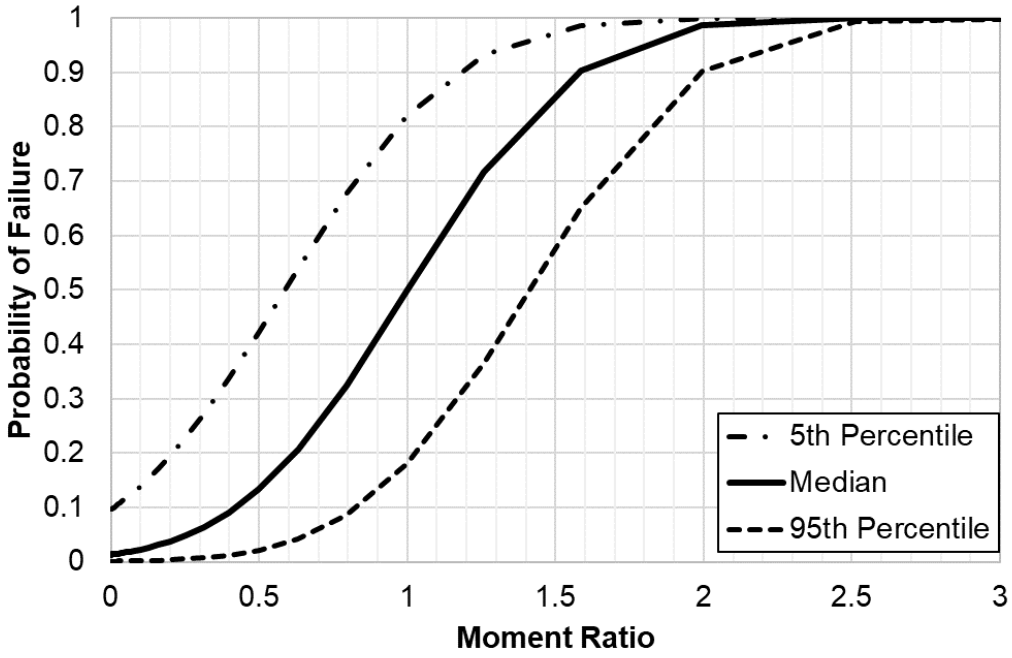

3.1 User Interface

The final component of *OpenSRA*, and the aspect that brings the backend calculations together is the graphical user interface (GUI). Further information about the graphical user interface and instructions on its use can be found in the User Manual.

The user interface consists of multiple tabs that follow the PBEE framework, outlined in Section 2.2.2 and shown in Figure 3.15. The visualization tab shows the inputs (infrastructure, ground motion, faults, and base maps) and will update once the analysis is performed. This tab allows the user to select specific infrastructure to see the results in tabular form (Figure 3.16).

Figure 3.15. The tabs in the GUI

Figure 3.16 Example of Visualization tab with tabulated values shown on the right

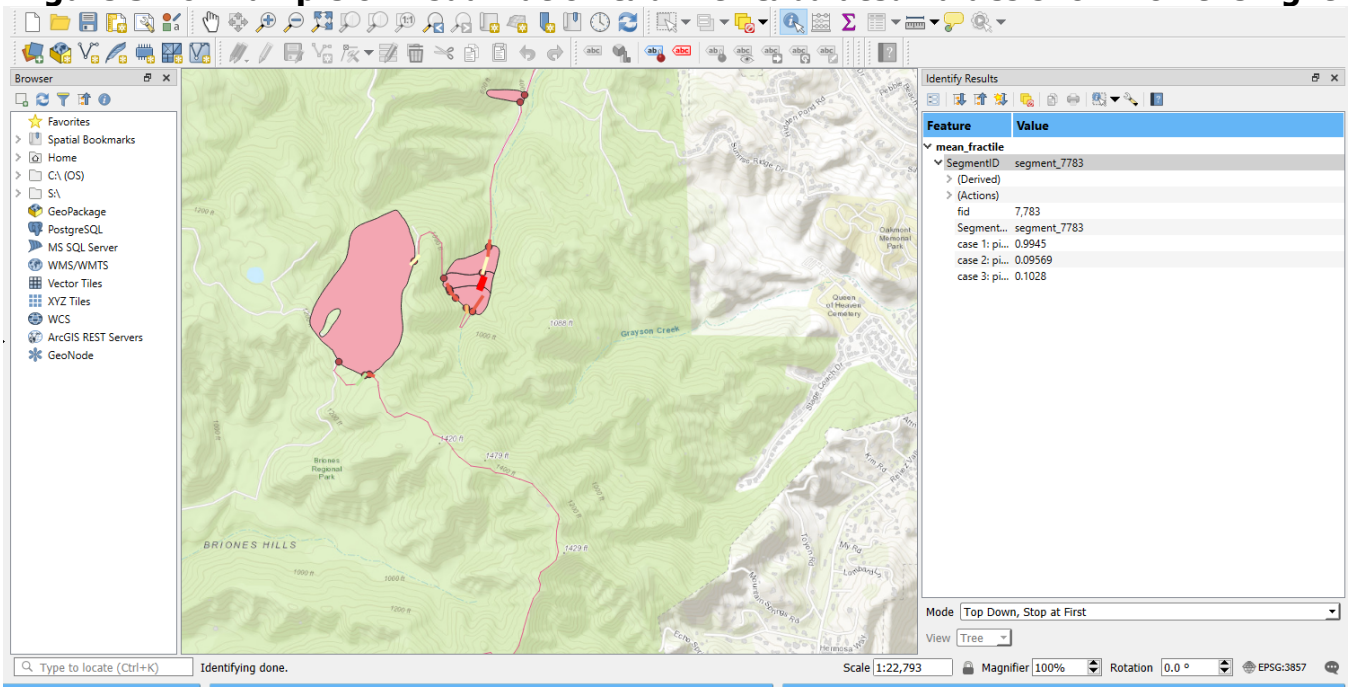

The "Infrastructure" tab is where the majority of the inputs are imported. The infrastructure can be imported as an excel file or as a GIS file. Each type of infrastructure has a slightly different layout. However, each is defined as a latitude and longitude coordinate, along with characteristics of the infrastructure. An example of this is shown in Figure 3.17.

Figure 3.17 Example of the input infrastructure table

fid	ID	LON_BEGIN	LAT_BEGIN	LON_END	LAT_END	LON_MID	LAT_MID	LENGTH_KM	OBJECTID	DIAMETER	PIPE_ID	SUB_SEGMENT_ID	L_ANCHOR_FULL_METER	SEGMENT_AZIMUTH_DEG
1	73	-122.0880298	37.4285453	-122.0880203	37.42831421	-122.08802505	37.428429755	0.02571	786	25.4	73	1	12.8	177.6
2	74	-122.0651995	37.40671103	-122.0649948	37.40665054	-122.06509715	37.406680785	0.019291	787	25.4	74	1	9.7	109.8
3	75	-122.0649948	37.40665054	-122.0654788	37.40607886	-122.0652368	37.4063647	0.076606	787	25.4	75	1	38.3	213.5
4	76	-122.0654788	37.40607886	-122.0657877	37.40582847	-122.06563325	37.405953665	0.038982	787	25.4	76	1	96	224
5	77	-122.0657877	37.40582847	-122.0662917	37.4054594	-122.0660397	37.405643935	0.060547	787	25.4	77	1	145.8	226.9
6	78	-122.0662917	37.4054594	-122.0667958	37.40509034	-122.06654375	37.40527487	0.060553	787	25.4	78	1	93	226.9
7	79	-122.0667958	37.40509034	-122.0673141	37.40470505	-122.06705495	37.404897695	0.062701	787	25.4	79	1	31.4	226.5
8	80	-122.0673141	37.40470505	-122.0672379	37.40459824	-122.067276	37.404651645	0.013651	787	25.4	80	1	6.8	149.8
9	81	-122.0672379	37.40459824	-122.0678024	37.40415827	-122.06752015	37.404378255	0.069854	787	25.4	81	1	34.9	225.1
10	82	-122.0678024	37.40415827	-122.068367	37.40371831	-122.0680847	37.40393829	0.06986	787	25.4	82	1	104.8	225.1
11	83	-122.068367	37.40371831	-122.0689316	37.40327835	-122.0686493	37.40349833	0.06986	787	25.4	83	1	42	225.1
12	84	-122.0689316	37.40327835	-122.0690015	37.40324827	-122.06896655	37.40326331	0.007022	787	25.4	84	1	3.5	241.1
13	85	-122.0690015	37.40324827	-122.0690231	37.40315628	-122.0690123	37.403202275	0.010405	787	25.4	85	1	5.2	190
14	86	-122.0690231	37.40315628	-122.0691605	37.4031601	-122.0690918	37.40315819	0.012144	787	25.4	86	1	6.1	271.4
15	87	-122.0691605	37.4031601	-122.0691681	37.40311813	-122.0691643	37.403139115	0.004715	787	25.4	87	1	2.4	187.7

The next few tabs are specifically following the PBEE framework (in reverse order). Each tab gives options for the different available models. Again, more information on these models can be found in the previous sections and in the User Manual.

The "Intensity Measure" tab allows the user to select the ground motion input. Currently, this is UCERF3 and NGAWest2, ShakeMaps, and a User Defined Rupture.

The "Input Value" tab is an additional input that changes based on the models chosen in the "Engineering Demand Parameter," "Damage Measure," and "Decision Variable" tabs. This tab

has the most complexities, as such there are extensive instructions included. There is also more information regarding this tab in the User Manual.

The final tab is the "Results" tab. This tab is a similar tab as "Visualization." The results are displayed; the "Visualization" tab allows for specific tables to be shown by selecting specific components.

As for outputting information to tables. The outputs are automatically exported to csv file format, to the working directory (in the general information tab).

CHAPTER 4: Conclusions/Recommendations

4.1 Implementation in *OpenSRA*

This report presents the implementation of demand and fragility models into *OpenSRA*. *OpenSRA* is a an open-source seismic risk assessment software developed for use in the natural gas industry. The goal of the overarching project is to address seismic demands through literature review and new research, and updating current and developing new models to estimate fragility of components of the natural gas system.

The seismic demands implemented into *OpenSRA* include fault displacement, ground shaking, and ground displacement (liquefaction, liquefaction induced settlement, lateral spreading, and seismic induced landsliding). Each of these demands were divided into "levels" of data, with the goal being to reduce uncertainty when data with higher resolution is available. Models are appropriately assigned to these levels based on data availability in order to provide a more accurate answer.

The fragility models included within *OpenSRA* are available for buried pipelines, wells and caprocks, and well-trees and pressure vessels (lumped together as above ground infrastructure). These models, described in detail in Watson-Lamprey et al. (2022), bridge the gap between seismic demands and decision variables as illustrated in the risk methodology presented in Chapter 2.

Using these implemented models, the end users can input data available to a site, a region, or statewide, predict the seismic demand, and compute the probability of failure both visually and tabularly. *OpenSRA* provides flexibility to the users by allowing use of default values recommended the researchers in the case where user-defined inputs are not available.

In closing, *OpenSRA* is a hub with research models and algorithms designed to interact (e.g., geospatial processing, random sampling, input/output operations). It is impossible for the team to test every combination of user inputs to these models. In order to better appreciate the results generated by *OpenSRA*, we highly recommend users inform themselves regarding the implemented research models. This includes the assumptions made to develop the models and any additional logic to implement them. Finally, users have the ability to use *OpenSRA* and the subsequent implementation of the included models in any way they prefer, but we cannot guarantee the performance of these models outside their intended purpose of research.

4.2 Recommendations for Further Research

This research effort has developed a user friendly, open-source risk software for natural gas infrastructure experiencing seismic loading. Given the timeframe of the project, and the lack of existing fragility curves currently available, this project focused on typical infrastructure to be broadly applicable. *OpenSRA* would benefit from additional research to:

1. Integrate directly with USGS for ShakeMap scenarios;
2. Incorporate real-time/monitoring data into risk assessment;
3. Allow for more flexibility in input datasets;

4. Develop more flexible output system for users to choose what to receive;
5. Integrate network/flow analysis into infrastructure types that have upstream/downstream dependencies;
6. Allow for more complex rupture scenarios (on top of simple fault planes);
7. Integrate other forms of natural hazards (i.e. rain induced landslides, fire danger, wind, etc.) in additional to seismic;
8. Further develop the backend to make better use of computer resource for computation efficiency;
9. Develop cloud-/server-based dissemination of datasets and updates, and/or extend the application to be web-based for broader access.

It is the hope of the authors to continue to expand the use of *OpenSRA* through additional research projects in years to come.

GLOSSARY AND LIST OF ACRONYMS

Term	Definition
Abaqus	Finite Element Software
CDF	Cumulative Distribution Function
CEC	California Energy Commission
CoV	Coefficient of Variation
CPT	Cone Penetration Test
DM	Damage Measure
DV	Decision Variable
EDP	Engineering Demand Parameter
IM	Intensity Measure
OpenSRA	Open Seismic Risk Assessment Tool
PBEE	Performance-Based Earthquake Engineering
PDF	Probability Density Function
PEER	Pacific Earthquake Engineering Research
PGA	Peak Ground Acceleration
PGV	Peak Ground Velocity
SPT	Standard Penetration Test
β	Pipeline-Ground Deformation Zone Interaction Angle (i.e., Crossing Angle)
c	Soil Cohesion
c_r	Root Cohesion
D_c	Distance to Nearest Coast
D_r	Distance to Nearest River
D_w	Distance to Nearest Waterbody
γ	Soil Unit Weight
GWT	Groundwater Table Depth
μ	Mean
ϕ	Soil Friction Angle
M_w	Moment Magnitude
Ψ	Polynomial Basis Functions

Term	Definition
σ	Standard Deviation and Aleatory Variability
σ_{epi}	Epistemic Uncertainty
t	Thickness of Slope Parallel to Ground Surface
θ	Fault-Well Intersection Angle
V_{s30}	Time-Weighted Average Shear Wave Velocity in the Top 30 Meters

REFERENCES

Abrahamson, N.A., Silva, W.J., Kamai, R. (2014). Summary of the ASK14 Ground Motion Relation for Active Crustal Regions: Earthquake Spectra, v. 30, no. 3, p. 1025-1155.

Abrahamson, N. (2022). Personal Communication.

ACI-318 (2019). Building Code Requirements for Structural Concrete and Commentary. American Concrete Institute, doi: 10.14359/51716937.

Bain, Chris; Hutabarat, Daniel; Bray, Jonathan D.; Abrahamson, Norman; O'Rourke, Thomas D.; Lindvall, Scott. (2022a). *Performance-Based Earthquake Engineering Assessment Tool for Natural Gas Storage and Pipeline Systems, Task B - Enhanced Liquefaction and Ground Deformation Report*. California Energy Commission.

Bedrossian, T.L., Roffers, P., Hayhurst, C.A., Lancaster, J.T. & Short, W.R. (2012) Geologic Compilation of Quaternary Surficial Deposits in Southern California (Special Report 217). Department of Conservation, California Geological Survey, Sacramento.

Boulanger, R. W., & Idriss, I. M. (2016). CPT-Based Liquefaction Triggering Procedure. Journal of Geotechnical and Geoenvironmental Engineering, 142(2), 04015065. https://doi.org/10.1061/(asce)gt.1943-5606.0001388.

Boore, D.M., Stewart J.P., Seyhan, E., and Atkinson, G.M., 2014, NGA-West2 Equations for Prediction PGA, PGV, and 5%-Damped PSA for Shallow Crustal Earthquakes: Earthquake Spectra, v. 30, no. 3, p. 1057-1085.

Bray, J.D., & Macedo, J. (2019). Procedure for Estimating Shear-Induced Seismic Slope Displacement for Shallow Crustal Earthquakes. J. of Geotechnical and Geoenvironmental Engineering, ASCE, V. 145(12), doi: 10.1061/(ASCE)GT.1943-5606.0002143.

Campbell, K.W., and Bozorgnia, Y. (2014). NGA-West2 Ground Motion Model for the Average Horizontal Component of PGA, PGV and 5% Damped Linear Acceleration Response Spectra: Earthquake Spectra, v. 30, no. 3, p. 1087-1115.

Cetin, K. O., Bilge, H. T., Wu, J., Kammerer, A. M., & Seed, R. B. (2009). Probabilistic Model for the Assessment of Cyclically Induced Reconsolidation (Volumetric) Settlements. Journal of Geotechnical and Geoenvironmental Engineering, 135(3), 387–398. https://doi.org/10.1061/(asce)1090-0241(2009)135:3(387).

CGS, (2016), The California Landslide Inventory, maps.conservation.ca.gov, California Geological Survey.

Chiou, B.S., and Youngs, R.R. (2014). Update of the Chiou and Youngs NGA Model for the Average Horizontal Component of Peak Ground Motion and Response Spectra: Earthquake Spectra, v. 30, no. 3, p. 1117-1153.

Cornell, C.A. (1968), Eng Seis Risk Analysis, Bull. Seismo. Soc. Am., V58(5), 1583-1606, doi: 10.1785/BSSA0580051583.

FEMA (2020). Hazus 4.2 SP3 Technical Manual. Federal Emergency Management Agency. https://www.fema.gov/sites/default/files/2020-10/fema_hazus_earthquake_technical_manual_4-2.pdf.

Field, E. H., T. H. Jordan, and C. A. Cornell (2003). OpenSHA: A Developing community-modeling environment for seismic hazard analysis, Seismological Research Letters 74, 406-419.

Field, E.H., Biasi, G.P., Bird, P., Dawson, T.E., Felzer, K.R., Jackson, D.D, Johnson, K.M., Jordan, T.H., Madden, C., Michael, A.J., Milner, K.R., Page, M.T., Parson, T., Powers, P.M., Shaw, B.E., Thatcher, W.R., Weldon, J.J. II, and Zeng, Y. (2013). Uniform California Earthquake Rupture Forecast, Version 3 (UCERF3) – The Time-Independent Model: U.S. Geological Survey Open-File Report 2013-1165.

Grant, A., Wartman, J., & Abou-Jaoude, G. (2016). Multimodal Method for Coseismic Landslide Hazard Assessment. Engineering Geology, 212, 146–160. doi: 10.1016/j.enggeo.2016.08.005.

Hutabarat, D., O'Rourke, T.D., Bray, J.D., Bain, C., Lindvall, S. (2022). Performance-Based Earthquake Engineering Assessment Tool for Natural Gas Storage and Pipeline Systems, Task B - Underground Pipeline Fragilities. Pacific Earthquake Engineering Research (PEER) Center Report, in preparation.

Idriss, I.M., & Boulanger, R.W. (2008). Soil Liquefaction During Earthquakes. EERI Publication, Monograph MNO-12, Earthquake Engineering Research Institute, Oakland. https://www.eeri.org/.

Jung, J. K., O'Rourke, T. D., & Argyrou, C. (2016). Multi-Directional Force–Displacement Response of Underground Pipe in Sand. Canadian Geotechnical Journal, 53(11), 1763–1781. https://doi.org/10.1139/cgj-2016-0059.

Ku, C.-S., Juang, C. H., Chang, C.-W., & Ching, J. (2012). Probabilistic Version of the Robertson and Wride Method for Liquefaction Evaluation: Development and Application. Canadian Geotechnical Journal, 49(1), 27–44. doi: 10.1139/t11-085.

Lacour, M., and Abrahamson, N. A. (2021) Efficient Risk Calculation for Performance-Based Earthquake Engineering Distributed Systems. Pacific Earthquake Engineering Research (PEER) Center Report.

Moehle, J.P., and Deierlein, G.G. (2004). A framework methodology for performance-based earthquake engineering, Proc., 13th World Conf. on Earthquake Engineering, Vancouver, BC, Canada, Paper No. 679.

Moss, R. E., Seed, R. B., Kayen, R. E., Stewart, J. P., Kiureghian, A. D., & Cetin, K. O. (2006). CPT-Based Probabilistic and Deterministic Assessment of In Situ Seismic Soil Liquefaction Potential. Journal of Geotechnical and Geoenvironmental Engineering, 132(8), 1032–1051. doi: 10.1061/(asce)1090-0241(2006)132:8(1032).

O'Rourke, M. J., & Liu, J. X. (2012). Seismic Design of Buried and Offshore Pipelines. Monograph MCEER-12-MN04, Multidisciplinary Center for Earthquake Engineering Research, Buffalo, NY.

O'Rourke, T. D., Jeon, S.-S., Toprak, S., Cubrinovski, M., Hughes, M., van Ballegooy, S., & Bouziou, D. (2014). Earthquake Response of Underground Pipeline Networks in Christchurch, NZ. Earthquake Spectra, 30(1), 183–204. https://doi.org/10.1193/030413eqs062m.

O'Rourke, T. D., Jung, J. K., & Argyrou, C. (2016). Underground Pipeline Response to Earthquake-Induced Ground Deformation. Soil Dynamics and Earthquake Engineering, 91, 272–283. https://doi.org/10.1016/j.soildyn.2016.09.008.

Pantoli, E., Hutchinson, T.C., Elfass, S.A., and McCallen, D.B. (2022). Performance-Based Earthquake Engineering Assessment Tool for Natural Gas Storage and Pipeline Systems, Task D Final Report - Seismic Response of Pipeline and Gas Storage Surface Infrastructure. California Energy Commission.

Petersen, M. D., Dawson, T. E., Chen, R., Cao, T., Wills, C. J., Schwartz, D. P., & Frankel, A. D. (2011). Fault displacement hazard for strike-slip faults. Bulletin of the Seismological Society of America, 101(2), 805-825.

Robertson, P. (2009). Performance Based Earthquake Design Using the CPT. Performance-Based Design in Earthquake Geotechnical Engineering. https://doi.org/10.1201/noe0415556149.ch1.

Robertson, P. K., & Wride, C. E. (1998). Evaluating Cyclic Liquefaction Potential using the Cone Penetration Test. Canadian Geotechnical Journal, 35(3), 442–459. doi: 10.1139/t98-017.

Rutqvist, Jonny; Tsubasa Sasaki; Keurfon Luu; Preston Jordan; Yingqi Zhang; William Foxall, Jennie Watson-Lamprey, Micaela Largent, Barry Zheng, (2022). Performance-Based Earthquake Engineering Assessment Tool for Natural Gas Storage and Pipeline Systems, Task C Final Report - Seismic Response of Wells and Caprocks. California Energy Commission.

Thompson, E. M. (2018). An updated Vs30 map for California with geologic and topographic constraints, U.S. Geol. Surv. Data Release, doi: 10.5066/F7JQ108S.

Thompson, Stephen. (2021). *Fault Displacement Hazard Characterization for OpenSRA*. California Energy Commission.

U.S. Geological Survey and California Geological Survey (USGS and CGS). 2006. Quaternary Fault and Fold Database of the United States: url http://earthquake.usgs.gov/hazards/qfaults/; accessed 3/13/2019.

Wald, D. J., B. C. Worden, K. Lin, and K. Pankow (2005). ShakeMap manual: technical manual, user's guide, and software guide, U.S. Geol. Surv. Tech. Methods 12-A1, 132 pp.

Wald DJ, Allen TI. (2007) Topographic Slope as a Proxy for Seismic Site Conditions. Bulletin of the Geological Society of America; 97 (5): 1379-1395.

Watson-Lamprey, Jennie, Bao Li Zheng, Micaela Largent, Norman Abrahamson, Chris Bain, Jonathan Bray, with Jens Birkholzer, Sherif Elfass, William Foxall, Sanjay Govinjee, Peter Hubbard, Tara Hutchinson, Grace Kang, Amarnath Kasalanati, Maxime Lacour, Scott Lindvall, David McCallen, Frank McKenna, Thomas O'Rourke, Elide Pantoli, Floriana Petrone, Jonny Rutqvist, Matt Schoettler, Kenichi Soga, Steve Thompson and Jeff Unruh. 2020. *Sensitivity Report for the Performance-Based Earthquake Engineering Assessment Tool for Natural Gas Storage and Pipeline systems.* California Energy Commission. Publication Number: CEC-500-202X-XXX.

Watson-Lamprey, Jennie, Micaela Largent, Bao Li Zheng. (2022). *System Wide Natural Gas Infrastructure Response and Fragility Model.* California Energy Commission. Publication Number: CEC-500-202X-XXX.

Wells, D. L., and K. J. Coppersmith. (1994). New empirical relationships among magnitude, rupture length, rupture width, rupture area, and surface displacement: Bulletin of the Seismological Society of America, v. 84, p. 974–1002.

Wills, C. J., and K. B. Clahan (2006). Developing a map of geologically defined site-condition categories for California, Bull. Seism. Soc. Am. 96, 1483–1501.

Wills, C. J., C. I. Gutierrez, F. G. Perez, and D. M. Branum (2015). A next generation VS30 map for California based on geology and topography, Bull. Seismol. Soc. Am. 105, no. 6, 3083–3091.

Witter, R.C., Knudsen, K.L, Sowers, J.M., Wentworth, C.M., Koehler, R.D., Randolph, C. E., Brooks, S.K., & Gans, K.D. (2006). Maps of Quaternary Deposits and Liquefaction Susceptibility in the Central San Francisco Bay Region, California: U.S. Geological Survey Open-File Report 06-1037 (http://pubs.usgs.gov/of/2006/1037/).

Youd, T. L., & Perkins, D. M. (1978). Mapping Liquefaction-Induced Ground Failure Potential. Journal of the Geotechnical Engineering Division, 104(4), 433–446.

Zhang G., Robertson, P.K., and Brachman, R.W.I. (2002). Estimating liquefaction-induced ground settlements from CPT for level ground, Canadian Geotechnical Journal, vol. 39., pp. 1168-1180.

Zhang, G., Robertson, P. K., & Brachman, R. W. I. (2004). Estimating Liquefaction-Induced Lateral Displacements Using the Standard Penetration Test or Cone Penetration Test. Journal of Geotechnical and Geoenvironmental Engineering, 130(8), 861–871. doi: 10.1061/(asce)1090-0241(2004)130:8(861).

Zhu, J., Baise, L. G., & Thompson, E. M. (2017). An Updated Geospatial Liquefaction Model for Global Application. Bulletin of the Seismological Society of America, 107(3), 1365–1385. doi: 10.1785/0120160198.

APPENDIX A:
DEFAULT DATA FOR *OPENSRA*

This appendix provides the default distributions and values for random and fixed variables, respectively. *OpenSRA* will use these values as default in the event where the users do not provide any inputs. The values and maps presented herein are recommended by the researchers from each Task Group.

A.1 Default Distributions for Parameters

The default values for all random and fixed variables used in *OpenSRA* are presented in Table A-1 Table to Table A-4 for buried pipelines, Table A-5 and Table A-6 for wells and caprocks, and Table A-7Table A-7 and Table A-8 for above ground infrastructure. For buried pipelines, the distributions for some of the random variables vary between Levels 1, 2, and 3; for wells and caprocks and above ground components, there is no variation in the distribution between levels.

Some notes for the tables:

- Parameters that have default values will be flagged with "True" under the column "Preferred Distribution Exists?"; otherwise "False" and the "Mean/Median" column will be flagged with "user provided".
- If the distribution varies with levels, then the parameter is flagged with "True" under the column "Distribution Varies with Level?"; otherwise "False".
- If a metric of the distribution is flagged with "internal GIS dataset", then this tells *OpenSRA* to search within the internal GIS datasets for the default values (see the next section).
- If a metric of the distribution is flagged with "depends", then the default values are based on atypical datasets, such as tables developed by the researchers (e.g., see Table B.15 in Bain et al. 2022).
- Only one of "Sigma" or "CoV" is required to define a distribution.
- Any empty cells under "Lower Bound" is interpreted as "-∞" for normal distributions and "0" for lognormal distributions.
- Any empty cells under "Upper Bound" is interpreted as "∞".

A.2 Default GIS Datasets

OpenSRA uses a number of default GIS datasets to infer the mean/median of the distributions of certain random variables. The parameters that utilize internal GIS data are flagged with "internal gis dataset" in Table A-1 to Table A-8Figure A-11. The statewide/regional review of the internal GIS maps are presented in Figure A-1 to Figure A-11. The names of maps are tabulated in the list below.

1. Mean annual precipitation – Zhu et al. (2017)

2. Distance to coast – Zhu et al. (2017)
3. Distance to river – Zhu et al. (2017)
4. Distance to water – Zhu et al. (2017)
5. Groundwater table depth – Zhu et al. (2017)
6. Statewide geologic maps - Wills et al. (2015)
7. Quaternary geologic map for Bay Area – Witter et al. (2006)
8. Quaternary geologic map for Los Angeles – Bedrossian et al. (2012)
9. Statewide Digital Elevation Model - Zhu et al. (2017)
10. Statewide Slope - Zhu et al. (2017)
11. Compound Topographic Index - Zhu et al. (2017)

Table A-1: Default Level 1 Distributions for Random Variables used in Buried Pipeline Analysis

Label used in *OpenSRA*	Preferred Distribution Exists?	Distribution Varies with Level?	Description	Unit	Mean/ Median	Sigma	CoV	Lower Bound	Upper Bound	Distribution Type
d_pipe	TRUE	TRUE	pipe diameter	mm	610		25	102	1067	normal
t_pipe	TRUE	TRUE	pipe wall thickness	mm	10.2		40	2.5	20.3	normal
sigma_y	TRUE	TRUE	pipe yield stress	kPa	359000		15	240000	600000	normal
n_param	TRUE	FALSE	Ramberg-Osgood parameter	unitless	10	3		depends	depends	normal
r_param	TRUE	FALSE	Ramberg-Osgood parameter	unitless	8.5	1.5		depends	depends	normal
def_length	TRUE	TRUE	length of ground deformation zone	m	100		90	10	400	lognormal
alpha_backfill	TRUE	TRUE	adhesion factor for clay	unitless	0.75	0.14		0.5	1	normal
s_u_backfill	TRUE	TRUE	undrained shear strength	kPa	40		45	20	120	lognormal
gamma_backfill	TRUE	TRUE	total unit weight of backfill soil	kN/m^3	19		9	16	21.5	lognormal
h_pipe	TRUE	TRUE	soil cover to centerline of pipeline	m	1.2		15	0.6	6	lognormal
phi_backfill	TRUE	TRUE	backfill friction angle	deg	38		15	30	45	lognormal
delta_backfill	TRUE	TRUE	sand/pipe interface friction angle ratio	unitless	0.75	0.14		0.5	1	normal
op_press	TRUE	FALSE	pipe internal operating pressure	kPa	8200		10	1	13800	lognormal
vs30	TRUE	FALSE	time-averaged shear wave velocity in the upper 30-meters	m/s	internal gis dataset		30			lognormal
gw_depth	TRUE	FALSE	depth to groundwater table	m	internal gis dataset		50			lognormal
dist_river	TRUE	FALSE	distance to nearest river	km	internal gis dataset		15	depends	depends	lognormal
dist_coast	TRUE	FALSE	distance to nearest coast	km	internal gis dataset		15	depends	depends	lognormal
dist_water	TRUE	FALSE	distance to nearest water body	km	internal gis dataset		15	depends	depends	lognormal
precip	TRUE	FALSE	mean annual precipitation	mm	internal gis dataset		40		2500	lognormal
slope	TRUE	FALSE	slope angle	deg	internal gis dataset		5			lognormal
t_slope	TRUE	FALSE	slope thickness (infinite-slope problem)	m	2		15	1	6	lognormal
gamma_soil	TRUE	FALSE	unit weight of soil	kN/m^3	17		7	16	21.5	lognormal
phi_soil	TRUE	FALSE	friction angle of soil	m	depends		depends	depends	depends	lognormal
coh_soil	TRUE	FALSE	cohesion of soil	kPa	depends		depends	depends	depends	lognormal
psi_dip	TRUE	FALSE	pipe-fault dip angle	deg	depends	10		15	90	normal
beta_crossing	TRUE	FALSE	slip-pipeline crossing angle	deg	depends	20		0.1	180	normal
l_anchor	TRUE	FALSE	pipeline anchored length	m	depends		40	1		lognormal

Table A-2: Default Level 2 Distributions for Random Variables used in Buried Pipeline Analysis

Label used in *OpenSRA*	Preferred Distribution Exists?	Distribution Varies with Level?	Description	Unit	Mean/ Median	Sigma	CoV	Lower Bound	Upper Bound	Distribution Type
d_pipe	FALSE	TRUE	pipe diameter	mm	user provided	0				normal
t_pipe	FALSE	TRUE	pipe wall thickness	mm	user provided	0				normal
sigma_y	FALSE	TRUE	pipe yield stress	kPa	user provided		7.5			normal
n_param	TRUE	FALSE	Ramberg-Osgood parameter	unitless	10	3		depends	depends	normal
r_param	TRUE	FALSE	Ramberg-Osgood parameter	unitless	8.5	1.5		depends	depends	normal
def_length	TRUE	TRUE	length of ground deformation zone	m	100		70	10	400	lognormal
alpha_backfill	TRUE	TRUE	adhesion factor for clay	unitless	0.75	0.12		0.5	1	normal
s_u_backfill	TRUE	TRUE	undrained shear strength	kPa	40		35	20	100	lognormal
gamma_backfill	TRUE	TRUE	total unit weight of backfill soil	kN/m^3	19		7	16	21.5	lognormal
h_pipe	TRUE	TRUE	soil cover to centerline of pipeline	m	1.2		15	0.6	6	lognormal
phi_backfill	TRUE	TRUE	backfill friction angle	deg	38		12	30	50	lognormal
delta_backfill	TRUE	TRUE	sand/pipe interface friction angle ratio	unitless	0.75	0.12		0.5	1	normal
op_press	FALSE	FALSE	pipe internal operating pressure	kPa	user provided		10	0	13800	lognormal
vs30	TRUE	FALSE	time-averaged shear wave velocity in the upper 30-meters	m/s	internal gis dataset		30			lognormal
gw_depth	TRUE	FALSE	depth to groundwater table	m	internal gis dataset		40			lognormal
dist_river	TRUE	FALSE	distance to nearest river	km	internal gis dataset		15	depends	depends	lognormal
dist_coast	TRUE	FALSE	distance to nearest coast	km	internal gis dataset		15	depends	depends	lognormal
dist_water	TRUE	FALSE	distance to nearest water body	km	internal gis dataset		15	depends	depends	lognormal
precip	TRUE	FALSE	mean annual precipitation	mm	internal gis dataset		40		2500	lognormal
slope	TRUE	FALSE	slope angle	deg	internal gis dataset		5			lognormal
t_slope	TRUE	FALSE	slope thickness (infinite-slope problem)	m	2		15	1	6	lognormal
gamma_soil	TRUE	FALSE	unit weight of soil	kN/m^3	17		7	16	21.5	lognormal
phi_soil	TRUE	FALSE	friction angle of soil	m	depends		depends	depends	depends	lognormal
coh_soil	TRUE	FALSE	cohesion of soil	kPa	depends		depends	depends	depends	lognormal
psi_dip	TRUE	FALSE	pipe-fault dip angle	deg	depends	10		15	90	normal
beta_crossing	TRUE	FALSE	slip-pipeline crossing angle	deg	depends	20		0.1	180	normal
l_anchor	TRUE	FALSE	pipeline anchored length	m	depends		40	1		lognormal

Table A-3: Default Level 3 Distributions for Random Variables used in Buried Pipeline Analysis

Label used in *OpenSRA*	Preferred Distribution Exists?	Distribution Varies with Level?	Description	Unit	Mean/ Median	Sigma	CoV	Lower Bound	Upper Bound	Distribution Type
d_pipe	FALSE	TRUE	pipe diameter	mm	user provided	0				normal
t_pipe	FALSE	TRUE	pipe wall thickness	mm	user provided	0				normal
sigma_y	FALSE	TRUE	pipe yield stress	kPa	user provided		7.5			normal
n_param	TRUE	FALSE	Ramberg-Osgood parameter	unitless	10	3		depends	depends	normal
r_param	TRUE	FALSE	Ramberg-Osgood parameter	unitless	8.5	1.5		depends	depends	normal
def_length	FALSE	TRUE	length of ground deformation zone	m	user provided		50	10	400	lognormal
alpha_backfill	FALSE	TRUE	adhesion factor for clay	unitless	user provided	0.1		0.5	1	normal
s_u_backfill	FALSE	TRUE	undrained shear strength	kPa	user provided		25	20	100	lognormal
gamma_backfill	FALSE	TRUE	total unit weight of backfill soil	kN/m^3	user provided		5	16	21.5	lognormal
h_pipe	FALSE	TRUE	soil cover to centerline of pipeline	m	user provided		10	0.6	6	lognormal
phi_backfill	FALSE	TRUE	backfill friction angle	deg	user provided		9	30	50	lognormal
delta_backfill	FALSE	TRUE	sand/pipe interface friction angle ratio	unitless	user provided	0.1		0.5	1	normal
op_press	FALSE	FALSE	pipe internal operating pressure	kPa	user provided		10	0	13800	lognormal
vs30	FALSE	FALSE	time-averaged shear wave velocity in the upper 30-meters	m/s	user provided		30			lognormal
gw_depth	FALSE	FALSE	depth to groundwater table	m	user provided		20			lognormal
dist_river	FALSE	FALSE	distance to nearest river	km	user provided		15	depends	depends	lognormal
dist_coast	FALSE	FALSE	distance to nearest coast	km	user provided		15	depends	depends	lognormal
dist_water	FALSE	FALSE	distance to nearest water body	km	user provided		15	depends	depends	lognormal
precip	FALSE	FALSE	mean annual precipitation	mm	user provided		40		2500	lognormal
slope	FALSE	FALSE	slope angle	deg	user provided		5			lognormal
t_slope	FALSE	FALSE	slope thickness (infinite-slope problem)	m	user provided		15	1	6	lognormal

Label used in *OpenSRA*	Preferred Distribution Exists?	Distribution Varies with Level?	Description	Unit	Mean/ Median	Sigma	CoV	Lower Bound	Upper Bound	Distribution Type
gamma_soil	FALSE	FALSE	unit weight of soil	kN/m^3	user provided		7	16	21.5	lognormal
phi_soil	FALSE	FALSE	friction angle of soil	m	user provided		depends	depends	depends	lognormal
coh_soil	FALSE	FALSE	cohesion of soil	kPa	user provided		depends	depends	depends	lognormal
psi_dip	FALSE	FALSE	pipe-fault dip angle	deg	user provided	10		15	90	normal
beta_crossing	FALSE	FALSE	slip-pipeline crossing angle	deg	user provided	20		0.1	180	normal
l_anchor	FALSE	FALSE	pipeline anchored length	m	user provided		40	1		lognormal

Table A-4: Default Values for Fixed Variables used in Buried Pipeline Analysis

Label used in *OpenSRA*	Preferred Distribution Exists?	Distribution Varies with Level?	Description	Unit	Value
soil_type	FALSE	FALSE	soil type (sand/clay) for model	mm	
steel_grade	TRUE	FALSE	steel grade: Grade-B, X-42, X-52, X-60, X-70, X-80	kPa	"NA"
soil_density	FALSE	FALSE	soil density: soft, medium stiff, or stiff for clay; medium dense, dense, or very dense for sand	unitless	

Table A-5: Default Distributions for Random Variables used in Wells and Caprocks Analysis

Label used in *OpenSRA*	Preferred Distribution Exists?	Distribution Varies with Level?	Description	Unit	Mean/ Median	Sigma	CoV	Lower Bound	Upper Bound	Distribution Type
theta	TRUE	FALSE	fault angle	deg	45	10		0		normal
w_fc	TRUE	FALSE	fault core width	m	0.017	1				lognormal
w_dz	TRUE	FALSE	damage zone width	m	1.1	0.5				lognormal
e_rock	TRUE	FALSE	Young's modulus of rock	GPa	11.147968	2.535		0		normal
phi_cmt	TRUE	FALSE	internal friction angle of cement	deg	25		20	0		normal
ucs_cmt	TRUE	FALSE	uniaxial compressive strength of cement	MPa	60		20	0		normal
h_wh	FALSE	FALSE	wellhead height, for all modes	m	user provided					normal
mpl_wh	FALSE	FALSE	wellhead mass per length, for all modes	kg/m	user provided					normal
phi_soil	FALSE	FALSE	soil friction angle, modes 1 and 2 only	deg	user provided					normal

Table A-6: Default Values for Fixed Variables used in Wells and Caprocks Analysis

Label used in *OpenSRA*	Preferred Distribution Exists?	Distribution Varies with Level?	Description	Unit	Value
mode	FALSE	FALSE	well mode: 1, 2, 4	unitless	
cement_flag	FALSE	FALSE	cemented casing/tubing (True/False)	unitless	

Table A-7: Default Distributions for Random Variables used in Above Ground Components Analysis

Label used in *OpenSRA*	Preferred Distribution Exists?	Distribution Varies with Level?	Description	Unit	Mean/ Median	Sigma	CoV	Lower Bound	Upper Bound	Distribution Type
h_t	TRUE	FALSE	tree height [m] - all subsystems	m	2.74	0.91		1.00E-03		normal
l_p2	TRUE	FALSE	length of pipe segment s2 [m] - subsystem p2	m	1.52	0.91		1.00E-03		normal
l_p6_sys23	TRUE	FALSE	length of pipe segment s6 [m] - subsystem p2 and p3	m	3.05	1.83		1.00E-03		normal
l_p6_sys4	TRUE	FALSE	length of pipe segment s6 [m] - subsystem p4	m	4.87	1.83		1.00E-03		normal
w_valve	TRUE	FALSE	valve weight [kN] - subsystem p4	kN	1.56	0.67		1.00E-03		normal
d_sys	TRUE	FALSE	pipe diameter (mm)	mm	114		25	0.001		normal
t_sys	TRUE	FALSE	pipe wall thickness (mm)	mm	8.6		40	1.00E-03		normal
op_press	TRUE	FALSE	pipe internal operating pressure	kPa	8200		10	1	13800	lognormal
sigma_y	TRUE	FALSE	yield stress [kPa]	kPa	360400		15	240000	600000	normal
d_vessel	TRUE	FALSE	height of pressure vessels [m]	m	10.68	2.43		1.00E-03		normal
h_d_ratio_vessel	TRUE	FALSE	height-to-diameter ratio for pressure vessels	unitless	5.5	1.5		1.00E-03		normal
p_vessel	TRUE	FALSE	design pressure for pressure vessels [MPa]	MPa	6.89	3.44		1.00E-03		normal
d_anchor	TRUE	FALSE	diameter for anchors [mm]	mm	31.75	3.8		1.00E-03		normal

Table A-8: Default Values for Fixed Variables used in Above Ground Components Analysis

Label used in *OpenSRA*	Preferred Distribution Exists?	Distribution Varies with Level?	Description	Unit	Value
steel_grade	TRUE	FALSE	steel grade: Grade-B, X-42, X-52 (default), X-60, X-70, X-80	unitless	above_ground_model
sys_type	FALSE	FALSE	subsystems: 2 for p2, 3 for p3, 4 for p4	unitless	
tee_flag	TRUE	FALSE	flag for tee-joints in subsystem: True/False	unitless	TRUE
elbow_flag	TRUE	FALSE	flag for elbows in subsystem: True/False	unitless	TRUE
stretch_length_flag	TRUE	FALSE	presence of stretch length for anchors: True/False	unitless	FALSE

Figure A-1: Map of Mean Annual Precipitation (Zhu et al. 2017)

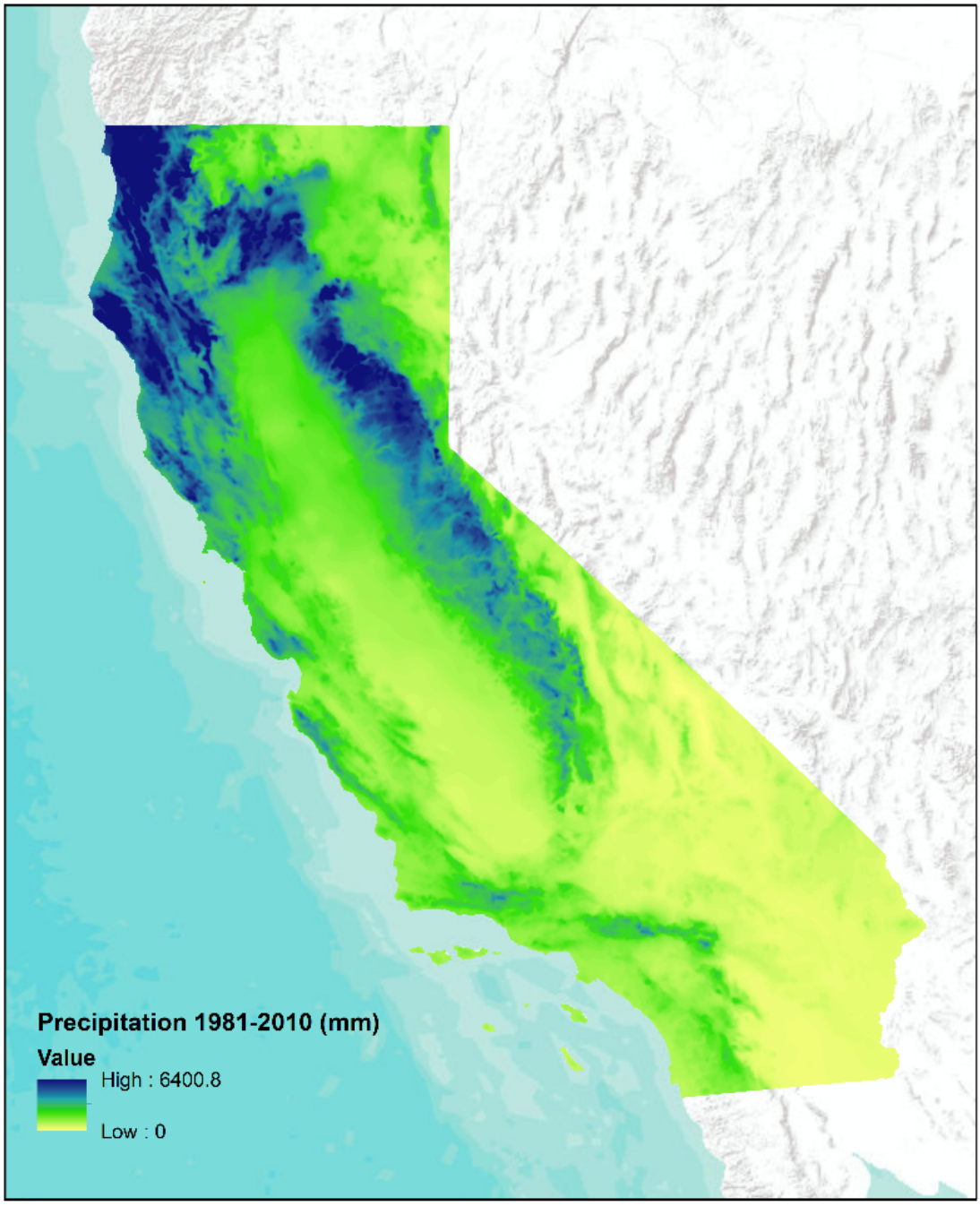

Figure A-2: Map of Distance to Nearest Coast (Zhu et al. 2017)

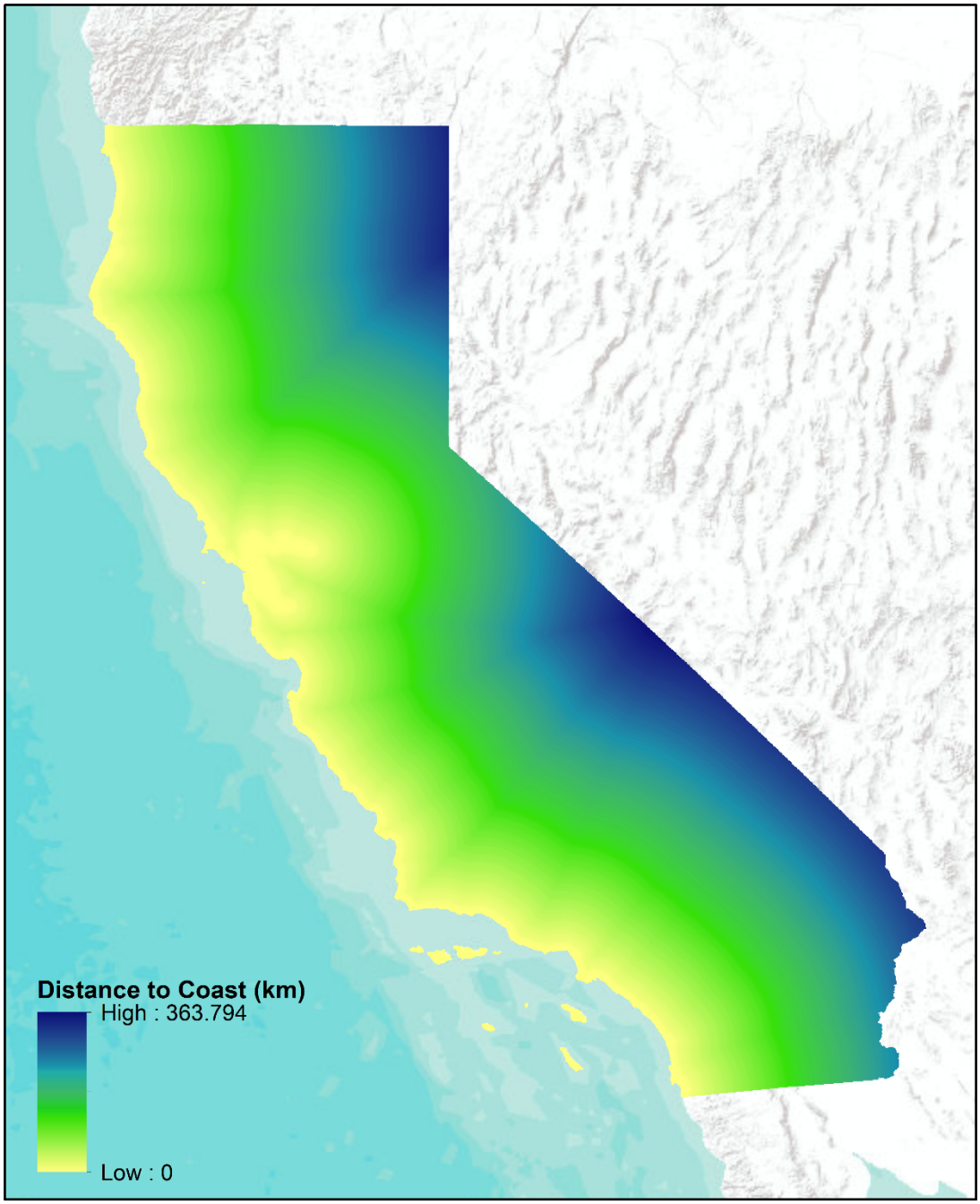

Figure A-3: Map of Distance to Nearest River (Zhu et al. 2017)

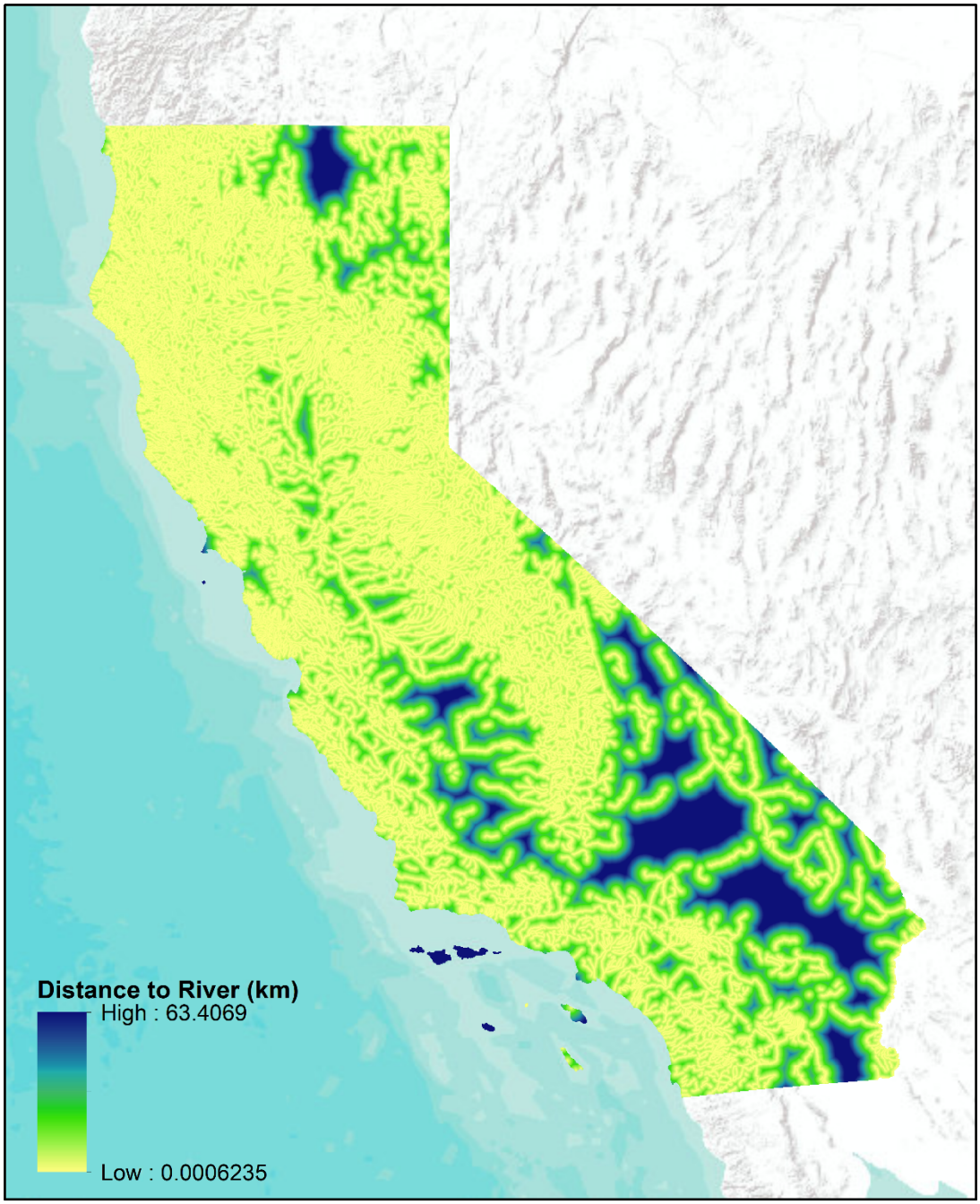

Figure A-4: Map of Distance to Nearest Waterbody (Zhu et al. 2017)

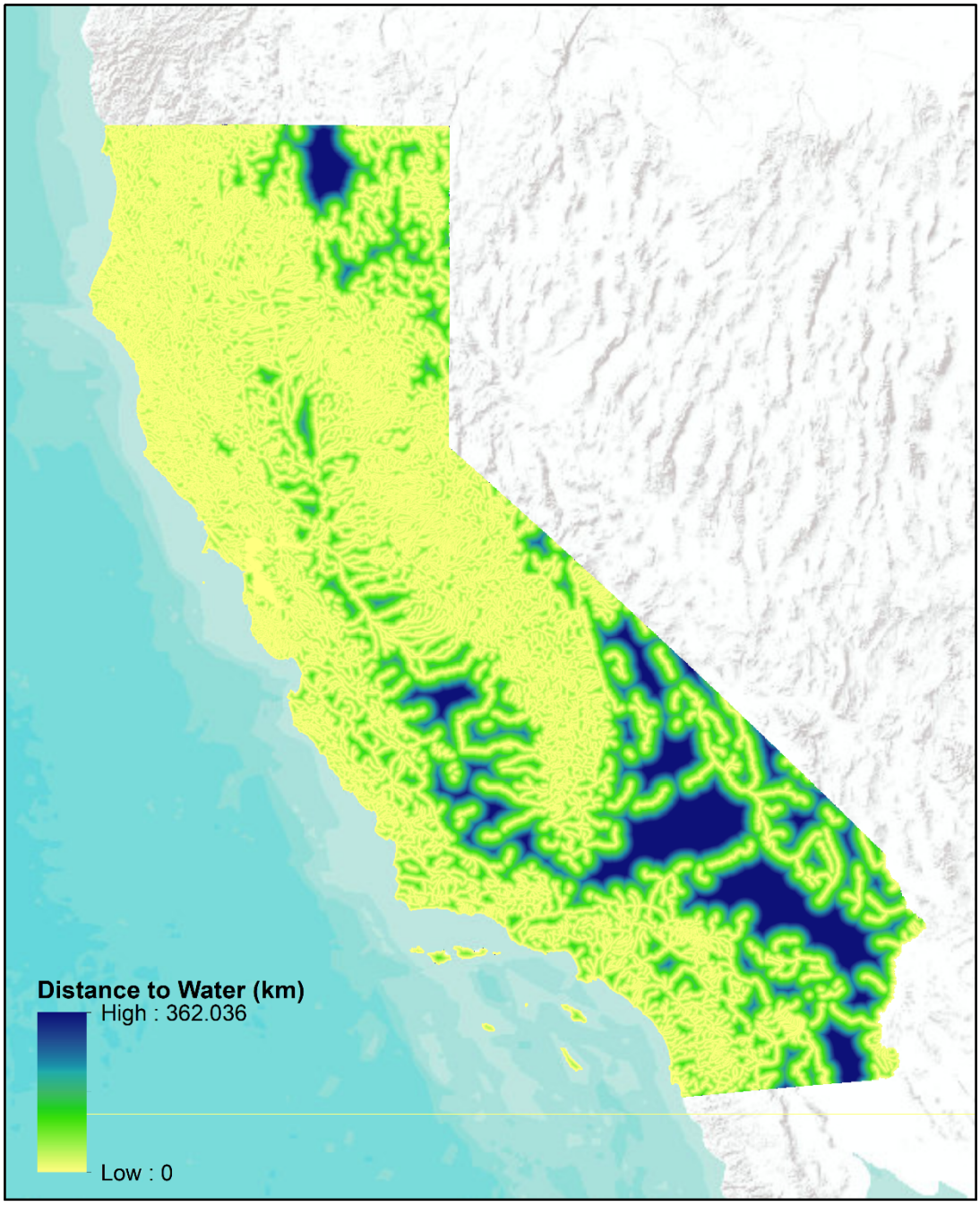

Figure A-5: Map of Depth to Groundwater Table Depth (Zhu et al. 2017)

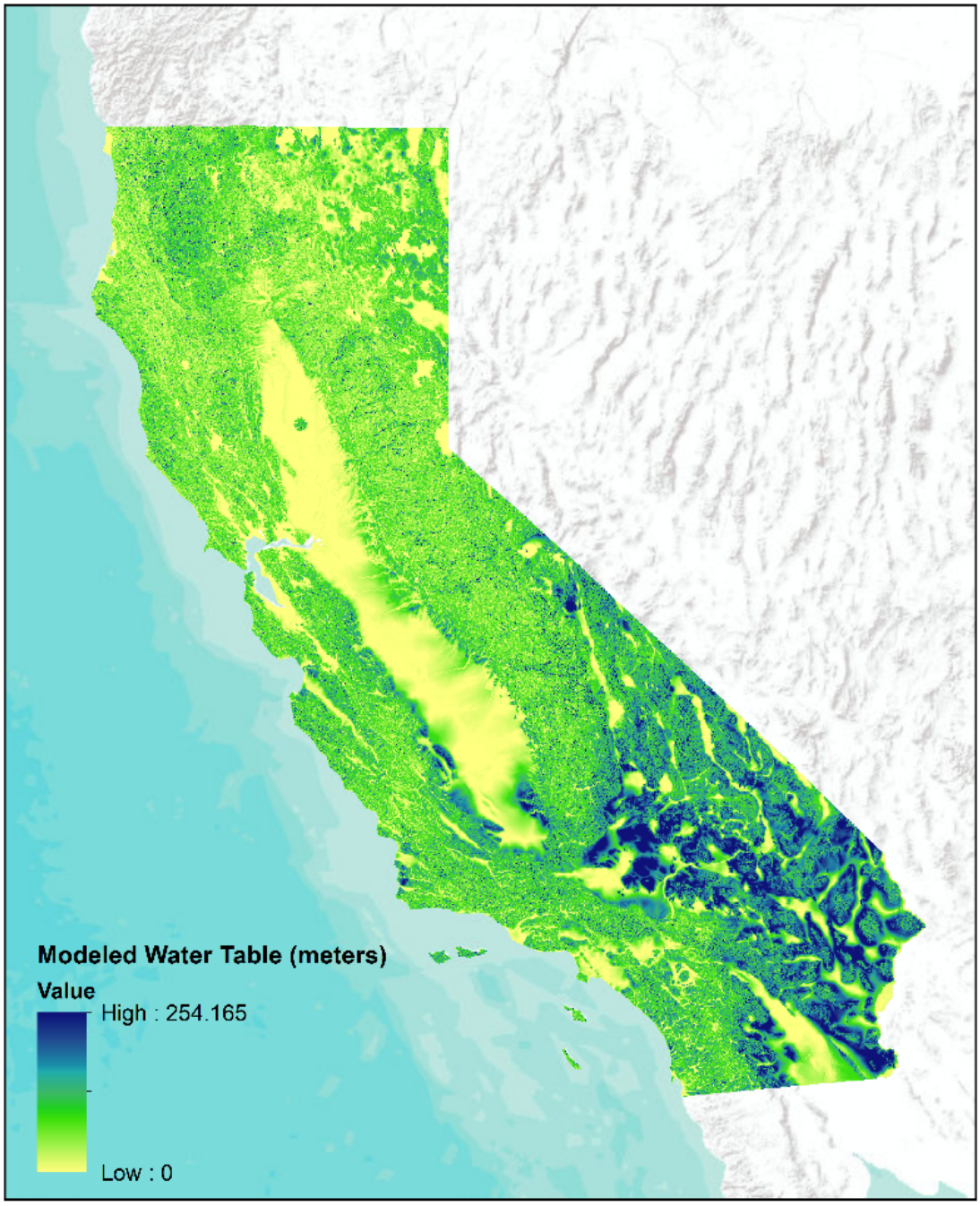

Figure A-6: Statewide Geologic Map from Wills et al. (2015)

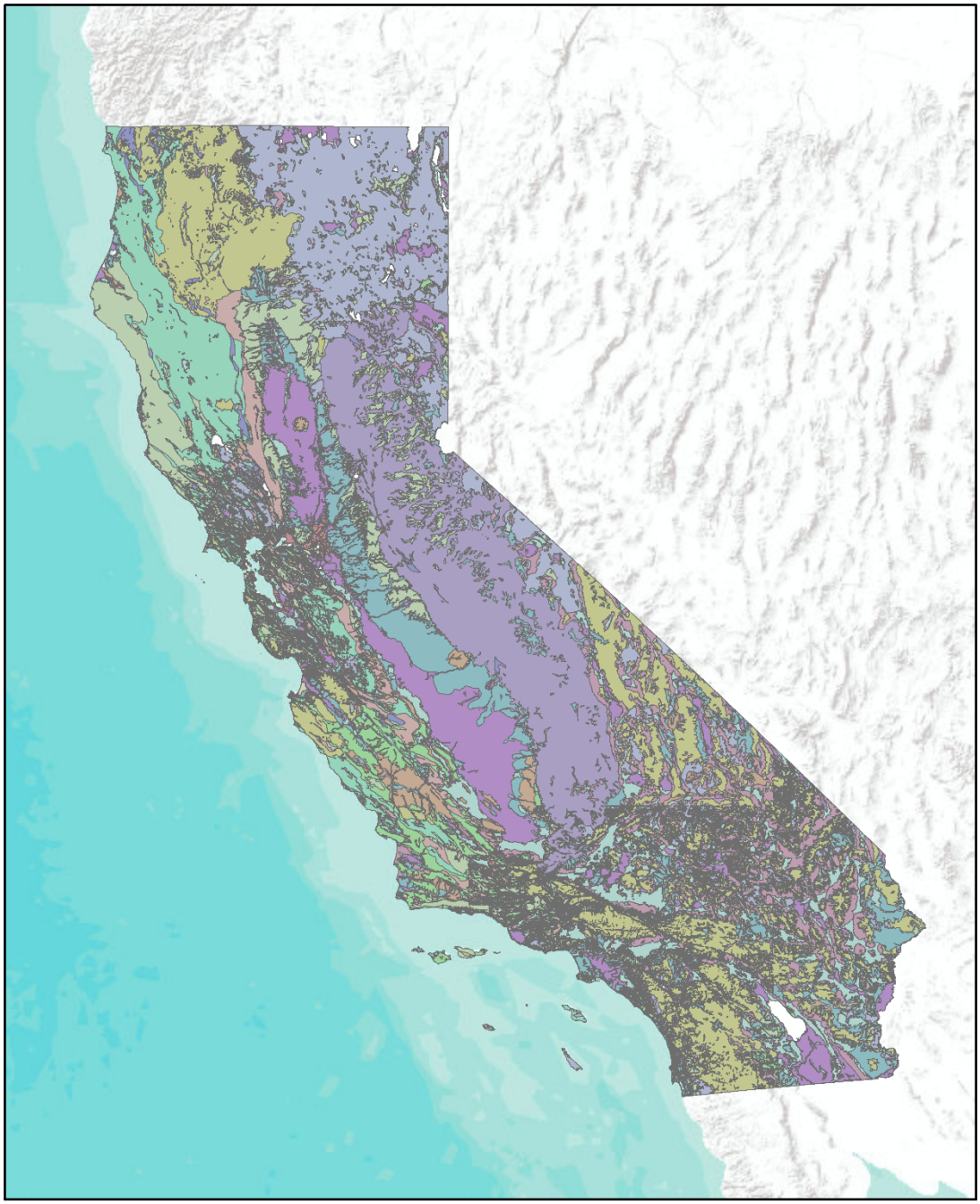

Figure A-7: Geologic Map the Bay Area Region from Witter et al. (2006)

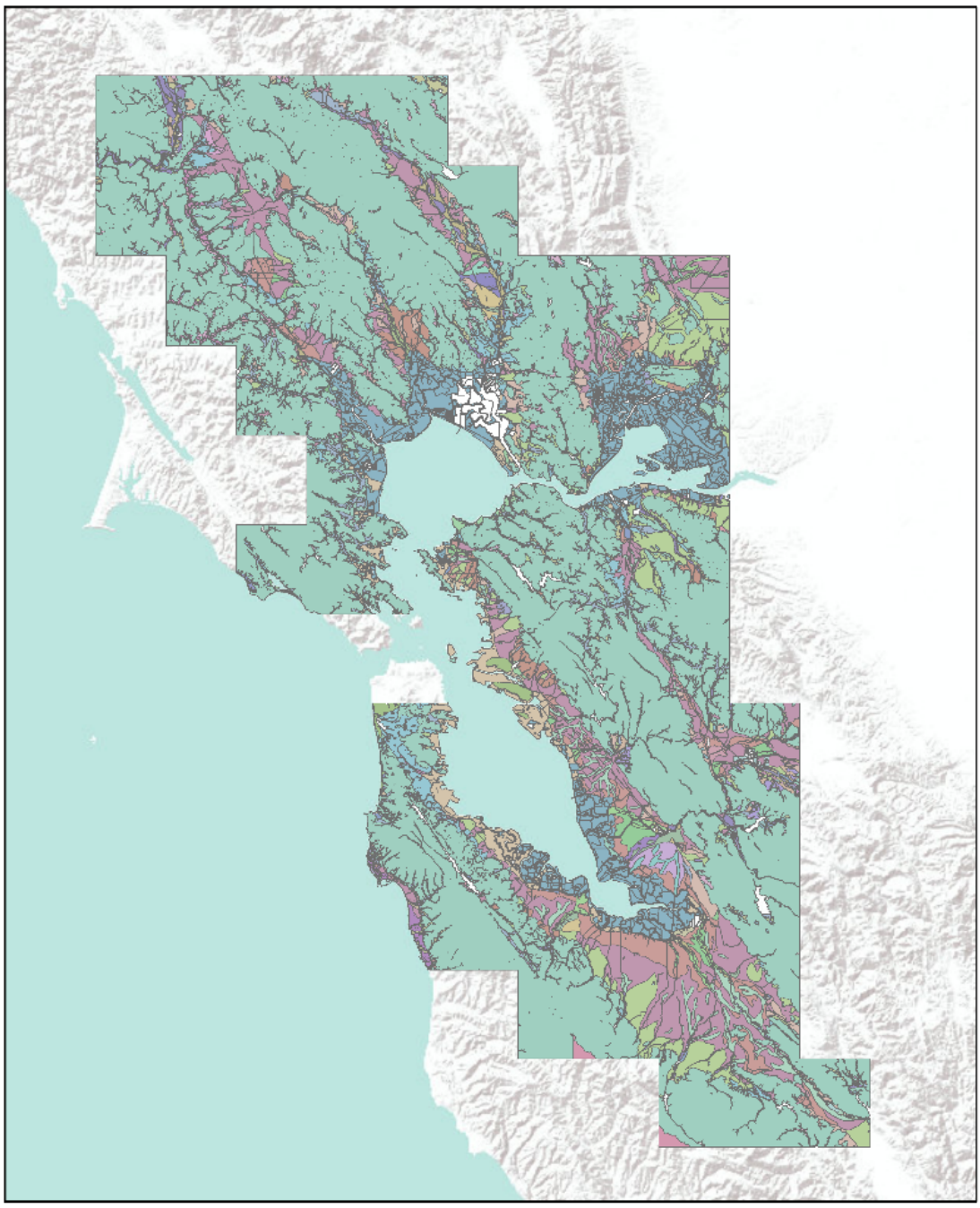

Figure A-8: Geologic Map the Los Angeles Region from Bedrossian et al. (2012)

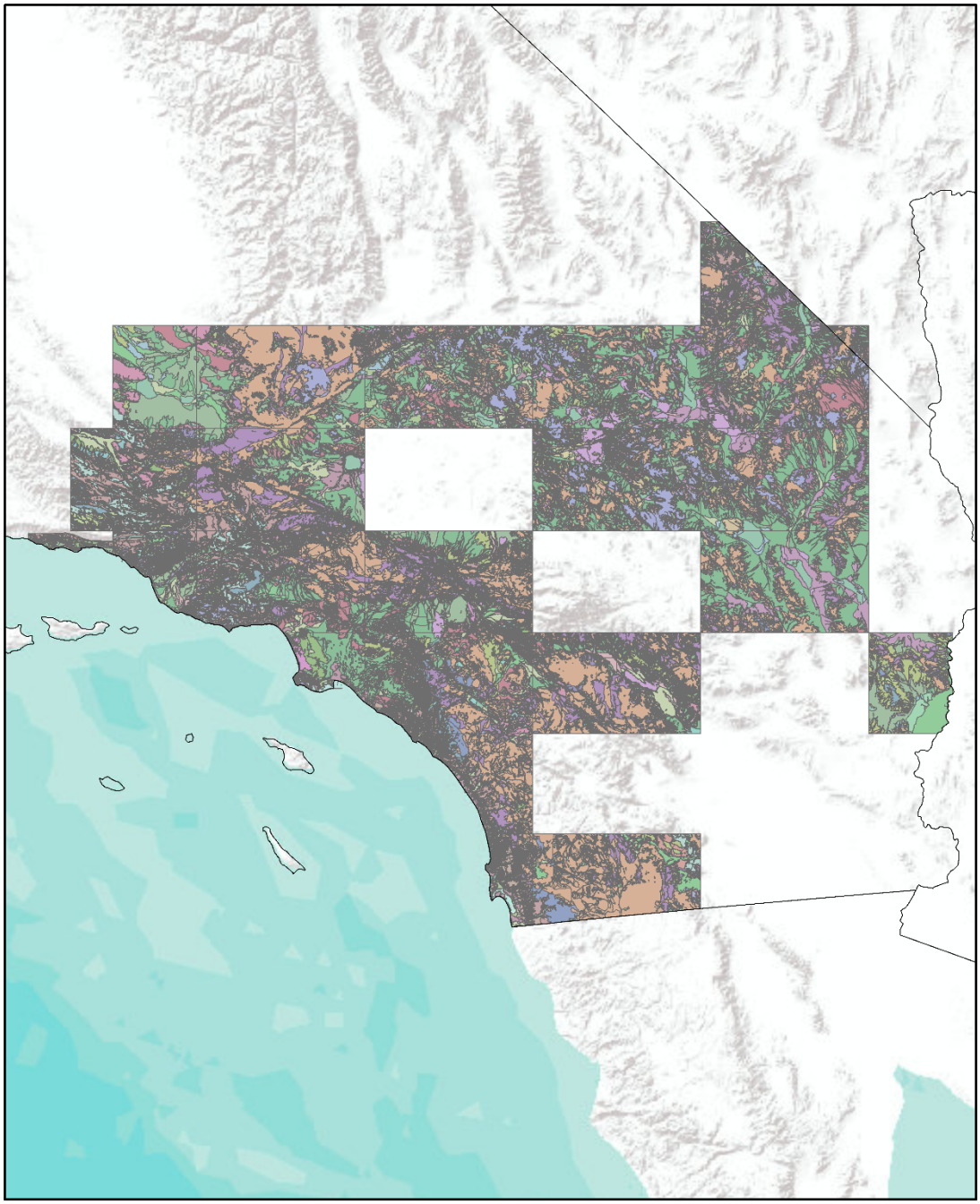

Figure A-9:Statewide Digital Elevation Model (Zhu et al. 2017)

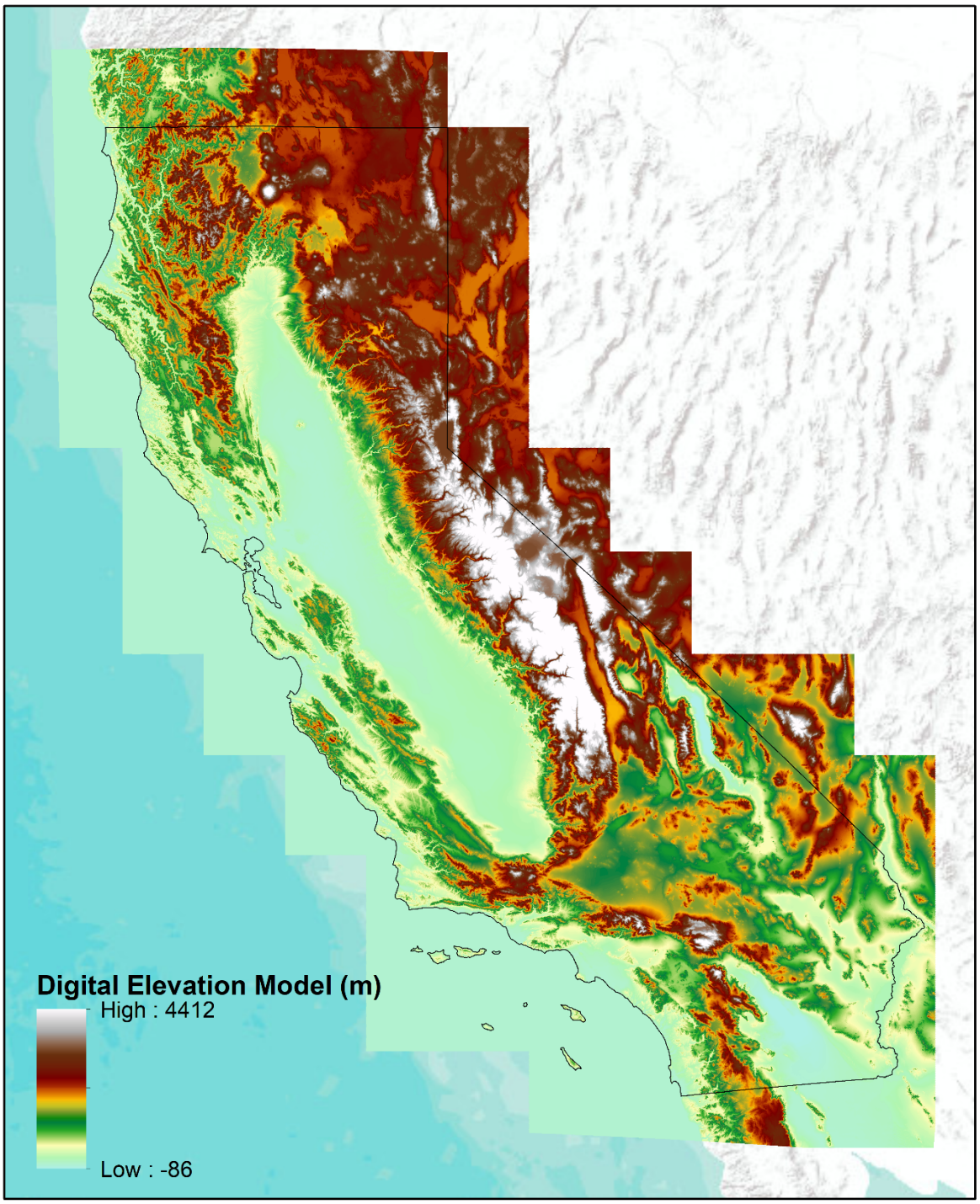

Figure A-10: Statewide Slope (Zhu et al. 2017)

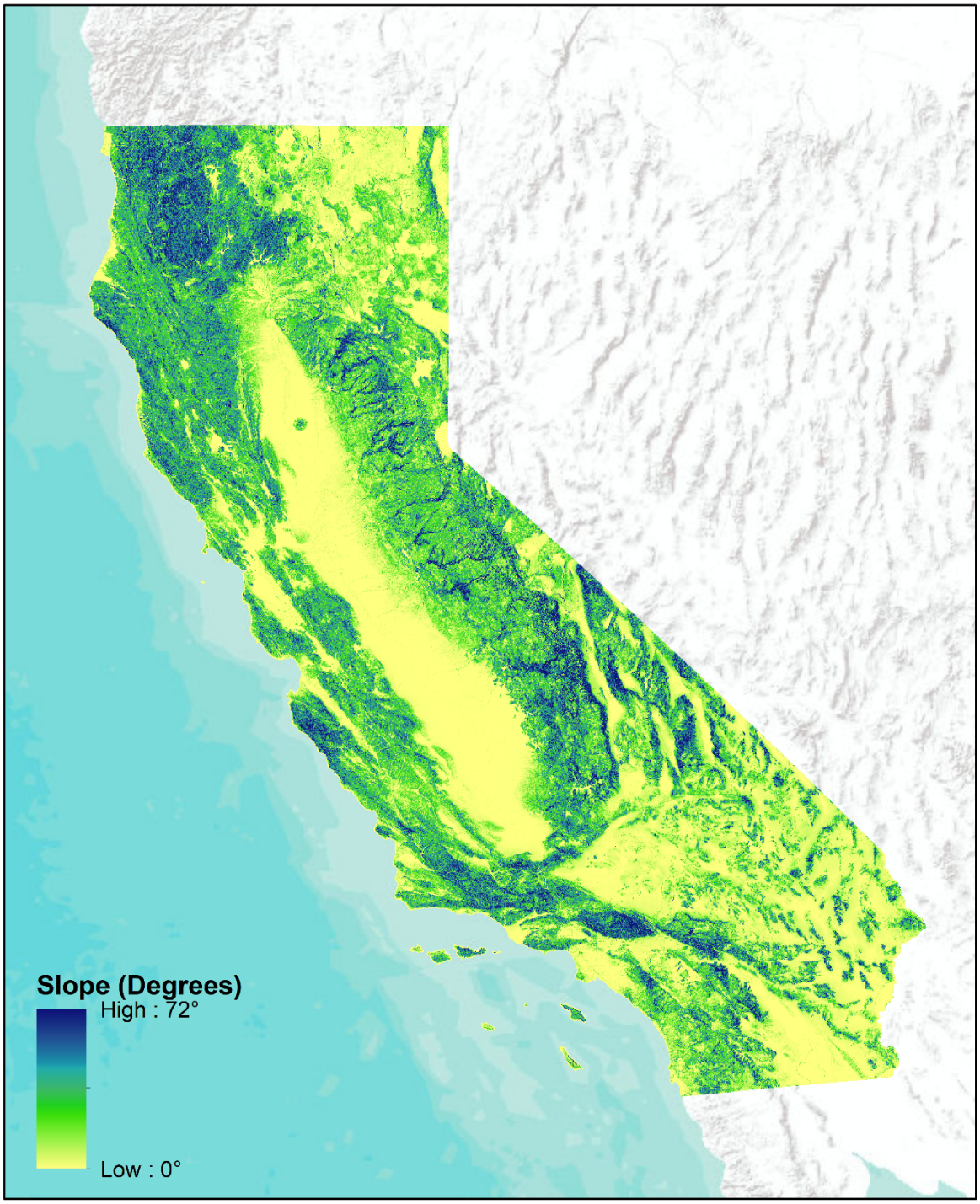

Figure A-11: Compound Topographic Index (Zhu et al. 2017)

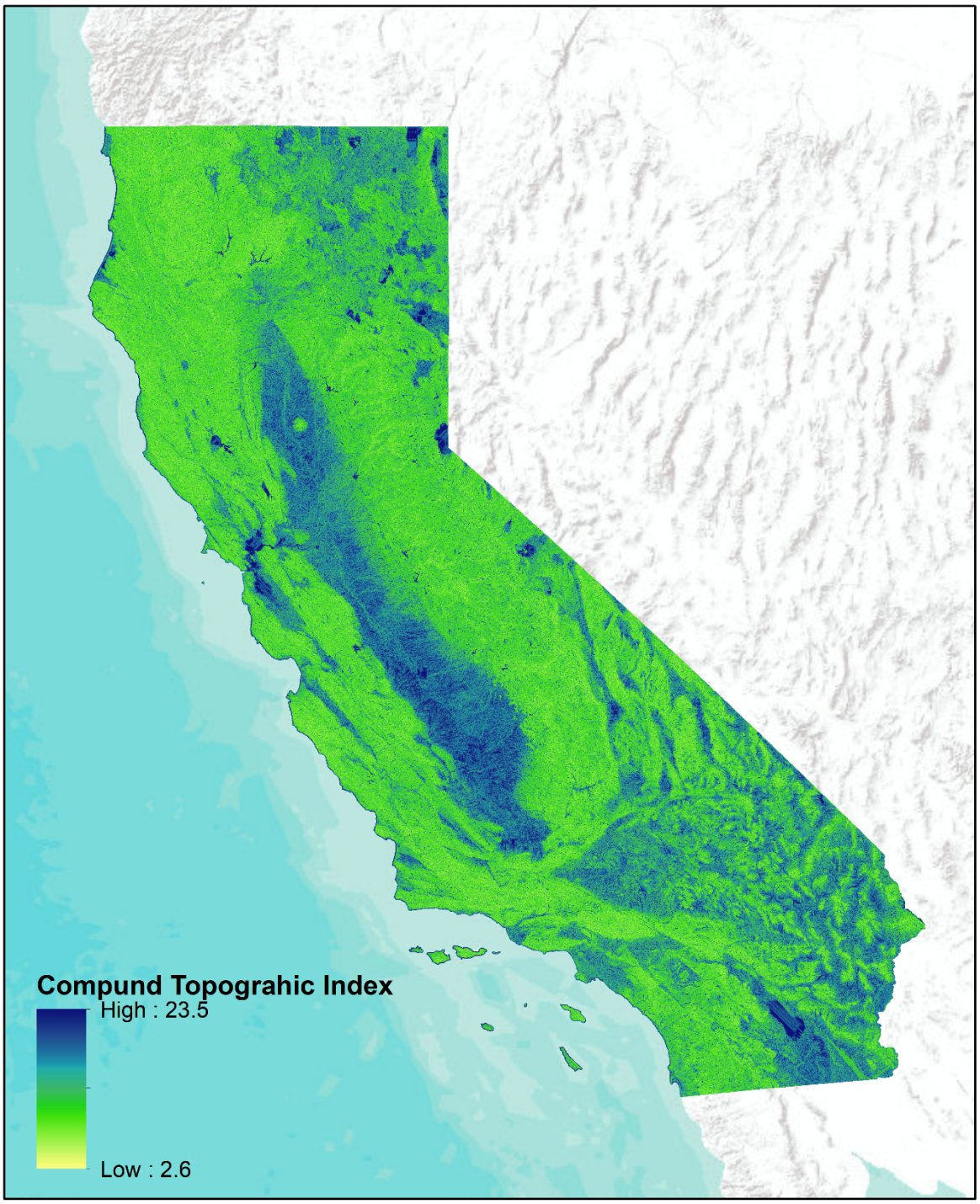

APPENDIX B:
LOGIC TREE FOR PIPELINE CROSSING

This appendix provides the logic tree to determine pipeline crossing and strain model to use for each of the geohazards: fault rupture, landslide, lateral spread, and liquefaction-induced lateral spread and settlement.

B.1 Default Distributions for Parameters

Three angles describe the problem geometry, and three-dimensional figures showing both the angles and ground movement, Δf, are provided for each type of pipeline-ground deformation crossing. For example, on page 3 the angles and Δf are shown for a pipeline subjected to left lateral strike-slip movement. The three angles are defined as follows:

β – pipeline obliquity angle ($0° < \beta < 180°$) is the smallest horizontal angle measured between the orientation of the longitudinal pipeline axis and the strike-slip component of motion on the failure plane. If the failure plane is pure dip-slip, β is the smallest horizontal angle measured between the orientation of the longitudinal pipeline axis and the strike of the failure plane according to the right-hand rule. The orientation of the pipeline is determined by vectorizing the pipeline to be pointing towards the hanging wall side of the fault (i.e., within 90 degrees or less of the dip direction azimuth). Failure planes may be faults or the edges of landslides, lateral spreads, or areas of liquefaction-induced ground settlement.

θ – rake angle ($-180° \leqslant \theta \leqslant 180°$) is measured on the failure plane, and is the angle measured from the failure plane's strike azimuth to the hanging wall displacement direction (relative to a fixed footwall). End member rake values are as follows: 0° defines pure left-lateral movement, 90° indicates pure reverse-slip movement, ±180° indicates pure right-lateral movement, and -90° indicates pure normal-slip movement. Angles between these end members represent a combination of lateral- and dip-slip movement. For example, -135° is right-lateral-normal displacement and 45° is left-lateral-reverse displacement.

ψ – dip angle ($0° < \psi \leqslant 90°$) is the vertical angle (within the range of 0° to 90°) from the horizontal plane to the ground deformation plane measured perpendicular to its strike.

B.2 Logic Tree for Pipelines Crossing Faults

At fault crossings, the preferred values of β, Ψ, and θ are derived from information in the Third Uniform California Earthquake Rupture Forecast (UCERF3) model. Specifically, the UCERF3 model prescribes fault-subsection-average values for θ, Ψ, and the azimuth of the down-dip direction (dip direction azimuth) of the fault plane. The strike of the fault plane needed to calculate β can be derived by adding or subtracting 90° to or from the dip direction azimuth.

All three angles are defined by the Uniform California Earthquake Rupture Forecast (UCERF) model (currently Version 3) at fault crossings, but the assessment can be simplified for cases that are predominantly strike-slip, normal-slip, or reverse-slip. This is common in practice

(e.g., the Hayward fault has a small vertical component of deformation but is often assessed assuming pure strike-slip deformation). We propose to simplify assessments at fault crossings as follows:

- $if \begin{cases} \frac{strike-slip\ deformation}{dip-slip\ deformation} > 4 \quad \rightarrow \quad Analyze\ as\ pure\ strike-slip \\ \frac{dip-slip\ deformation}{strike-slip\ deformation} > 4 \quad \rightarrow \quad Analyze\ as\ pure\ dip-slip \end{cases}$
- $else \quad \rightarrow \quad Use\ full\ offset\ method\ patch\ (currently)\ to\ assess\ oblique\ movements$

The limiting ratio values of > 4 noted above translate to rake angles that are more than 14° from the end-member values of 0° and 180° (for strike-slip faulting) or -90° and 90° (for normal and reverse dip-slip faulting, respectively). The analysis method and corresponding rake angle ranges are listed in the following table:

Analysis method	**Range of Rake Angle (degrees)**
Pure Strike-Slip	-14 to 14 (Pure Left-Lateral); θ ≤ -166 or θ ≥ 166 (Pure Right-Lateral)
Pure Dip-Slip	-104 to -76 (Pure Normal); 76 to 104 (Pure Reverse)
Oblique (Full-Offset Method)	All Other Rakes

The cases outlined here apply at Levels 1, 2, and 3.

Case 1: Left Lateral Strike-Slip Fault Displacement

Parameter Range for Case 1:

$0° < \beta < 180°$

$-14° \leq \theta \leq 14°$

$0° < \Psi \leq 90°$

Pipe Strain Assessment Model to Use Based on β:

IF $0° < \beta \leq 90°$: Hutabarat et al. Strike-Slip Tension Model with Parameters:

$\beta = \beta$

$\Delta_f = \Delta_f|\cos(\theta)|$

IF $90° < \beta < 180°$: Hutabarat et al. Strike-Slip Compression Model with Parameters:

$\beta = \beta$

$\Delta_f = \Delta_f|\cos(\theta)|$

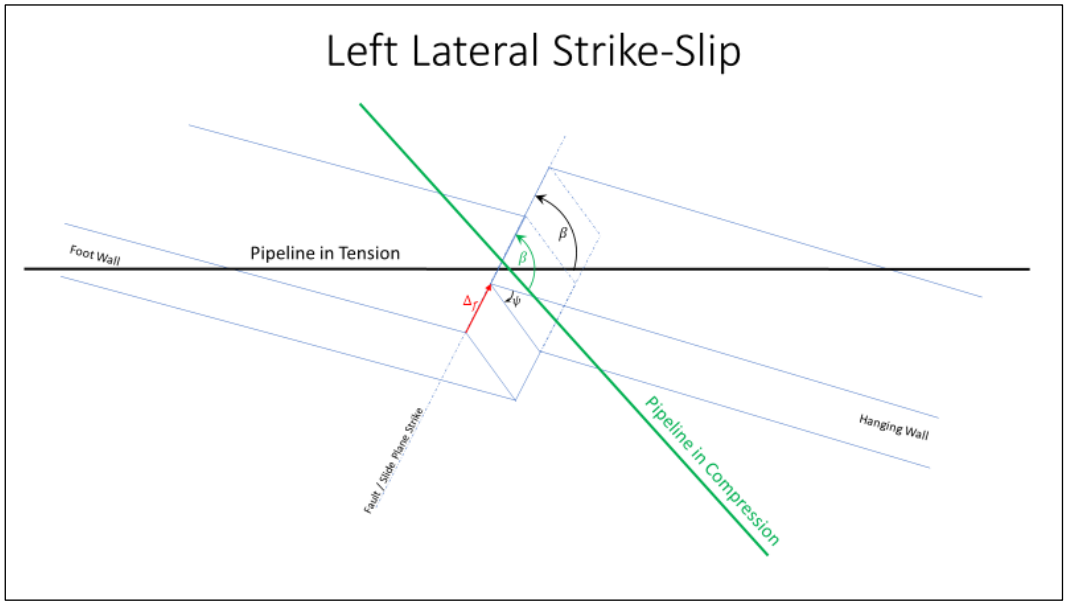

Case 2: Oblique Normal with Left Lateral Strike-Slip

Parameter Range for Case 2:

$0° < \beta < 180°$

$-76° < \theta < 14°$

$0° < \Psi \leq 90°$

Pipe Strain Assessment Model to Use Based on β:

IF $0 < \beta \leq 90°$: Full-Offset Method with Hutabarat et al. Strike-Slip Tension and Normal-Slip Models with Parameters:

$$\beta = \beta\ for\ Strike-Slip\ Tension\ Model$$

$$\Delta_f = \Delta_f\ for\ Strike-Slip\ Tension\ Model$$

$$\psi = \psi\ for\ Normal-Slip\ \ Model$$

$$\Delta_f = \Delta_f \left(\frac{1}{|\cos(90-\beta)|}\right)\ for\ Normal-Slip\ Model$$

IF $90° < \beta < 180°$: Worst Case Scenario Between Hutabarat et al. Strike-Slip Compression and Normal-Slip Models (Likely to be Strike-Slip Compression Model) with Parameters:

$$\beta = \beta\ for\ Strike-Slip\ Compression\ Model$$

$$\Delta_f = \Delta_f\ for\ Strike-Slip\ Compression\ Model$$

$$\psi = \psi\ for\ Normal-Slip\ \ Model$$

$$\Delta_f = \Delta_f \left(\frac{1}{|\cos(90-\beta)|}\right)\ for\ Normal-Slip\ Model$$

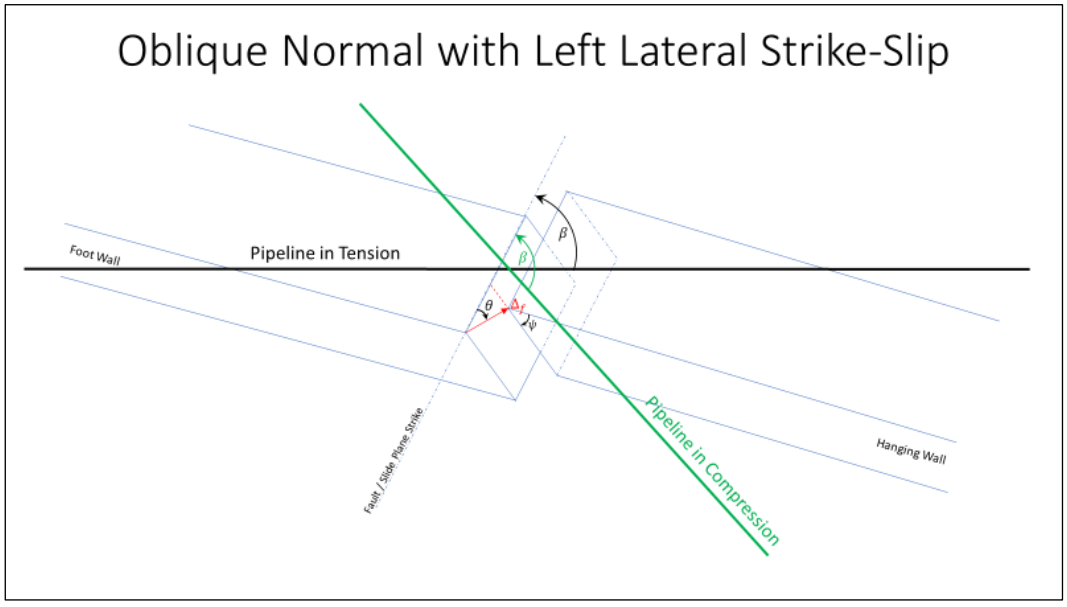

Case 3: Normal-Slip

Parameter Range for Case 3:

$0° < \beta < 180°$

$-104° \leq \theta \leq -76°$

$0° < \Psi \leq 90°$

Pipe Strain Assessment Model to Use Based on θ:

Hutabarat et al. Normal-Slip Model with Parameters:

$$\Delta_f = \Delta_f * \left(\frac{1}{|\cos(90-\beta)|}\right) \; for \; Normal - Slip \; Model$$

$$\psi = \psi \; for \; Normal - Slip \;\; Model$$

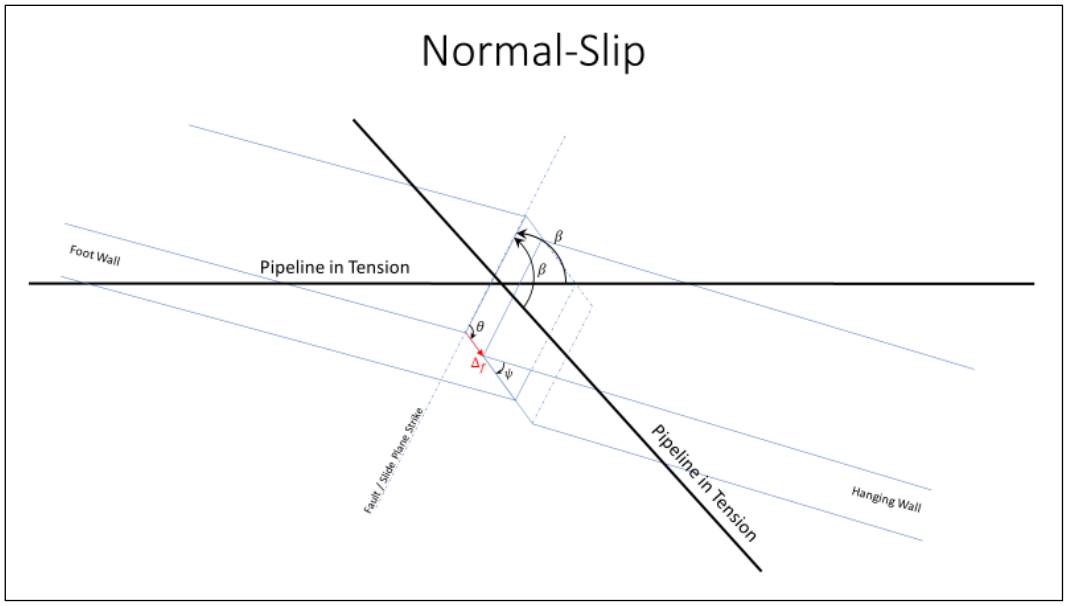

Case 4: Oblique Normal with Right Lateral Strike-Slip

Parameter Range for Case 4:

$0° < \beta < 180°$

$-166° < \theta < -104°$

$0° < \Psi \leq 90°$

Pipe Strain Assessment Model to Use Based on β:

IF $0 < \beta \leq 90°$: Full-Offset Method with Hutabarat et al. Strike-Slip Tension and Normal-Slip Models with Parameters:

$$\beta = \beta\ for\ Strike-Slip\ Tension\ Model$$

$$\Delta_f = \Delta_f\ for\ Strike-Slip\ Tension\ Model$$

$$\psi = \psi\ for\ Normal-Slip\ \ Model$$

$$\Delta_f = \Delta_f * \left(\frac{1}{|\cos(90-\beta)|}\right)\ for\ Normal-Slip\ Model$$

IF $90° < \beta < 180°$: Worst Case Scenario Between Hutabarat et al. Strike-Slip Compression and Normal-Slip Models (Likely to be Strike-Slip Compression) with Parameters:

$$\beta = \beta\ for\ Strike-Slip\ Compression\ Model$$

$$\Delta_f = \Delta_f\ for\ Strike-Slip\ Compression\ Model$$

$$\psi = \psi\ for\ Normal-Slip\ \ Model$$

$$\Delta_f = \Delta_f * \left(\frac{1}{|\cos(90-\beta)|}\right)\ for\ Normal-Slip\ Model$$

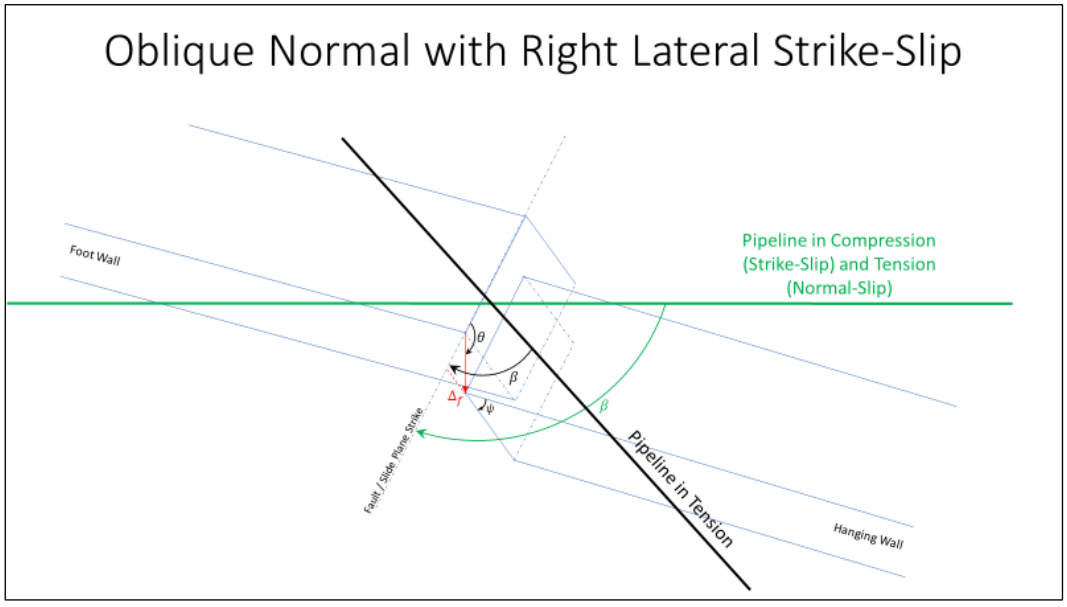

Case 5: Right Lateral Strike-Slip

Parameter Range for Case 5:

$0° < \beta < 180°$

$166° \leq \theta \leq -166°$

$0° < \Psi \leq 90°$

Pipe Strain Assessment Model to Use Based on β:

IF $0 < \beta \leq 90°$: Hutabarat et al. Strike-Slip Tension Model with Parameters:

$\beta = \beta$

$\Delta_f = \Delta_f$

IF $90° < \beta < 180°$: Hutabarat et al. Strike-Slip Compression Model with Parameters:

$\beta = \beta$

$\Delta_f = \Delta_f$

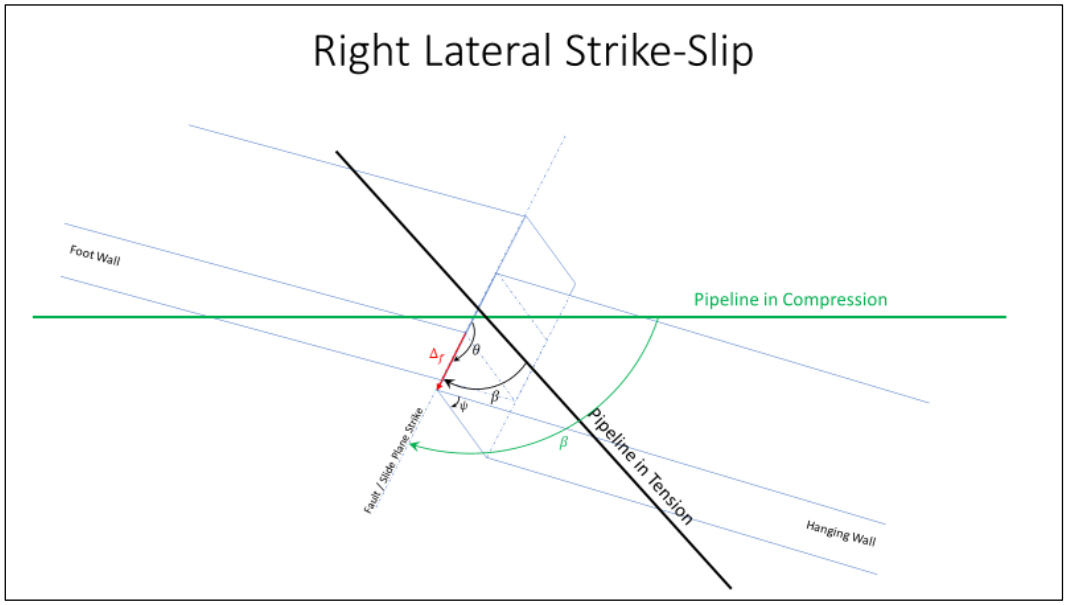

Case 6: Oblique Reverse with Left Lateral Strike-Slip

Parameter Range for Case 6:

$0° < \beta < 180°$

$14° < \theta < 76°$

$0° < \Psi \leq 90°$

Pipe Strain Assessment Model to Use Based on θ:

IF $0 < \beta \leq 90°$: Use Worst Case Scenario Between Hutabarat et al. Strike-Slip Tension and Reverse-Slip Models (Likely to be Reverse-Slip Model) with Parameters:

$$\beta = \beta\ for\ Strike-Slip\ Tension\ Model$$

$$\Delta_f = \Delta_f\ for\ Strike-Slip\ Tension\ Model$$

$$\psi = \psi\ for\ Reverse-Slip\ \ Model$$

$$\Delta_f = \Delta_f * \left(\frac{1}{|\cos(90-\beta)|}\right)\ for\ Reverse-Slip\ Model$$

IF $90° < \beta < 180°$: Full-Offset Method with Hutabarat et al. Strike-Slip Compression and Reverse-Slip Models with Parameters:

$$\beta = \beta\ for\ Strike-Slip\ Compression\ Model$$

$$\Delta_f = \Delta_f\ for\ Strike-Slip\ Compression\ Model$$

$$\psi = \psi\ for\ Reverse-Slip\ \ Model$$

$$\Delta_f = \Delta_f * \left(\frac{1}{|\cos(90-\beta)|}\right)\ for\ Reverse-Slip\ Model$$

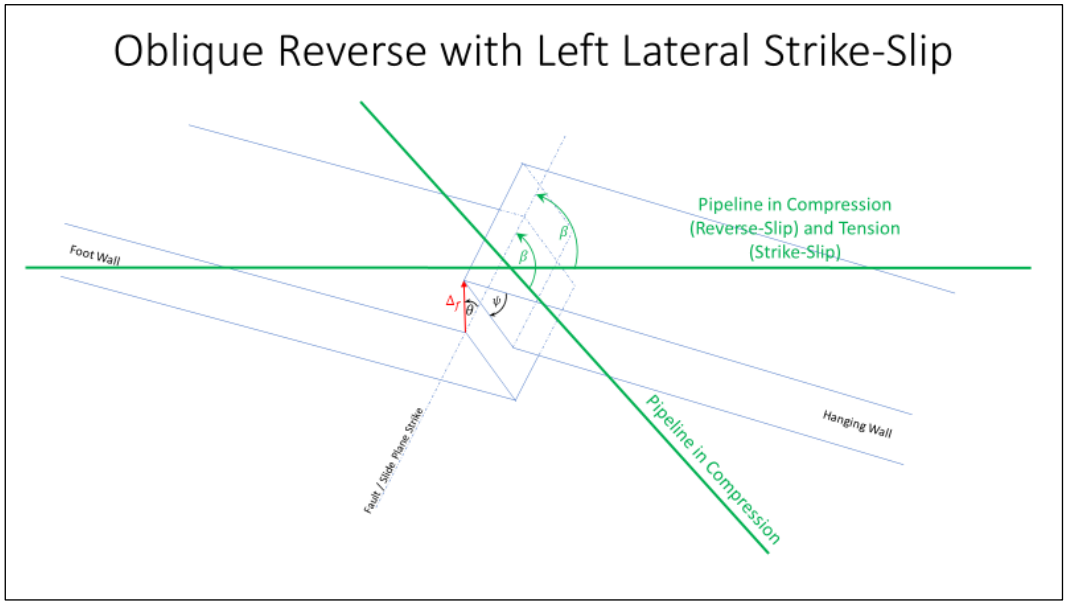

Case 7: Reverse-Slip

Parameter Range for Case 7:

$0° < \beta < 180°$

$76° \leq \theta \leq 104°$

$0° < \Psi \leq 90°$

Pipe Strain Assessment Model to Use Based on θ:

Hutabarat et al. Reverse-Slip Model with Parameters:

$$\psi = \psi \; for \; Reverse - Slip \;\; Model$$

$$\Delta_f = \Delta_f * \left(\frac{1}{|\cos(90-\beta)|}\right) \; for \; Reverse - Slip \; Model$$

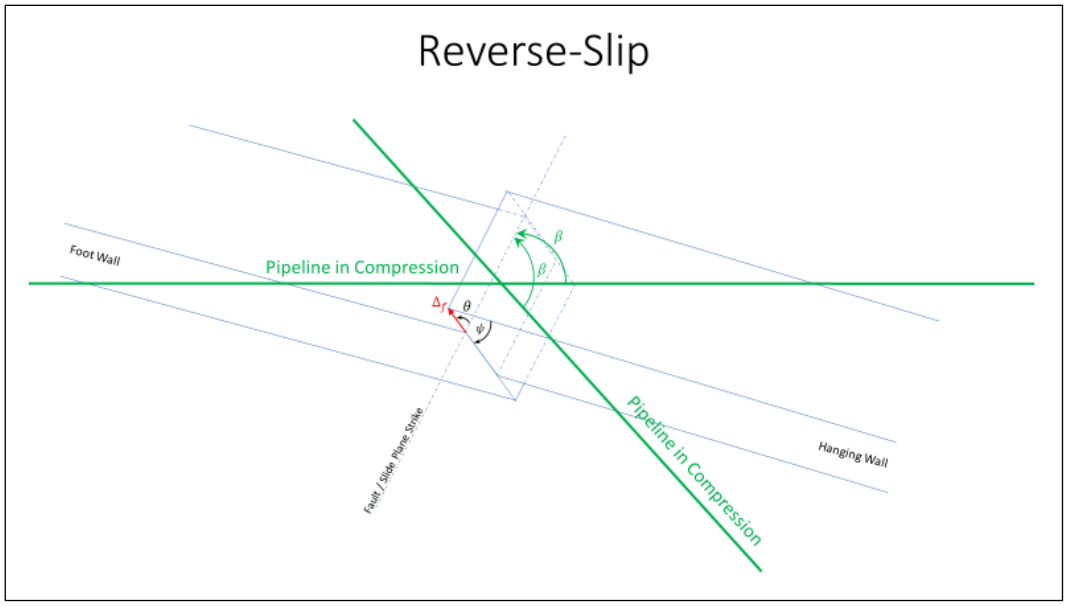

Case 8: Oblique Reverse with Right Lateral Strike-Slip

Parameter Range for Case 8:

$0° < \beta < 180°$

$104° < \theta < 166°$

$0° < \Psi \leq 90°$

Pipe Strain Assessment Model to Use Based on β:

IF $0 < \beta \leq 90°$: Worst Case Scenario Between Hutabarat et al. Strike-Slip Tension and Reverse-Slip Models (Likely to be Reverse-Slip Model) with Parameters:

$$\beta = \beta\ for\ Strike - Slip\ Tension\ Model$$

$$\Delta_f = \Delta_f\ for\ Strike - Slip\ Tension\ Model$$

$$\psi = \psi\ for\ Reverse - Slip\ \ Model$$

$$\Delta_f = \Delta_f * \left(\frac{1}{|\cos(90-\beta)|}\right)\ for\ Reverse - Slip\ Model$$

IF $90° < \beta < 180°$: Full-Offset Method with Hutabarat et al. Strike-Slip Compression and Reverse-Slip Models with Parameters:

$$\beta = \beta\ for\ Strike - Slip\ Compression\ Model$$

$$\Delta_f = \Delta_f\ for\ Strike - Slip\ Compression\ Model$$

$$\psi = \psi\ for\ Reverse - Slip\ \ Model$$

$$\Delta_f = \Delta_f * \left(\frac{1}{|\cos(90-\beta)|}\right)\ for\ Reverse - Slip\ Model$$

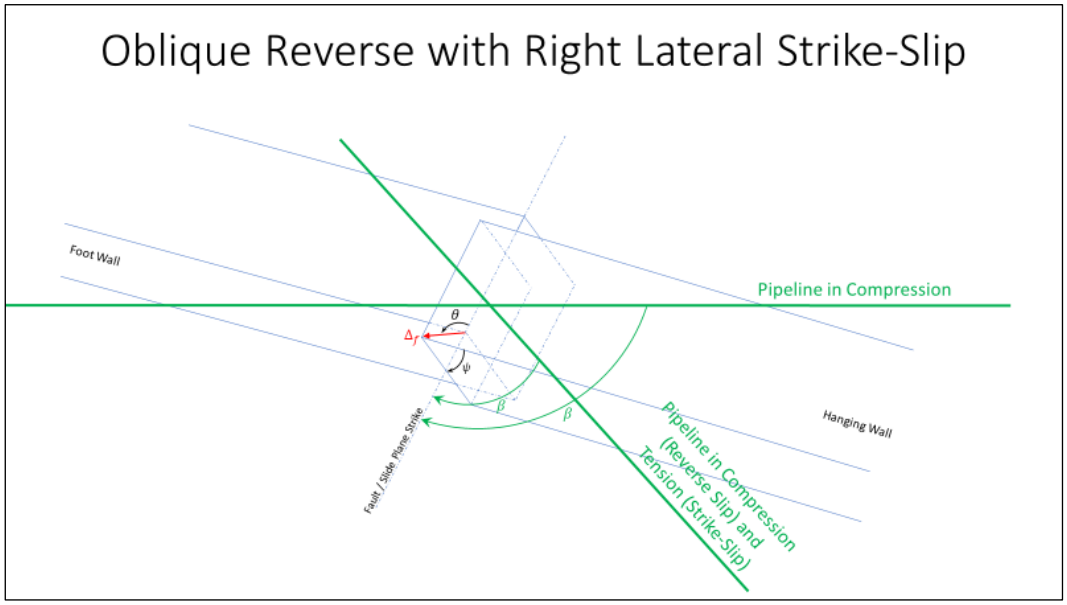

B.3 Logic Tree for Pipelines Crossing Landslides

To assess risk from earthquake-induced slope displacement, *OpenSRA* will first discretize the pipelines into approximately 100-m long segments. At the midpoint of each segment, each of the parameters necessary to perform the seismic slope displacement assessment are sampled from their respective distributions to get a sense of the epistemic uncertainty. For each combination of parameters, the seismic slope displacement is calculated and if the estimated displacement is less than or equal to 5 cm, the displacement is assumed to be negligible (i.e., zero), and the probability of leakage or rupture is assumed to be zero. For non-negligible seismic slope displacement (greater than 5 cm), the probability of tensile leakage or rupture or compressive rupture is estimated. Finally, *OpenSRA* reports the risk as the percentiles (i.e., 5^{th}, 16^{th}, 50^{th}, 84^{th}, and 95^{th}) for the probability of tensile leakage or rupture and the probability of compressive rupture at each pipe segment.

At Level 1, no landslide polygons are available at the statewide level. Rather, the ground displacement hazard is evaluated assuming infinite slope type failures with distributions of geotechnical strength parameters correlated to the units in the statewide Wills et al. (2015) geologic map and slope based on a statewide slope map with approximately 30 m resolution. The steps for assessing risk from seismic slope displacement at Level 1 are outlined below:

1. If the estimated seismic slope displacement for a combination of the input parameters is less than or equal to 5 cm, assume no (i.e., negligible) displacement of the landslide. The probability of tensile leakage or rupture and the probability of compressive rupture is therefore zero for this combination of parameters.
2. If non-negligible seismic slope displacement (greater than 5 cm) is calculated for a combination of the input parameters, assume a pipeline in this zone has a 25% chance of crossing the edge of a landslide. This is applied by multiplying the resulting probability of leakage or rupture by 0.25.
3. At Level 1, there is insufficient information without polygons to check if a pipeline crosses the scarp or toe of a landslide; therefore, assume pipeline/landslide interaction can be assessed as strike-slip ground deformation. Assess the pipeline using the Hutabarat et al. strike-slip compression model.

At Level 2, the landslide polygons from the CGS landslide inventory are used unless the user inputs an alternative set of landslide polygons. A Level 2 assessment does not have site-specific geotechnical strength data. The analysis steps at Level 2 are as follows:

1. First, check location of pipeline crossings in an area defined as a landslide using the polygons from the CGS landslide inventory, or as an alternative, a set of user-defined landslide polygons. The length of the landslide is defined by the length of a line from the highest point of the landslide feature (i.e., scarp) to the lowest point of the landslide feature (i.e., toe). This vector from the scarp to the toe of the landslide is also assumed to define the direction of the landslide movement. If the pipeline crosses in the upper 15% of the line that defines the landslide length, assume it crosses the scarp. If it crosses in the bottom 15% of the line that defines the landslide length, assume it crosses the toe. If it crosses the middle 70%, assume it crosses the body of the landslide. *OpenSRA* will determine the locations of pipeline/landslide intersections and perform the assessment at those locations.

2. Second, check the pipeline crossing angle relative to the direction of the landslide movement. Refer to the figures that follow which illustrate the cases described in this step.
    - If the pipeline crosses within ±20° of the orientation of the line that defines the length of the landslide, assume pure normal-slip at the scarp and pure reverse-slip at the toe.
    - If the pipeline crosses within 20° - 45° of the orientation of the line that defines the length of the landslide, assume the pipeline is in a transition zone between pure normal-slip and pure strike-slip at the upper part of the landslide with a linear weighting factor or it is in a transition zone between pure reverse-slip and pure strike-slip at the lower part of the landslide with a linear weighting factor.
    - If the pipeline crosses at an angle greater than 45° from the orientation of the line that defines the length of the landslide AND it crosses the landslide body, assume pure strike-slip displacement.
    - If it crosses at an angle greater than 45° from the orientation of the line that defines the length of the landslide AND it crosses the landslide scarp area, assume pure normal-slip displacement.
    - If it crosses at an angle greater than 45° from the orientation of the line that defines the length of the landslide AND it crosses the landslide toe area, assume pure reverse-slip displacement.
3. For pure normal-slip, assume $\theta = -90°$ and a mean value of $\Psi = 65°$. Lower and upper limits of Ψ are $\Psi = 45°$ and $\Psi = 90°$. For pure reverse-slip, assume $\theta = 90°$ and a mean value of $\Psi = 35°$. Lower and upper limits of Ψ are $\Psi = 25°$ and $\Psi = 50°$.
4. In the transition zones, assume mean value of $\Psi = 65°$ and $\theta = -90°$ for pure normal-slip, a mean value of $\Psi = 35°$ and $\theta = 90°$ for pure reverse-slip, and $\theta = 0°$ or $\theta = 180°$ (pure left or right lateral movement, respectively) for strike-slip. *OpenSRA* will determine if the pipeline will be in the strike-slip compression or tension mode based on the β angle and relative motion (left lateral or right lateral) of the landslide and the stable, non-moving ground.

At Level 3, the user should input landslide polygons; the CGS landslide inventory landslide polygons are used as a default if the user chooses not to input landslide polygons. The analysis steps at Level 3 are as follows:

1. First, check the location of pipeline crossings in an area defined as a landslide using the user input landslide polygons, or if not provided, using the CGS landslide inventory landslide polygons as a default. The user-defined landslide polygons must include an attribute indicating the slip direction azimuth. The length of the landslide is defined by the length of a line from the highest point of the landslide feature (i.e., scarp) to the lowest point of the landslide feature (i.e., toe) by sampling from a DEM map. If the pipeline crosses in the upper 15% of the line that defines the landslide length, assume it crosses the scarp. If it crosses in the bottom 15% of the line that defines the landslide length, assume it crosses the toe. If it crosses the middle 70%, assume it crosses the body of the landslide.

2. Second, check the pipeline crossing angle relative to the direction of the landslide movement. Refer to the figures that follow which illustrate the cases described in this step. These five assumptions are the same as used in Level 2 analyses.
    - If the pipeline crosses within ±20° of the orientation of the landslide slip direction vector, assume pure normal-slip at the scarp and pure reverse-slip at the toe.
    - If the pipeline crosses within 20° - 45° of the orientation of the landslide slip direction vector, assume the pipeline is in a transition zone between pure normal-slip and pure strike-slip at the upper part of the landslide with a linear weighting factor or it is in a transition zone between pure reverse-slip and pure strike-slip at the lower part of the landslide with a linear weighting factor.
    - If the pipeline crosses at an angle greater than 45° from the orientation of the landslide slip direction vector AND it crosses the landslide body, assume pure strike-slip displacement.
    - If it crosses at an angle greater than 45° from the orientation of the landslide slip direction vector AND it crosses the landslide scarp area, assume pure normal-slip displacement.
    - If it crosses at an angle greater than 45° from the orientation of the line landslide slip direction vector AND it crosses the landslide toe area, assume pure reverse-slip displacement.
3. For pure normal-slip, assume $\theta = -90°$ and a mean value of $\Psi = 65°$. Lower and upper limits of Ψ are $\Psi = 45°$ and $\Psi = 90°$. For pure reverse-slip, assume $\theta = 90°$ and a mean value of $\Psi = 35°$. Lower and upper limits of Ψ are $\Psi = 25°$ and $\Psi = 50°$.
4. In the transition zones, assume mean value of $\Psi = 65°$ and $\theta = -90°$ for pure normal-slip, a mean value of $\Psi = 35°$ and $\theta = 90°$ for pure reverse-slip, and $\theta = 0°$ or $\theta = 180°$ (pure left or right lateral movement, respectively) for strike-slip. *OpenSRA* will determine if the pipeline will be in strike-slip compression or tension mode based on the β angle.

Landslide Crossings – Levels 2 and 3
Check Location of Pipe in Slide

First, check location of pipeline crossings in landslide

- IF upper 15% – scarp
- IF bottom 15% – toe
- IF middle 70% – body

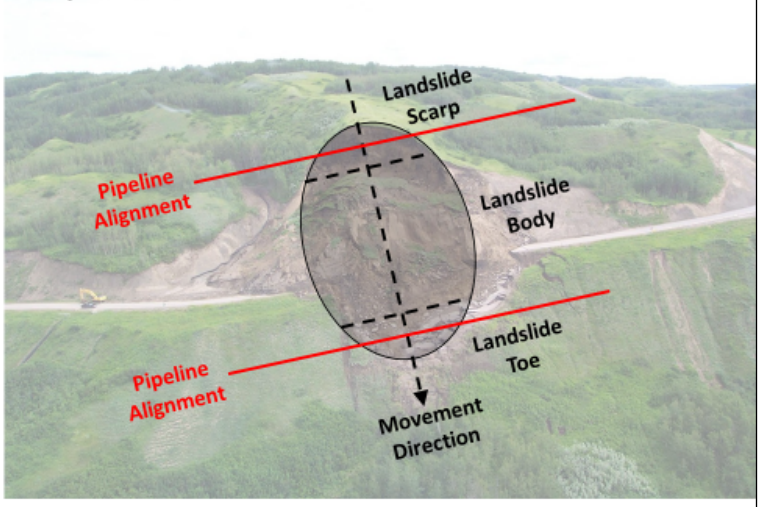

Landslide Crossings – Levels 2 and 3 (Cont.)
Check Relative Pipeline/Slip Direction

Second, check pipeline crossing angle relative to direction of movement as follows:

- Pure normal-slip or pure reverse-slip
- Transition Zone: Pure normal-slip and pure strike-slip with linear weighting factor or pure reverse-slip and pure strike-slip with linear weighting factor
- Pure strike-slip if crossing body; pure normal-slip if crossing scarp; pure reverse-slip if crossing toe

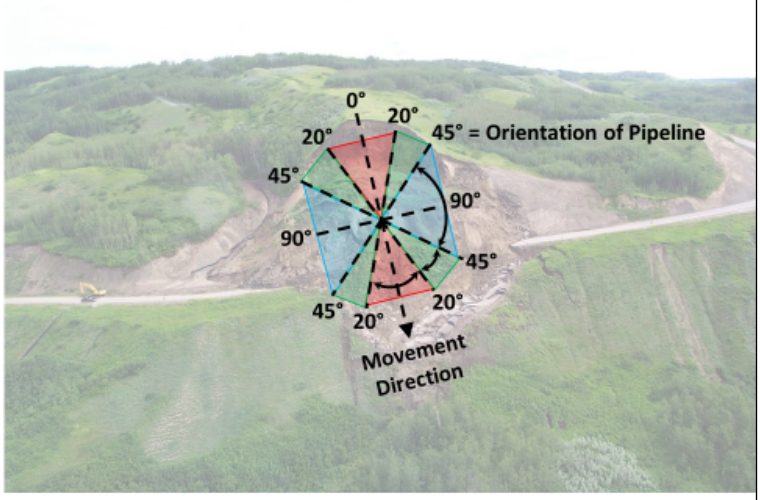

B.4 Logic Tree for Pipelines Crossing Lateral Spreads

To assess risk from liquefaction-induced lateral spreading, *OpenSRA* will first discretize the pipelines into approximately 100-m long segments. At the midpoint of each segment, each of the parameters necessary to perform the lateral spread displacement assessment are sampled from their respective distributions to get a sense of the epistemic uncertainty. For each combination of parameters, the lateral spread displacement (D_H) is calculated and if the estimated displacement is less than or equal to 5 cm, the displacement is assumed to be negligible (i.e., zero), and the probability of leakage or rupture is assumed to be zero. For non-negligible lateral spread displacement (greater than 5 cm), the probability of tensile leakage or rupture or compressive rupture is estimated. Finally, *OpenSRA* reports the risk as the percentiles (i.e., 5^{th}, 16^{th}, 50^{th}, 84^{th}, and 95^{th}) for the probability of tensile leakage or rupture and the probability of compressive rupture at each pipe segment.

Lateral spreading can be differentiating into two cases: lateral spreads influenced by a free-face condition and lateral spreading influenced by a gently sloping ground condition. The free-face ratio (L/H) is used to estimate the displacement for lateral spreads near a free-face condition and is defined as the distance from a point in question to the bottom of the free-face (L) divided by the height of the free-face (H). Topographic slope (%) is used to estimate the displacement for lateral spreads on gently sloping ground.

At Level 1, we do not differentiate between the free face condition and the gently sloping ground condition. At Level 1, if the estimated lateral spread displacement is less than or equal to 5 cm, the displacement is negligible and the probability of tensile leakage or rupture or compressive rupture is zero. For non-negligible displacement (displacement greater than 5 cm), assume that a pipeline has a 25% probability of crossing the edge of a lateral spread. This is applied by multiplying the resulting probability of leakage or rupture by 0.25. Use the Bain et al. idealized block model to estimate pipe strain, assume the estimated pipe strain is in compression.

At Level 2, regardless of which Level 2 method is used to estimate lateral spread displacement, we assume geometry for a generic lateral spread. As at Level 1, if the displacement is negligible (less than or equal to 5 cm), the displacement is assumed to be zero. For non-negligible displacement (displacement greater than 5 cm), assume that a pipeline has a 25% probability of crossing the edge of a lateral spread. This is applied by multiplying the resulting probability of leakage or rupture by 0.25. Next, check the pipeline crossing angle relative to the direction of the lateral spread displacement movement. Refer to the figure that follows which illustrate the cases described in this step.

- If the pipeline crosses within ±30° of the orientation of the lateral spread slip direction vector, assess the pipe strain using the Bain et al. model. Assume the strain is compressive.
- If the pipeline crosses within 30° - 45° of the orientation of the lateral spread slip direction vector, assume the pipeline is in a transition zone between the Bain et al. model and the Hutabarat et al. strike-slip with a linear weighting factor. Assume the pipe strain is compressive.

- If the pipeline crosses at an angle greater than 45° from the orientation of the lateral spread, assess the pipe strain with the Hutabarat et al. strike-slip model. Assume the pipe strain is compressive.
- The lateral spread slip direction is estimated by sampling a statewide slope aspect map.

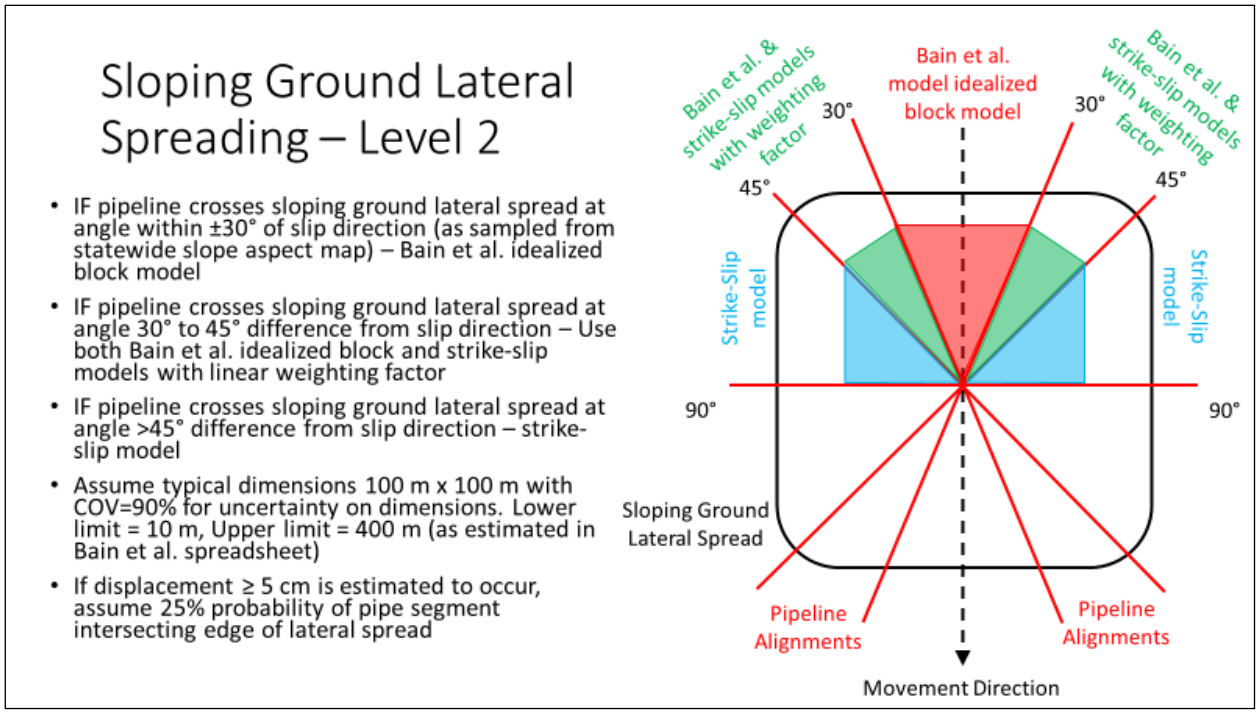

At Level 3, the liquefaction triggering and lateral spread displacement assessment is performed using CPTs, or soil exploratory borings if CPTs are not available. A Level 3 assessment cannot be performed without site-specific data from a CPT or a soil boring. *OpenSRA* takes the CPTs or soil borings data and estimates a lateral spread polygon rather than assuming generic dimensions for a lateral spread. As at Levels 1 and 2, if the estimated displacement is negligible (less than or equal to 5 cm), assume that the displacement is zero.

At Level 3, *OpenSRA* determines whether the free-face condition or gently sloping ground condition controls. To do this, for gently sloping ground lateral spreads, *OpenSRA* will sample an approximately 30 m resolution slope map to estimate the topographic slope at the site in question and calculate the lateral spread displacement. If near a free-face condition, the user should input a shapefile (line feature) indicating the location of the bottom of nearby free-face features and it must include an attribute indicating the height of the free-face feature. *OpenSRA* will then calculate the shortest distance to the free-face feature (L), calculate the free-face ratio (L/H) using the height attribute (H) in the user provided shapefile, and calculate the lateral spread displacement (D_H). The lateral spread displacement is taken as the maximum from the gently sloping ground and free-face conditions. If the user does not provide a shapefile indicating the location of the bottom of nearby free-face feature, *OpenSRA* will assume the gently sloping ground condition controls. If the gently sloping ground condition controls, the pipe strain is calculated as follows:

- If the pipeline crosses within ±30° of the orientation of the lateral spread slip direction vector, assess the pipe strain using the Bain et al. model. Assume the strain is tensile on the upslope side of the lateral spread and compressive on the downslope side.
- If the pipeline crosses within 30° - 45° of the orientation of the lateral spread slip direction vector, assume the pipeline is in a transition zone between the Bain et al. model and the Hutabarat et al. strike-slip models with a linear weighting factor. Assume the strain is tensile on the upslope side of the lateral spread and compressive on the downslope side.
- If the pipeline crosses at an angle greater than 45° from the orientation of the lateral spread slip direction vector, assess the pipe strain with the Hutabarat et al. strike-slip models. Assume the strain is tensile on the upslope side of the lateral spread and compressive on the downslope side.

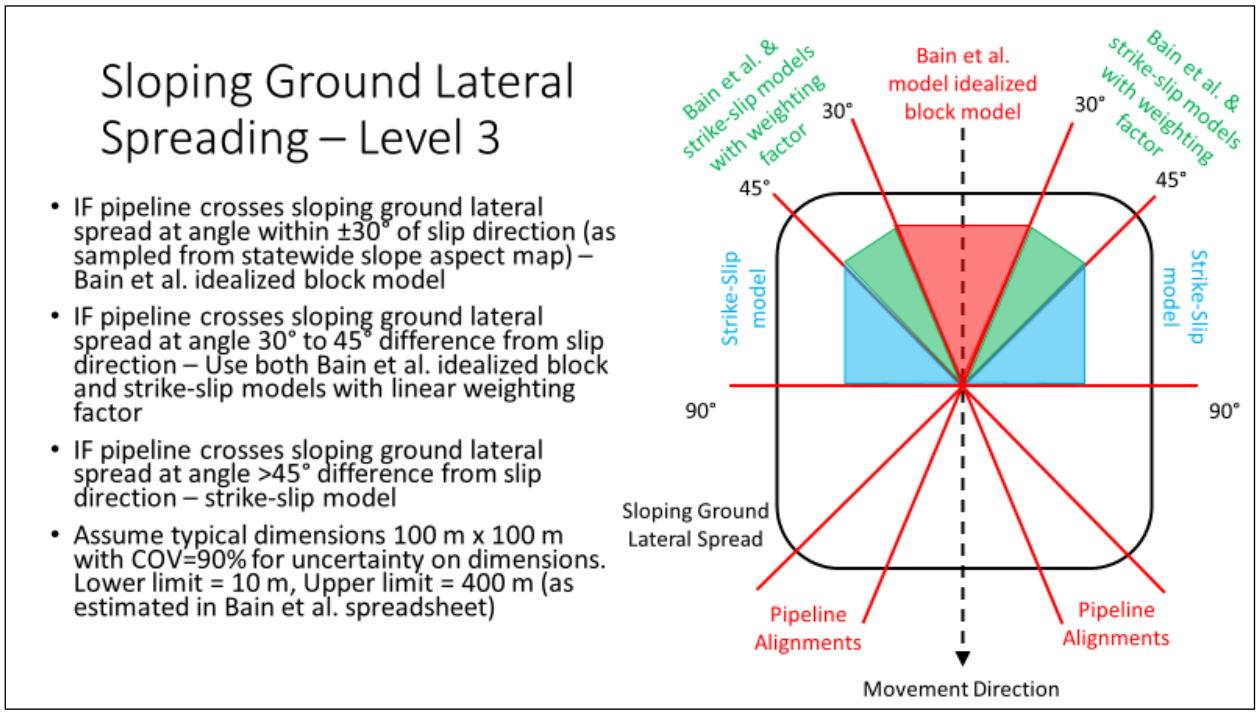

If the free-face condition controls, the logic for assessing pipe strain is as follows:

- If the pipeline crosses a free-face lateral spread, the free-face ratio (L/H) is less than or equal to 10, and the pipeline crosses within ±30° of the orientation of the lateral spread slip direction vector, estimate the pipe strain as the maximum value calculated from the Bain et al. model and the Hutabarat et al. pure normal-slip tension model with a mean value of dip angle, $\Psi = 45°$ (assumes equal vertical and outward horizontal ground deformation). Assume the strain in both models is tensile because the lateral spread extension zone typically produces the greatest displacement demand on a buried pipeline in a free-face lateral spread.
- If the pipeline crosses a free-face lateral spread, the free-face ratio (L/H) is less than or equal to 10, and the pipeline crosses at an angle within 30° - 45° of the orientation of

the lateral spread slip direction vector, estimate the pipe strain as the maximum value calculated from the Bain et al. model and the Hutabarat et al. pure normal-slip tension model with a value of dip angle, $\Psi = 45°$. Apply a linear weighting factor to the two models.

- If the pipeline crosses a free-face lateral spread, the free-face ratio (L/H) is less than or equal to 10, and the pipeline crosses at angle greater than 45° from the slip direction vector, estimate the pipe strain as the maximum value calculated from the Hutabarat et al. pure normal-slip tension model.
- If the pipeline crosses within ±30° of the orientation of the lateral spread slip direction vector and L/H > 10, assess the pipe strain using the Bain et al. model. Assume the strain is tensile, because the lateral spread extension zone typically produces the greatest displacement demand on a buried pipeline in a free-face lateral spread.
- If the pipeline crosses within 30° - 45° of the orientation of the lateral spread slip direction vector and L/H > 10, assume the pipeline is in a transition zone between the Bain et al. model and the Hutabarat et al. pure strike-slip model with a linear weighting factor. Assume the strain is tensile.

- If the pipeline crosses at an angle greater than 45° from the orientation of the lateral spread slip direction vector and L/H > 10, assess the pipe strain with the Hutabarat et al. pure strike-slip tension model. Assume the strain is tensile for a free-face lateral spread.

B.5 Logic Tree for Pipelines Crossing Areas of Liquefaction-Induced Settlement

To assess risk from liquefaction-induced ground settlement, *OpenSRA* will first discretize the pipelines into approximately 100-m long segments. At the midpoint of each segment, each of the parameters necessary to perform the liquefaction-induced settlement assessment are sampled from their respective distributions to get a sense of the epistemic uncertainty. For each combination of parameters, the liquefaction-induced settlement is calculated and if the estimated settlement is less than or equal to 5 cm, the settlement is assumed to be negligible (i.e., zero), and the probability of leakage or rupture is assumed to be zero. For non-negligible liquefaction-induced settlement (greater than 5 cm), the probability of tensile leakage or rupture or compressive rupture is estimated. Finally, *OpenSRA* reports the risk as the percentiles (i.e., 5^{th}, 16^{th}, 50^{th}, 84^{th}, and 95^{th}) for the probability of tensile leakage or rupture and the probability of compressive rupture at each pipe segment.

At Level 1, if the estimated liquefaction-induced settlement is less than or equal to 5 cm, the settlement is negligible, and the probability of rupture is zero. For non-negligible settlement (settlement greater than 5 cm), assume that a pipeline has a 25% probability of crossing the edge of an area with liquefaction-induced ground settlement. This is applied by multiplying the resulting probability of leakage or rupture by 0.25. Use the Hutabarat et al. pure normal-slip (rake angle, $\theta = -90^o$) model to estimate pipe strain given the estimate of liquefaction-induced ground settlement, assuming the dip angle, $\Psi = 75^o$ and the pipeline obliquity, $\beta = 90°$.

At Level 2, the quality of the data used to calculate liquefaction-induced settlement is improved (see data matrix) and the pipeline data are also improved. However, the logic tree for performing the liquefaction-induced ground settlement assessment is similar at Level 1 and Level 2. If the settlement is negligible (less than or equal to 5 cm), the settlement is assumed to be zero. For non-negligible settlement (greater than 5 cm), assume that a pipeline has a 25% probability of crossing the edge of an area with liquefaction-induced ground settlement. This is applied by multiplying the resulting probability of leakage or rupture by 0.25. Use the Hutabarat et al. pure normal-slip (rake angle, $\theta = -90^o$) model to estimate pipe strain given the estimate of liquefaction-induced ground settlement, assuming the dip angle, $\Psi = 75^o$ and the pipeline obliquity, $\beta = 90°$.

At Level 3, the liquefaction triggering and ground settlement assessment is performed using CPT or soil boring data, which is a significant improvement in the quality of the geotechnical data relative to the data available at Levels 1 and 2. A Level 3 assessment cannot be performed without site-specific data from a CPT or a soil boring. *OpenSRA* takes the CPTs or soil borings data and creates a polygon to estimate the spatial extent of liquefaction-induced ground settlement. If the estimated settlement is negligible (less than or equal to 5 cm), assume that the ground settlement is zero, and the probability of leakage or rupture due to this hazard is zero. For non-negligible estimated liquefaction-induced ground settlement (greater than 5 cm), use the Hutabarat et al. pure normal-slip (rake angle, $\theta = -90^o$) model to estimate pipe strain for given the estimate of liquefaction-induced ground settlement, assuming a default dip angle, $\Psi = 75^o$, which can be overridden by a user-defined dip angle based on the geometry of the ground settlement area. *OpenSRA* will estimate the pipeline obliquity (β) based on the intersection angle of the pipeline with the edges of the ground

settlement area (see figure below). If insufficient information is available for *OpenSRA* to estimate pipeline obliquity, β will be assumed to be equal to 90°.